Planification du réseau de distribution basse tension avec intégration de sources photovoltaïques et stockage : cas du réseau du Cambodge

Vannak Vai

Communauté UNIVERSITÉ Grenoble Alpes

THÈSE

Pour obtenir le grade de

DOCTEUR DE LA COMMUNAUTE UNIVERSITE GRENOBLE ALPES

Spécialité : **Génie Electrique**

Arrêté ministériel : 25 mai 2016

Présentée par

Vannak VAI

Thèse dirigée par **Bertrand RAISON** et
codirigée par **Marie-Cécile ALVAREZ-HERAULT**

préparée au sein du **Laboratoire G2Elab**
dans **l'École Doctorale EEATS**

Planning of low voltage distribution system with integration of PV sources and storage means - Case of power system of Cambodia

Planification du réseau de distribution basse tension avec intégration de sources photovoltaïques et stockage - Cas du réseau du Cambodge

Thèse soutenue publiquement le **27 Septembre 2017**,
devant le jury composé de :

M. Bruno FRANCOIS
Professeur, Ecole Centrale de Lille — Président

M. Cristian NICHITA
Professeur, Université du Havre — Rapporteur

M. Marc PETIT
Maître de conférences, CentraleSupélec — Rapporteur

M. Bertrand RAISON
Professeur, Université de Grenoble Alpes — Directeur

Mme Marie-Cécile ALVAREZ-HERAULT
Maître de conférences, Grenoble INP — Co-encadrant

M. Long BUN
Docteur, Institut de Technologie du Cambodge — Invité

គោរពជូនលោកឪពុក និង អ្នកម្តាយរបស់ខ្ញុំ

À mes parents

To my parents

ទីកន្លែងកំណើត :

ភូមិតាហ៊ី ឃុំព្រៃខ្ពស់ ស្រុកបវេល ខេត្តបាត់ដំបង ប្រទេសកម្ពុជា

Place of Birth :

Tahy, PreyKhpuos, Bavel, Battambang, Cambodia

Acknowledgments

This PhD thesis has been completed in the Laboratoire de Génie Electrique de Grenoble (G2Elab) of the Institut Polytechnique de Grenoble (Grenoble INP) and Institut de Technologie du Cambodge (ITC). I would like to express my sincere appreciation to my directeur de thèse, Bertrand RAISON, my co-encadrants: Marie-Cécile ALVAREZ-HERAULT and Long BUN, for their inspiration, guidance, encouragement, and friendship, without whom this work would not have been possible. BR, you have been being always with me, you were always patient even I had little progress. MC, you constantly guided me even we were so far away (Cambodia-France-California), you have been so kind to provide me with valuable suggestions. BL, you have been always encouraging me with positive thinking. Believe me, 36 months working with them has been a rewarding and enjoyable experience.

I also would like to express my heartfelt gratitude to the rapporteurs, Cristian NICHITA and Marc PETIT, and the member of the committee, Bruno FRANCOIS, for their valuable comments and review of this thesis. Cristian and Marc, you both permitted me to send a manuscript one month after the deadline, that was very kind of you.

I would like to say special thanks to Bong Seihakkiry RANN (Electricité du Cambodge-EDC) for discussing and providing me the documents related to current issues of power system in Cambodia. He guided me to select the site study of rural area in Cambodia for my PhD thesis.

Without the financial support of the Bourses du Gouvernement Français (BGF) and G2Elab which offered me a scholarship, this work would not have been possible. I would like to say special thanks to Michael GRAS (BGF) and James ROUDET (Directeur du G2Elab) for granting me the rare opportunity in wonderful city, Grenoble.

Special appreciation is extended to Nadine MICHEL and Florence FRANCOIS, administrative staffs of G2Elab, for their help, kindness, and encouragement. We and Bertrand were at Angkor Wat temple together from 19th to 23rd November, 2016, I will never forget these days of mine.

I wish also to thank Bong Sophal, president of Cambodia association in Grenoble. Bong Sophal, you are warm welcome to me not only in Grenoble, but also first time in France, Paris-Charles de Gaulle (CDG) Airport. We were together on the way from Paris to Grenoble by car on 30th August, 2012.

I would like to say many thanks to both Bong Khanna and Khanmony, and their families in Paris. It was my first night I got a good sleep in your home in France, 29th August, 2012.

I am thankful to Om Seth and Om Eam for being so kind to me in Grenoble. Your home always opened and welcome to me, it was my second home in Grenoble. Khmer foods in France were at your home for me.

Also, I am very much thankful to Association Française de Solidarité (AFS)-Cambodge for being so supportive to provide me financial support for high school and bachelor of engineering in Battambang and Phnom Penh. AFS has been with me since 2006. I am extremely grateful to Marie et loïc, AFS members in Grenoble for their kindness. It was first time for me on mountain in your home; Noël day.

I am grateful to Anne-thérèse and her brother Damien for being my second Maman in AFS. She is always so gentle to me. On 6th December, we were enjoyable together for la Fête des lumières 2014 in Lyon city.

Special acknowledgement for Dr. Egor Gladkikh and Dr. Alexander MC for giving me the algorithm of MIQCP and Reorder number; it was part of this thesis. You asked me what was my problem and objective, and then you developed it for me in one week. You are very nice to me.

I am especially indebted to Bong Nimol KHIM, Victor and Geoffrey for their encouragement and help for administration process of doctoral school; soutenance de thèse.

I would also like to thank all PhD Students from the laboratory: Ahmed, Kevin, Hadi, Bhargav, Stéphane, Olivier… for their kindness. Also, I am very thankful to all my friends: Panha, Puthea, Samnith, Kimsin, Kakada, Chen, Roun, Chanthan, Daya, Bunthern, Sokchea, Rothmony, Savda, Malen, Sokcheat... for their encouragement and friendship.

Lastly and most importantly, I would like to express my deepest gratitude for my parents (Vai CHUCH, Kimseak SORN), my brothers (Vannsak, Kimsan, Savta), my sister (Savet), nephews, nieces, and my lovely fiancée (Chanra, called AYA) for their unconditional love and support. Chanra, you have been being with me since 2006, you never give up me, you are always next to me, and I do love you!!!

Grenoble, September 27th, 2017

Vannak VAI

Résumé

La consommation d'énergie augmente d'année en année en raison de la croissance de la population et des conditions économiques. Dans ce contexte, le gouvernement Cambodgien a mis en place une politique de promotion et d'encouragement du développement de l'électrification ; tous les villages devront être électrifiés d'ici 2020 et au moins 70% des domiciles auront accès au réseau électrique d'ici 2030. Par ailleurs, de nombreux foyers non électrifiés sont équipés de panneaux solaires afin d'avoir accès à l'électricité. L'objectif de cette thèse est donc de développer des outils de planification du réseau de distribution basse tension afin de contribuer à l'électrification du pays. La première partie de cette thèse se concentre sur le développement d'outils d'optimisation de l'architecture afin de minimiser le coût d'investissement (CAPEX) et d'exploitation (OPEX) qui respecte l'ensemble des contraintes topologies et électriques (courant et tension) tout en intégrant les incertitudes liées au développement des consommateurs basse tension. La deuxième partie de la thèse propose une nouvelle solution de planification afin d'intégrer les productions solaires présentes et à venir sur le réseau basse tension. Cette solution consiste à ajouter du stockage centralisé (en milieu urbain et rural) et du stockage décentralisé (en milieu rural). Les principaux avantages seraient d'une part de réduire le pic de consommation du transformateur moyenne tension/basse tension et donc de réduire les investissements moyenne tension mais également le dimensionnement de « microgrids » basse tension pouvant être autonomes une grande partie de l'année. Une comparaison technico-économique avec la solution classique de renforcement permet d'évaluer l'intérêt de cette nouvelle solution.

Mots clés: *Méthode de Monte Carlo, optimisation, planification, photovoltaïque, réseau de distribution basse tension, stockage, théorie de graphe*

Abstract

The energy consumption increases year by year due to the growth of the population and the economic conditions. In this context, the Cambodian government promotes and encourages the development of the electrification through several policies; all the villages must be electrified by 2020 and at least 70 % of the households will be connected to the network by 2030. Besides, lots of non-electrified homes are equipped with solar panels so as to have access to the electricity. Then, the objective of this thesis is to develop planning tools of the low voltage distribution network to contribute to the electrification of the country. The first part of this thesis focusses on the development of architecture's optimization methods to minimize the capital expenditure (CAPEX) and operational expenditure (OPEX) while respecting both topological and electrical constraints (current and voltage) and integrating the uncertainties on the future development of the low voltage customers. The second part of the thesis proposes a new planning solution so as to integrate the current and future solar productions on the low voltage network. This solution consists in adding centralized storage (in urban and rural areas) and decentralized storage (in rural areas). The main advantages would be first to reduce the consumption peak of the medium voltage /low voltage transformer and consequently to reduce the medium voltage investments but also to size low voltage "microgrids" which can be autonomous a big part of the year. A technical and economic comparison with the classic solution of reinforcement allows estimating the interest of this new solution.

Keywords: *Monte Carlo method, optimization, planning, photovoltaic, low voltage distribution system, storage, graph theory*

Table of Contents

List of Figures

List of Tables

List of Principal Symbols and Abbreviations

B_{ij}	: Susceptance between the bus i and j
CAPEX	: Capital Expenditure
CeBES	: Centralized Battery Energy Storage
$C_{invest}(t)$	: Investment cost at the year t
$C_{total-act}$	: Total actualized cost over planning study
DeBES	: Decentralized Battery Energy Storage
d_{ij}	: Distance between two buses i and j
EAC	: Electricity Authority of Cambodia
EDC	: Electricité du Cambodge
ENS	: Energy Non-Supplied
FFBP	: First-Fit Bin-Packing
GA	: Genetic Algorithm
G_{ij}	: Conductance between the bus i and j
HV	: High Voltage
ICT	: Information Communication Technology
IPP	: Independent Power Producer
$I_{\alpha,neutral}^{bus}$	: Phase and neutral currents injected in the bus, $\alpha =$ A, B or C
$I_{\alpha,neutral}^{line}$	: Phase and neutral currents of line, $\alpha =$ A, B or C
$load\_ph_i^{\alpha}$	: Phase connection of load i, $\alpha =$ A, B or C
LV	: Low Voltage
MCS	: Monte-Carlo Simulation
MIME	: Ministry of Industry, Mines and Energy
MIQCP	: Mixed Integer Quadratically Constrained Programming
MV	: Medium Voltage
NASA	: National Aeronautics and Space Administration
OPEX	: Operational Expenditure
$Pbes_k^t$	: Power injection of battery for i^{th} bus at time t
$Ploss(t)$	: Power loss at the year t
p_i, q_i	: Active and reactive power of load i

$P_{ij}, p_{ij}^{\max}$	: Active power flow and maximal active power flow on line ij
PV	: Photovoltaic
$Q_{ij}, q_{ij}^{\max}$	: Reactive power flow and maximal reactive power flow on line ij
RES	: Renewable Energy Source
RGC	: Royal Government of Cambodia
SAIDI	: System Average Interruption Duration Index
SAIFI	: System Average Interruption Frequency Index
SoCmin,SoCmax	: Minimum and maximum of Stage of Charge of battery
SHS	: Solar Home System
SP	: Shortest Path
TolCon	: Constraint Tolerance
TolFun	: Function Tolerance
VUF	: Voltage Unbalance Factor
$V_{\alpha n}$	: Phase voltage, $\alpha =$ A, B or C
$V_{i,neg,pos}$	: Negative and positive sequences of voltages of the i^{th} bus
V_{lr}	: Receiving end voltage of branch
V_{ls}	: Sending end voltage of branch
V_{set}	: Voltage reference of DeBES
$x_{ij}, x_{ph\_ij}^{\alpha}$	: State of connection between two buses i and j, $\alpha =$ A, B or C
Z_{ij}	: Impedance of the conductor between two buses i and j
θ_{α}	: Power factor angles, $\alpha =$ A, B or C
δ_{α}	: Phase voltage angles, $\alpha =$ A, B or C
$\delta^{in}(i)$	: Set of incoming edge for i^{th} vertex
$\delta_{ij} = \delta_i - \delta_j$	: Voltage angle between the bus i and j
ΔV	: Voltage drop of branch

General Introduction

Day by day, the energy consumptions have continuously increased throughout the world due to a growing number of inhabitants with more comfortable lifestyles. Presently, energy needs have raised concerns regarding fossil fuel depletion, energy efficiency and global warming issues, thus leading our societies to search for alternative energy sources. Renewable energy sources have been put forward to reduce our dependency on fossil fuel by converting the energy from natural resources into thermal and electric energy. Today, the renewable energy sources are more and more used to provide energy. These sources are usually small size production units lower than 12 MW and located close to the end users. For that reason they are called distributed generations and are connected to the distribution system. As they can have either a positive or negative impacts on the distribution network, lots of research and development works are studied around the world to make to distribution network evolve toward a more reliable, economic and environmentally friendly grid.

In developing country such as Cambodia, the context is quite different. Even if the the low-voltage distribution systems are being reinforced and expanded in the recent years, about 75% of the population living in rural areas has currently no access to the electricity. In order to meet the need of the population and society regarding electricity, the Cambodian government has established a policy to promote and encourage the development of electrification [*REFE13*][1]; all the villages will have electricity by the year 2020, and at least 70% of the households will have access to grid-quality electricity by the year 2030. These objectives compel the Cambodian government and electricity distributors to perform planning and develop master plans for the development of the distribution network.

In addition, in Cambodia, the electricity is recently supplied by four main different sources, i.e. diesel, hydropower, coal and imports from neighboring countries. In the master plan of the electricity sector development of the country, the government sets hydropower and coal as the two main sources of electricity production. Nevertheless, more and more people having no access to the electricity invest in small photovoltaic production units connected to the LV distribution network and called Solar Home System (SHS). These small production units can have an impact on planning decisions in the low voltage network development because they can change the direction of power flows and even create situation of reverse power flows, i.e. electricity going from the LV grid to the MV grid

[1]*[REFE13] REFEDC, "Program for the development of rural electrification of Electricité Du Cambodge (EDC) through department of Rural Electrification Fund (REF)," 2013. [Online]. Available: http://ref.gov.kh/page/home.*

through the MV/LV substation. It is mandatory to integrate them in planning studies and to find economic solution to best take advantage of their potential benefits.

In that purpose, this thesis investigates novel methodologies and concepts to expand and design the low voltage distribution systems in a long term planning purposes in order to increase the electrification of developing countries such as Cambodia and to maximize the use of SHS. The research tasks performed in this PhD thesis are organized as it follows:

Chapter I will give a state of the art of the power systems in Cambodia focusing on the LV distribution network both in urban and rural areas. The planning principles used for developing the distribution network will also be presented.

In chapter II, optimization tools for the planning of distribution networks using current rules will be developed for both rural and urban areas. The objectives are the minimization of the capital expenditure (CAPEX) and the operation expenditure (OPEX) and the improvement of the load balancing while respecting a set of topological and electrical (current and voltage) constraints. Two novel algorithms will be developed to search for the optimal architecture: a Mixed Integer Quadratically Constrained Programming (MIQCP) and a Shortest Path and First Fit Bin Packing (SP-FFBP) algorithms. The presence of productions will not be considered at this stage. The impacts of uncertainties on the power and location of LV customers will be integrated using Monte Carlo simulations to evaluate the flexibility of the proposed tools.

In chapter III, SHS will be integrated in the planning tools. The maximum amount of PV without causing technical constraints is computed and located in the LV network. Then, the association of storage devices will be studied in order to solve the constrained induced by the PV connections and loads. Different kind of algorithms will enable to locate, size and control theses BES. Finally, a technical and economic analysis will be performed on a simple case study to compare the traditional planning method with the new one.

In chapter IV, the new planning methods developed in chapter III will be applied on two case studies (urban and rural) and compared with the traditional planning method. Uncertainties on the hourly load profiles will be integrating to evaluate the robustness of the new planning approach. These two case studies will lead to some conclusions and propositions for the development of LV microgrids in developing countries.

Chapter I

State of the Art of the Power System in Cambodia

Chapter I

State of the art of the power system in Cambodia

Summary

I.1 Introduction

Cambodia, officially known as the Kingdom of Cambodia, is a country located in Southeast Asia as depicted by Figure I-1. It has an area of 181 035 km^2 with a population of over 15 million in 2014 [*KING14*]. Currently, the electricity in Cambodia is supplied by four main different sources, i.e. diesel, hydropower, coal and imports from neighboring countries [*EAC16*]. Furthermore, the renewable energy sources such as photovoltaic and biomass already exist, but they are small and still isolated from the national grid. Also, Cambodia is an agricultural country, where over 80 % of the people live in rural areas with agriculture as the main source of subsistence [*FAO11*]. Among the Southeast Asian region, Cambodia has one of the most expensive electricity tariff {i.e. ~0.18 USD/kWh (Urban-LV) and ~0.3 USD/kWh (Rural-LV)} according to a report from [*KOSA12*]and [*EAC16*]. Presently, 74.80 % of the villages, and 65 % of households access to grid quality electricity [*MME16*]. Also, only about 25 % of Cambodian households have access to the electricity in rural area even if this country has a high potential for renewable [*PHOK16*]. They survive by using diesel engine, battery, kerosene for lighting, TV, multimedia and some other household appliances.

Likewise, to reduce poverty, improve the standard of living and foster economic development, Cambodian government has established the policy to promote and encourage the development of electrification [*REF17*]; all the villages in the Kingdom of Cambodia will have access to electricity of any type by the year 2020 and at least 70 % of all households in the Kingdom of Cambodia will have access to quality electricity grid by the year 2030.

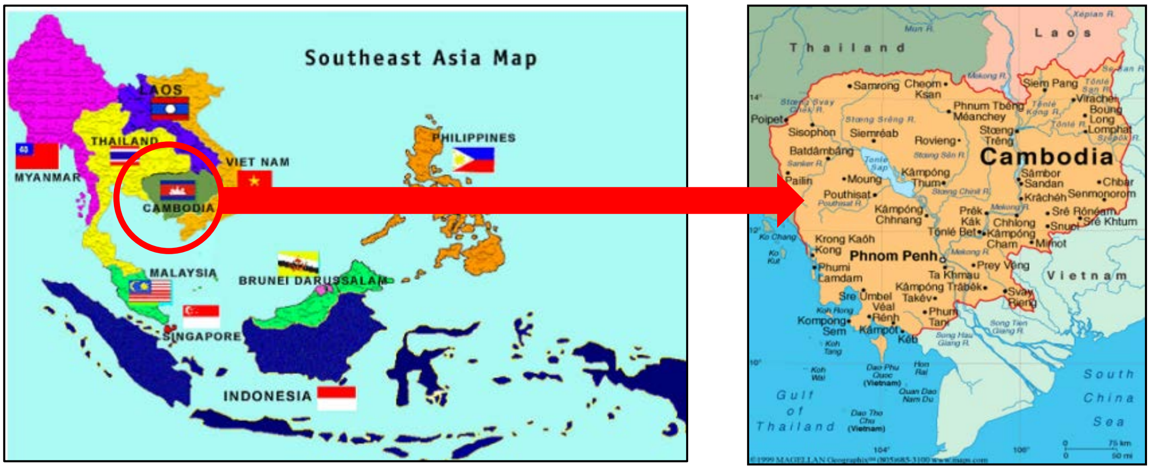

Figure I- 1 : Cambodia map

Besides, in the master plan of the electricity sector development in the country, the government sets hydropower and coal as the two main sources of electricity production [*KEIR09*][*EAV11*]. However, as renewable energy sources such as solar are abundant only in some particular areas, the government seems to neglect it in his development plan for the electricity sector [*MME16*]. It is thus very interested to highlight the benefits of small scale distributed generations (i.e. photovoltaic and battery energy storage) integration into the low-voltage distribution system in order to encourage the Cambodian government and electricity distributors with these sources. Moreover, in order to apply the concept of planning on low-voltage distribution system, it is necessary to understand the background of the power system such as its current situation and its evolution, and also the architecture of the low-voltage distribution system in Cambodia. The first part of this chapter will describe the current situation of the power system in Cambodia. In the second part, we will provide the structure of the low-voltage distribution system in two different areas (i.e. rural and urban). Finally, we will detail the principles of planning the power distribution system in the last part of this chapter.

I.2 Institutional framework of the Cambodian power sector

The electricity law of the Kingdom of Cambodia defines the responsibility of the Ministry of Industry, Mines and Energy (MIME) and Electricity Authority of Cambodia (EAC) separately. The MIME is mainly responsible for setting and administrating the government policies, strategies, planning, and setting the technical standards for the power sector. The EAC is responsible for issue rules, regulation and procedures and for monitoring, guiding and coordinating the operators in the power sector both suppliers and consumers and also making sure they follow the policy, guidelines and technical standards issued by MIME [*EAC15*]. The roles of these organizations are summarized in Figure I-2.

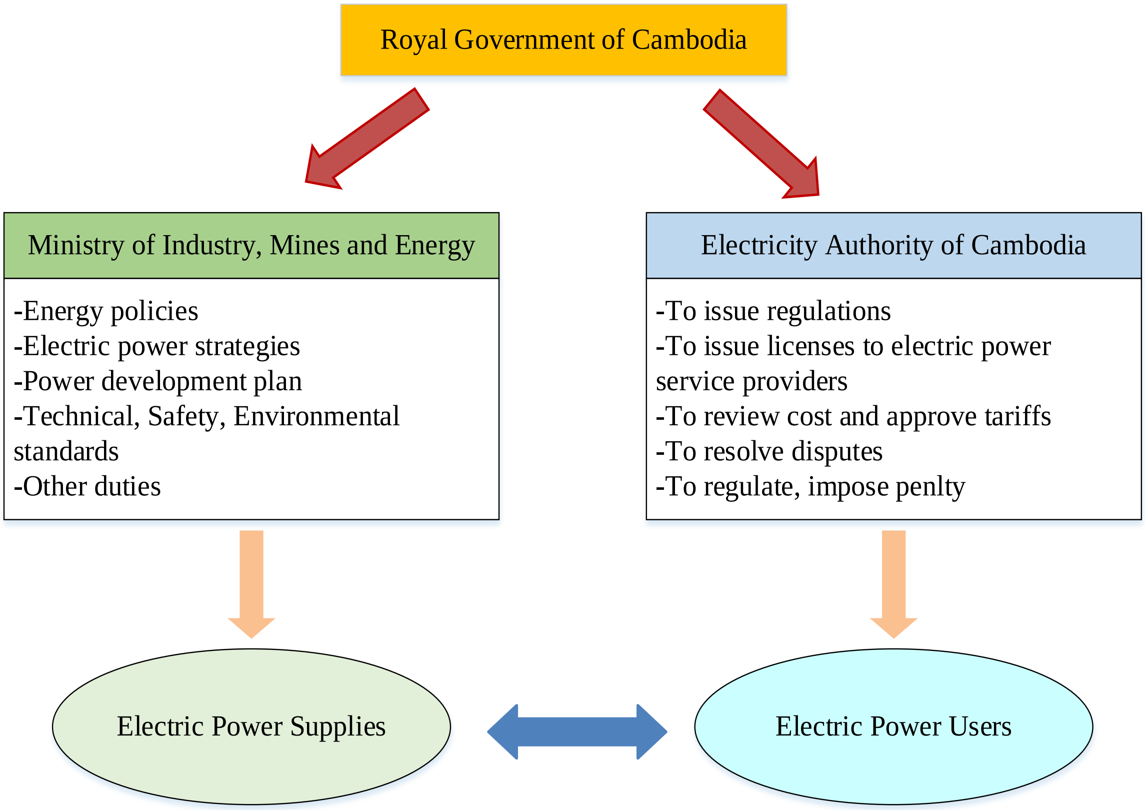

Figure I- 2 : Governance of the electricity sector in Cambodia [*KOSA12*]

I.3 Generation, import and consumption of electricity

I.3.1 Power generation

I.3.1.1 Power generation by type of licenses

There are two types of licensees that generate electricity in the Kingdom of Cambodia not including Electricité du Cambodge (EDC) which is the only licensee in the public sector. The first are Independent Power Producers (IPPs), having generation license to generate and sell electricity to suppliers or industries in compliance with the power purchase agreement. The seconds are Consolidated Licensees, having generation license to generate electricity for supplying the consumers through their distribution system [*EAC15*]. Moreover, the energy generated and sent out by all the licensees in Cambodia during 2015 is 4489.27 GWh, which is 46.79% more than the energy sent out during 2014. The percentage of energy sent out by the Independent Power Producers, Consolidated licensees and EDC is depicted by the pie chart of Figure I-3 [*EAC16*].

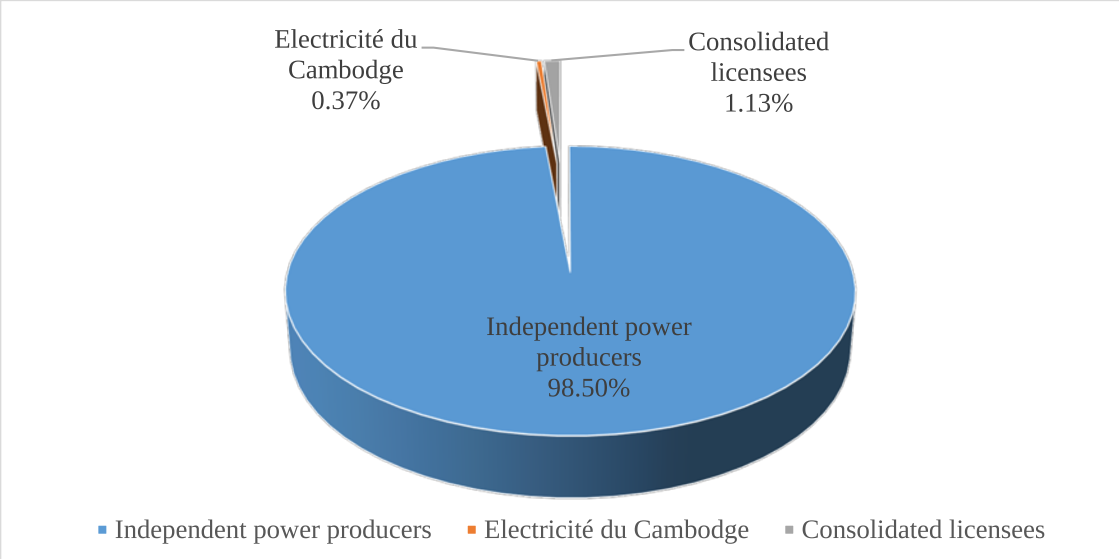

Figure I- 3 : Proportion of energy sent out by licenses at the end of 2015 (%)

I.3.1.2 Power generation by type of generation facilities

In the year 2015, the electricity generation facilities in Cambodia are divided into four types: 1-Hydropower plants, 2- Diesel power plants, 3- Thermal power plants using coal and 4- Thermal power plants using wood or biomass. The total energy generated by all the generation types is 4489.27 GWh in 2015 [*EAC16*] compared to 3058.36 GWh in 2014 [*EAC15*]. Figure I-4 provides the proportion of energy sent out by the four types of generation.

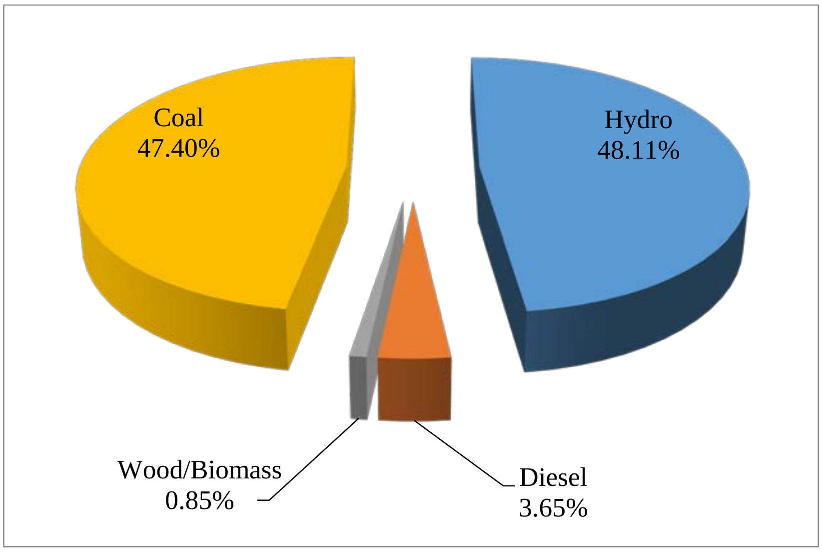

Figure I- 4 : Proportion of energy sent out by types of generation at the end of 2015 (%)

I.3.2 Energy imported from neighboring countries

With the rapid increase in demand following the trend of economic growth, Cambodia does not have sufficient supply for its demand, thus the Royal Government of Cambodia (RGC) needs power from its neighboring countries such as Laos, Thailand, and Vietnam under the power sector cooperation agreement between the Greater Mekong Subregion (GMS) [*Asso10*] nations. The percentage of productions in Cambodia as well as the amount of imports of electricity (total: 6015.36 GWh) are shown in Figure I-5 [*Eac16*].

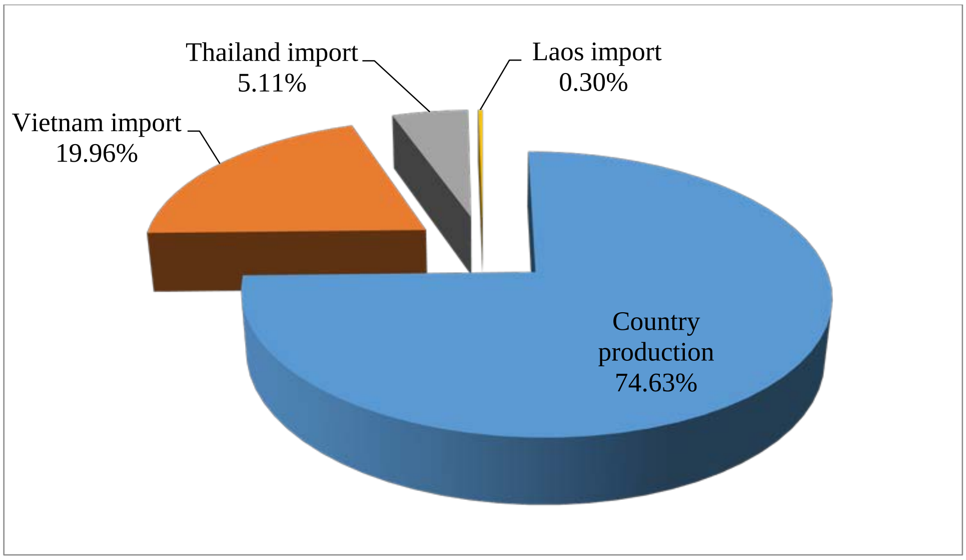

Figure I- 5 : Percentage of productions by Cambodia and necessary imports at end of 2015 (%)

I.3.3 Supply of electricity to consumers

Each year, the size of the electrical infrastructure to provide electricity to consumers and the number of villages supplied with electricity grow up due to the increase of new licenses and the expansion of the area to supply. A comparison of data on the electricity generation in Cambodia, the imports from neighboring countries by licensees and on consumers and consumption for the years 2014 and 2015 are provided in Table I-1. As it can be noticed, the energy import from neighboring countries has been decreased by 15% due to the increase of the country production.

Table I- 1 : Data of the electricity sector at a glance in Cambodia [*EAC16*]

Description	Unit	2014	2015	%Change
Electricity generated	GWh	3058.36	4489.27	46.79
Electricity imported from Thailand	GWh	523.56	307.39	-41.29
Electricity imported from Vietnam	GWh	1256.72	1200.39	-5.16
Electricity imported from Laos	GWh	13.77	18.31	32.96
Total electricity import	GWh	1803.05	1526.08	-15.36
Total electricity available	GWh	4861.41	6015.35	23.74
Installed Generating Capacity	MW	1511.338	1657.274	9.66
Number of consumers	#	1424735	1859204	30.49
Electricity sold to consumers	GWh	4144.12	5205.34	25.61
Average losses	%	14.75	13.47	-8.68

I.3.4 Electricity consumption

According to the EAC, consumers' demand for electricity increases every year; hence, the demand for installed electricity-producing capacity must also be increased. In the meantime, energy sold has increased by around 880 % from 614.03 GWh in 2002 [*EAC12*] to 6015.35 GWh in 2015 [*EAC16*] as shown in Figure I-6. Also, the number of consumers has increased by around 20% in 14 years as given in Figure I-7.

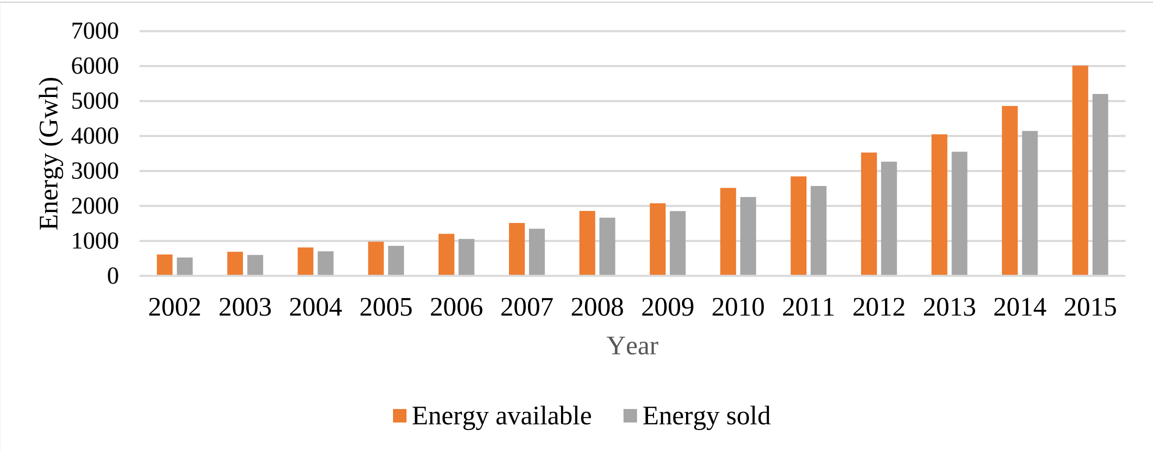

Figure I- 6 : Energy available and sold between 2002 to 2015

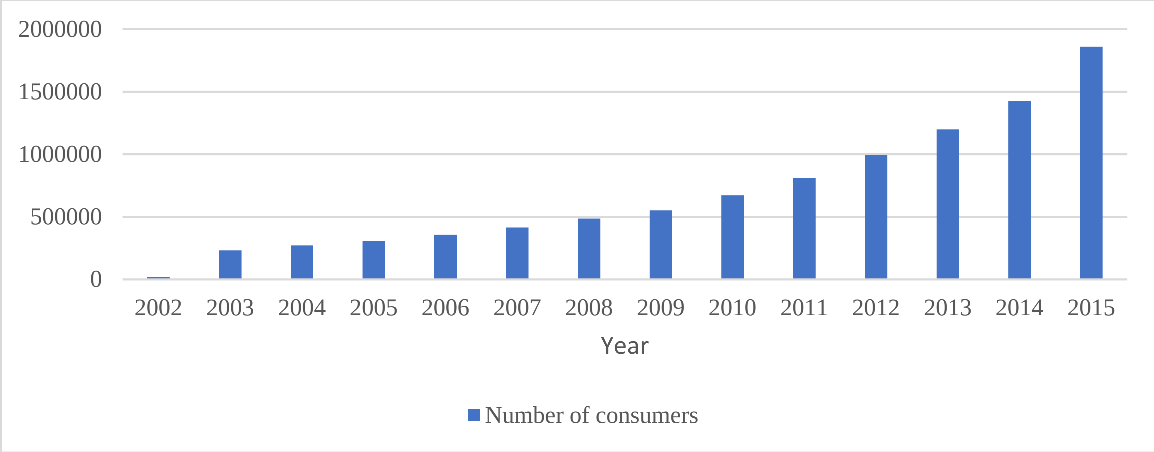

Figure I- 7 : Number of consumers between 2002 to 2015[*EAC12*][*EAC16*]

I.4 Power distribution system

The distribution system is the final link between the bulk power system and the end users. It provides electricity to the end users from the high voltage (HV) / medium voltage (MV) substations [*BENO15*]. It consists of the MV and the low voltage (LV) systems. In Cambodia, the MV distribution system consists of three phases (urban areas) and single phases (some rural areas). The line voltage is usually 22 kV in MV system and it is designed as a looped system, but is operated radially. The LV distribution system is perfectly radial and consists of single phase and three phases including a distributed neutral wire. The phase and line voltages are usually 230/400 V. Moreover, the length of distribution systems, both medium and low voltage, is approximately 7145 km with about 3282 MV/LV substations [*EAC15*]. In addition, the voltage standards in the kingdom of Cambodia are illustrated in the following table:

Table I- 2 : Voltage levels in Cambodia [*KING04*]

Classification of voltage	**Range of nominal voltage**	**Nominal voltage**	**Highest voltage**
High Voltage (HV)	U > 35 kV	230 kV	245 kV
		115 kV	123 kV
Medium Voltage (MV)	600 < U ≤ 35 kV	22 kV	24 kV
Low Voltage (LV)	U ≤ 600 V	230 / 400 V	

Moreover, low voltage at the supply point shall be maintained between -10 and + 6% of the nominal value as shown in Table I-3. Also, the rating frequency in Cambodia is 50 Hz and the variation of the frequency shall be between 49.5 Hz and 50.5 Hz.

Table I- 3 : Variation of low voltage in Cambodia [*KING04*]

Nominal system voltage	Value to be maintained
230 V	207 V≤ U ≤ 244 V
400 V	360 V≤ U ≤ 424 V

I.4.1 Supplying of the medium voltage (MV) systems

The MV distribution system is supplied by either the HV national grid through HV/MV substations or through the 22 kV distribution lines coming from Vietnam grid, Thai grid and Laos grid in the border area or MV isolated networks from the bulk power system. The map of the MV distribution system of Cambodia is depicted in Figure I-8.

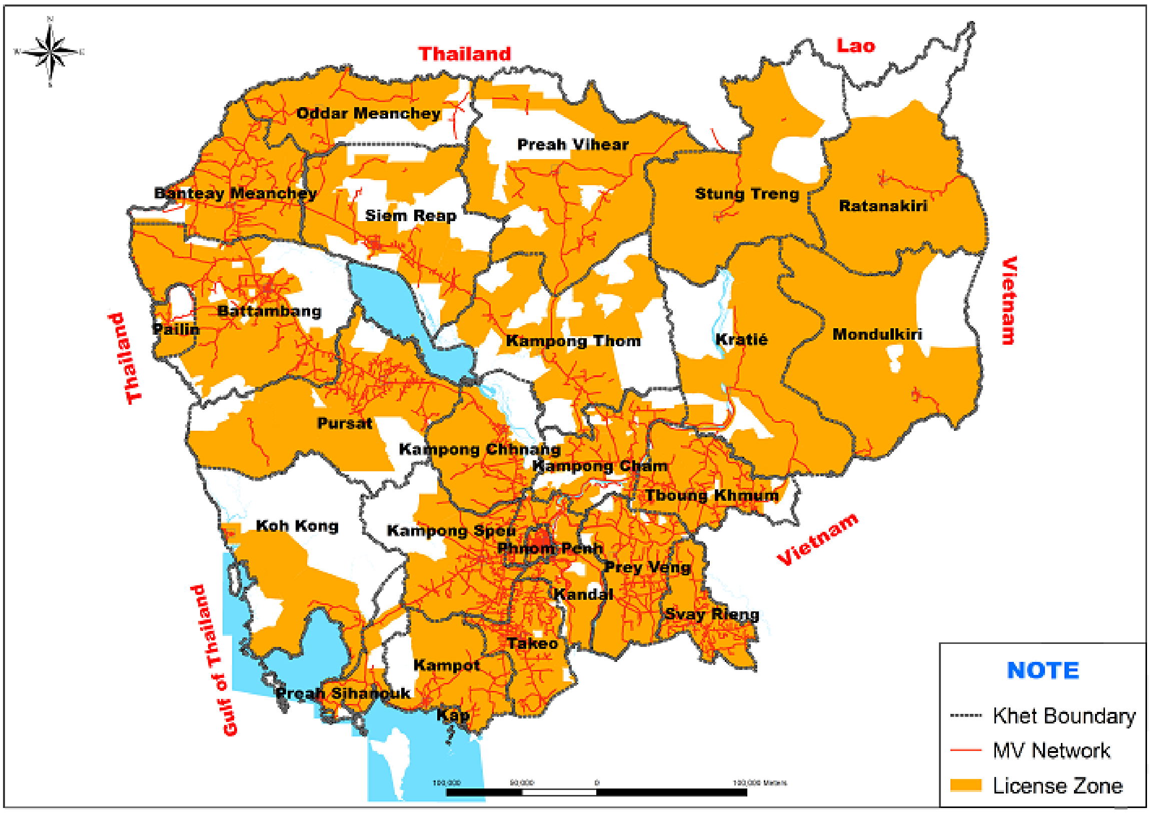

Figure I- 8 : Map of the MV distribution system at the end of 2015 [*EAC16*]

The information on the percentage of the energy input of the MV grid system in Cambodia is illustrated in Figure I-9. It can be noticed the almost all the power supplying the MV grid is national.

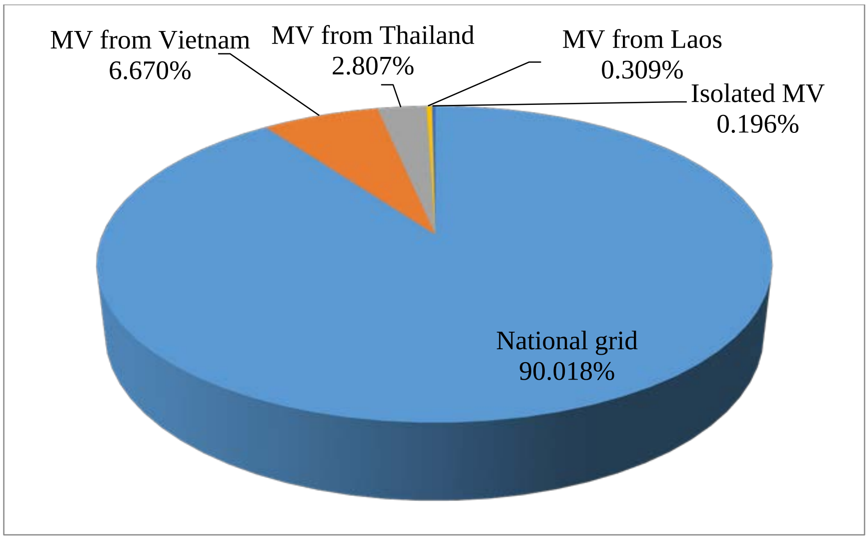

Figure I- 9 : Percentage of energy input of MV grid at the end of 2015 [*EAC16*]

I.4.1.1 National grid

The MV lines connected to the national grid provide electric power supply in areas around the grid substations. It is the case in Phnom Penh and the provinces of Kandal, Kampong Speu, Takeo, Kampot, Sihanoukville, Kampong Cham, Kampong Thom, Prey Veng, Banteay Meanchey, Battambang, Siem Reap, Pursat and Kampong Chhanang [*EAC16*].

I.4.1.2 MV grid connected from neighboring countries

- MV grid connected to the Vietnam system

Cambodia imports electricity from Vietnam through 22 kV connections at 18 locations in the provinces of Kampong Cham, Svay Rieng, Kampot, Mondulkiri, Kandal, Takeo, Kratie, Prey Veng and Ratanakiri. The supply is then extended to other licensees. By the end of 2015, 46 licensees got supply from the Vietnam grid.

- MV grid connected to the Thailand system

Cambodia imports electricity from Thailand through 22 kV connections at 8 locations in the provinces of Battambang, Pailin, Banteay Meanchey, Koh Kong and Oddor Meanchey. The supply is extended to other licensees. By the end of 2015, 8 licensees got supply from the Thai grid.

- MV grid connected to the Laos system

EDC imports power from Laos to supply to city of Steung Treng and some areas of Preah Vihear. By the end of 2015, 9 licensees got supply from the Lao grid.

I.4.1.3 Isolated supply systems

Isolated systems consist of local MV grids having their own generation and supplying a small area, generally belonging to one licensee. The information on number of consumers, energy available and supplied to consumers for these isolated systems has been listed in Table I-4.

Table I- 4 : Information of province for MV isolated system at the end of 2015

Name of Province	Number of Licensees	Number of consumers	Installed Capacity (kW)	Energy generated (MWh)	Energy Sold to consumers (MWh)
Kampong Cham	3	2447	1272	432.24	384.97
Kampong Chhnang	2	783	206	155.04	129.54
Kampong Thom	5	3833	1959	1228.01	1015.28
Koh Kong	2	762	760	481.34	426.46
Kratie	4	2298	896	951.05	834.20
Oddor Meanchay	2	1941	2372	612.52	529.96
Preah Vihear	6	6111	6218	6025.66	4862.76
Pursat	1	821	847	636.65	584.86
Ratanakiri	1	349	220	274.20	253.43
Siem Reap	3	1832	640	893.09	750.72
Stueng Treng	1	443	425	103.20	87.60
Total	30	21620	15815	11793.00	9859.78

I.4.2 Architecture of the low-voltage distribution system

The MV/LV substations are the interface between the MV and LV systems. The MV/LV substations are different whether the area is rural or urban. The main topological constraints depend on geographic and demand of loads. So, both rural and urban topologies are described in the following subsections.

I.4.2.1 Rural areas

The rural areas are characterized by a low load density (big zone with low consumption). Thus, the conductor length is long, usually with overhead lines with a single-phase and three-phase distribution called main lines along the road. Therefore, the main technical problems in rural areas are the voltage drop at the end of the line. Figure I-10 and Figure I-11 illustrate the simple architecture in rural areas with single phase and three phases distribution presently implemented in Cambodia.

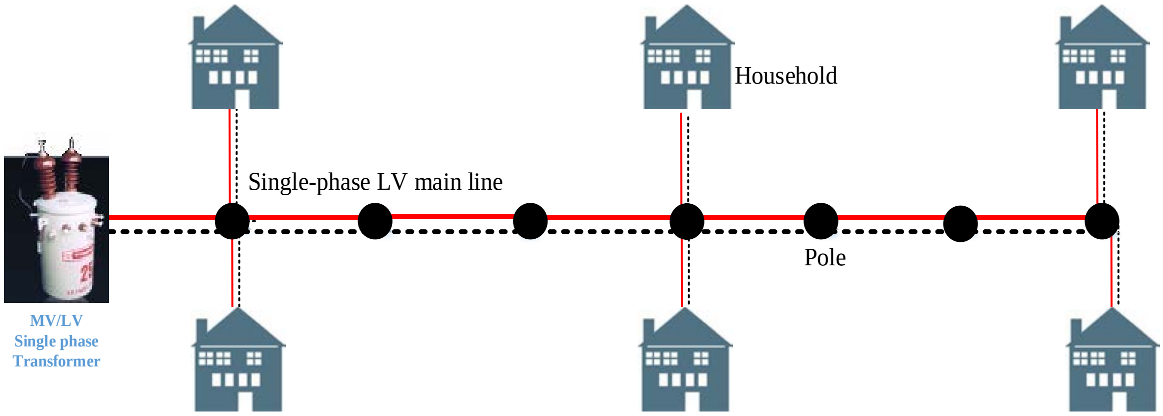

Figure I- 10 : Simple architecture of low-voltage distribution with a single phase main line in rural area

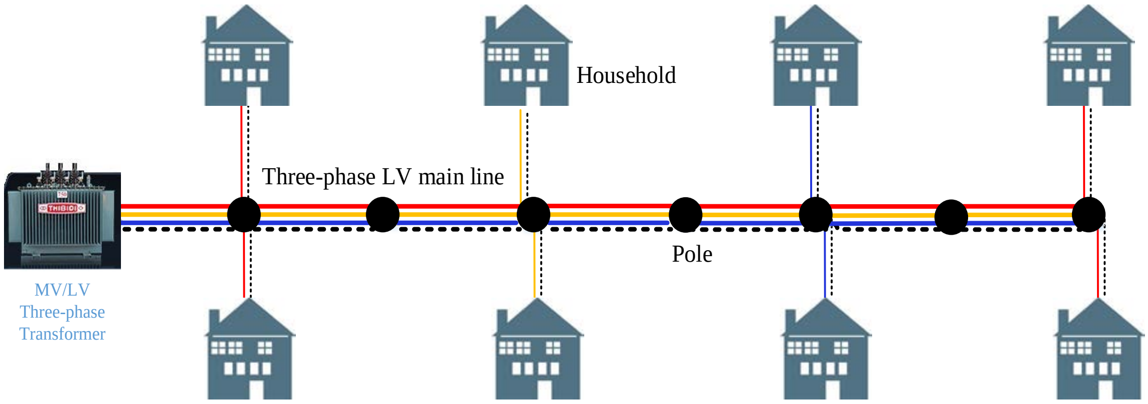

Figure I- 11 : Simple architecture of low-voltage distribution with a three-phase main line in rural area

I.4.2.2 Urban areas

The urban area is different from rural because its load density is high with short conductor length. Consequently, the main problem to take into account is permissible current in conductor. Currently, almost all the main lines are distributed with three-phase main lines. Figure I-12 shows the principle of the architecture of low voltage distribution system in rural area which is presently implemented in Cambodia.

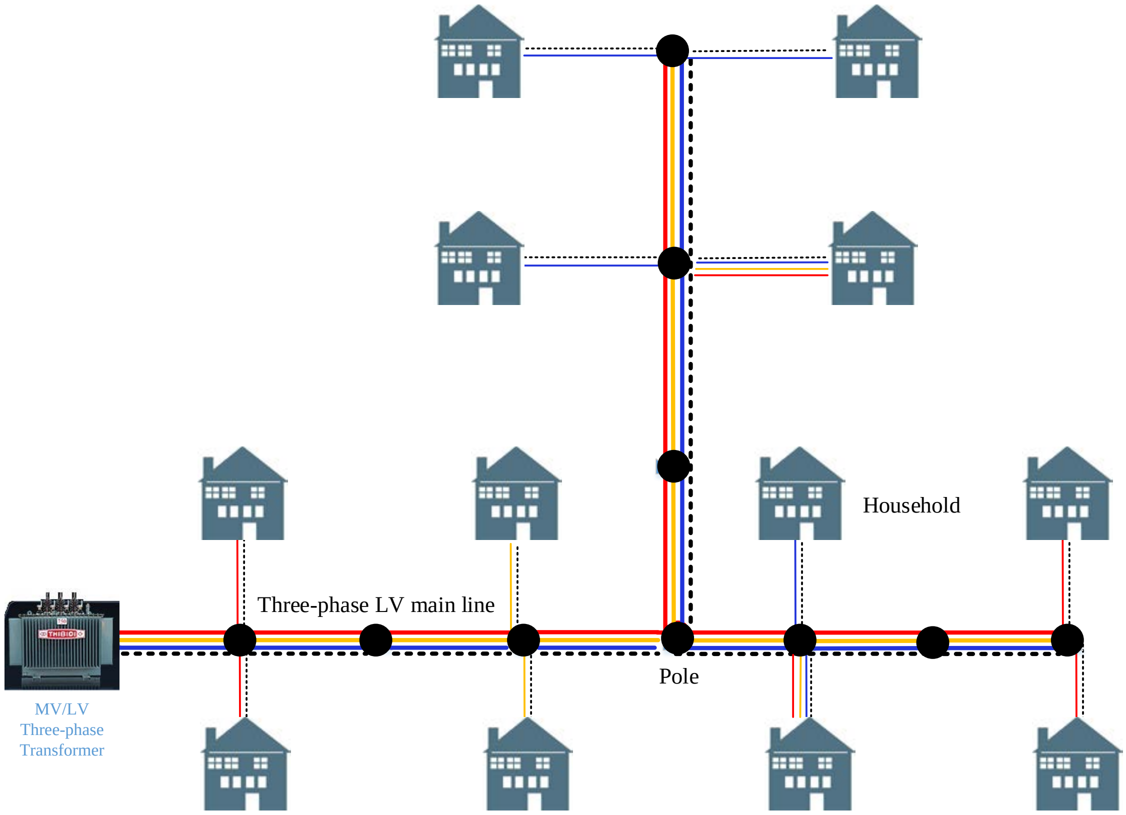

Figure I- 12 : Simple architecture of low-voltage distribution in urban area

I.5 Solar energy

The solar energy is abundant in the whole country with an average daylight of about 12 h per day and consequently 4380 h per year. Figure I-13 shows the monthly average daylight in Cambodia. The longest day is 12.46 hours long in June and the shortest day is in December with 11.27 hours of daylight.

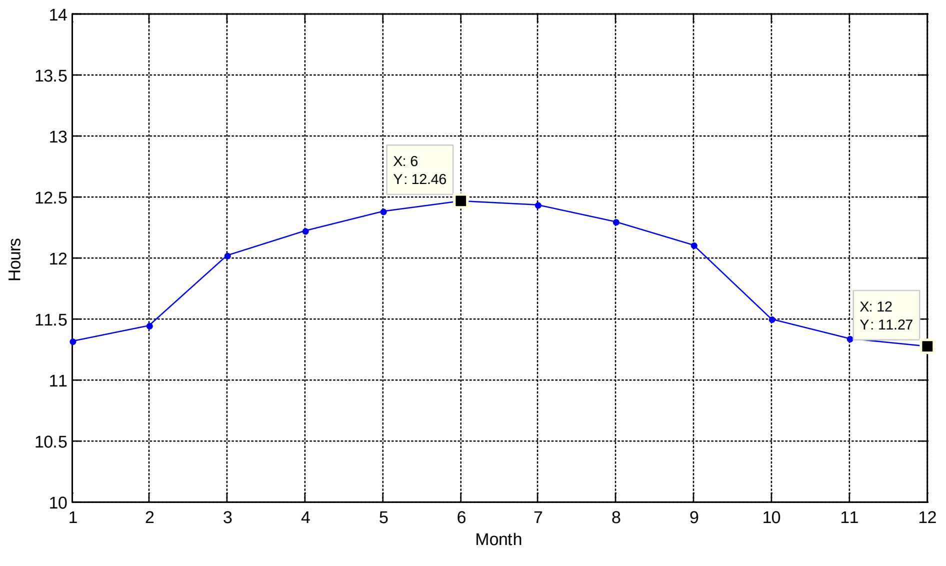

Figure I- 13 : Monthly average daylight in Phnom Penh, Cambodia [*CLIM17*]

Since there is no surface irradiation data available to our study, satellite data have been collected to grasp the potential of solar energy over the whole country. The data were downloaded from the National Aeronautics and Space Administration (NASA) home page [*NASA17*] via HOMER software [*HOME15*] and [*NREL16*]. Figure I-14 represents the monthly average and maximal solar radiation over the country. The monthly average radiation varies between 0.34 kW/m^2 and 0.44 kW/m^2. with an annual average of 0.40 kW/m^2. The maximum radiation is higher than 1.3 kW/m^2.

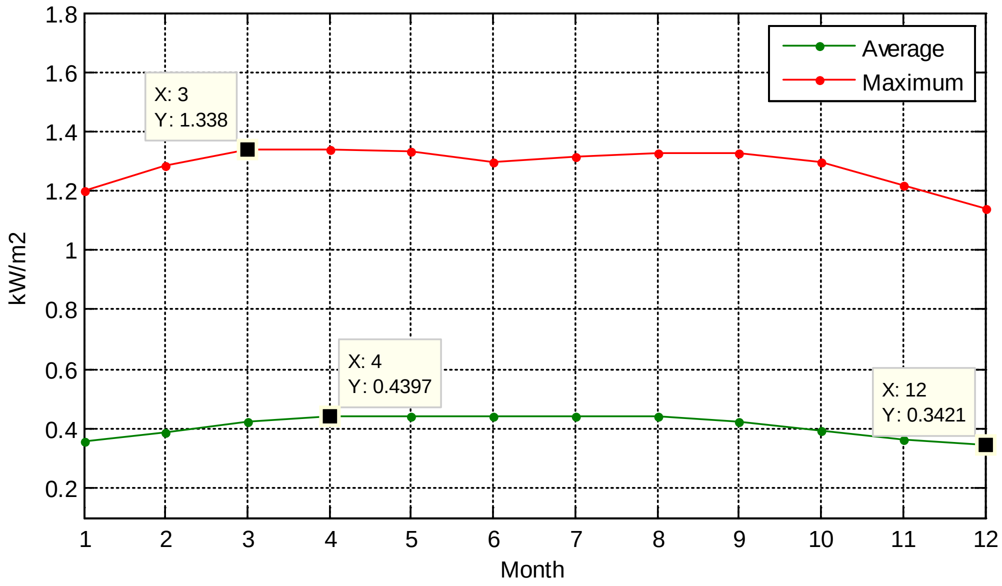

Figure I- 14 : Monthly average and highest solar radiation

Figure I-15 shows the spatial distribution of the solar irradiation based on the annual average satellite data. The southern and southwestern regions have the lowest irradiation whereas the latter increases gradually towards central region where it reaches the maximum value. It decreases slightly towards the eastern and northeastern regions but remains higher than the southern and southwestern regions.

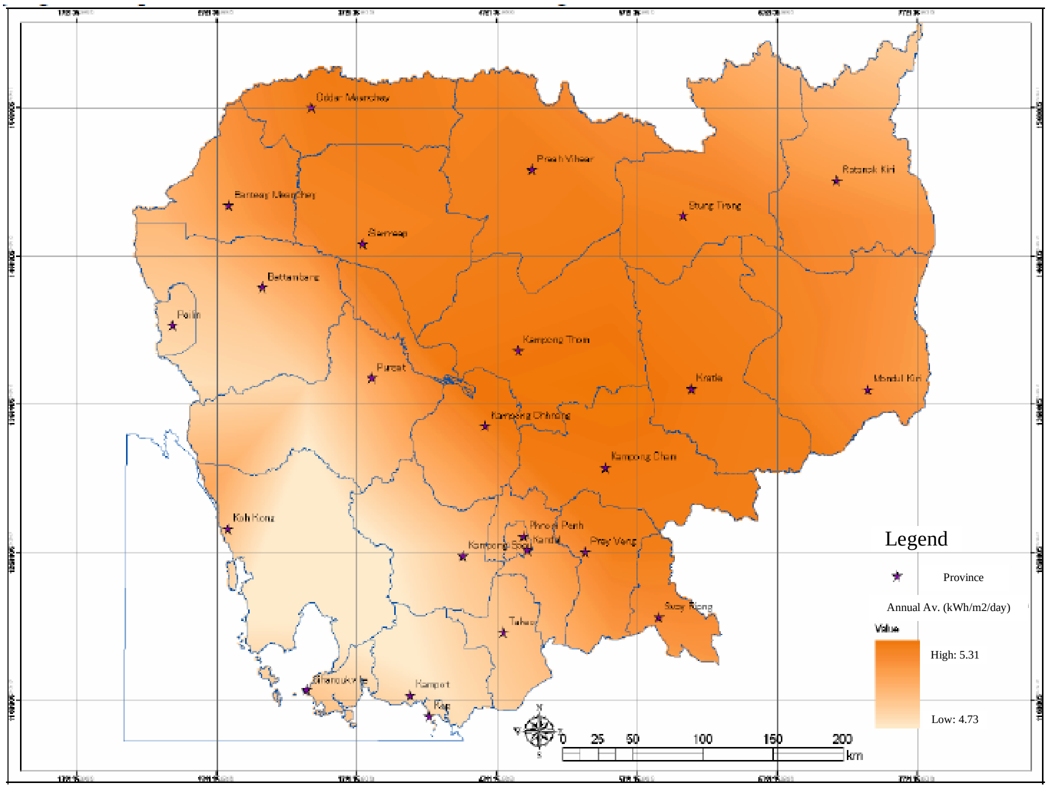

Figure I- 15 : Annual average solar irradiation [*JICA06*]

I.6 Objective of planning

The objectives of planning are to develop the power system in a long term planning perspective (usually 30 years) in order to improve its reliability and quality of service while respecting the technical constraints, being more environmentally-friendly and minimizing the global costs.

I.6.1 Reliability and quality of service

Three indicators usually define the reliability and quality of service in planning studies and are the following ones:

- The SAIDI (System Average Interruption Duration Index) is the average duration of power outage per year per customer.
- The SAIFI (System Average Interruption Frequency Index) is the average power outage frequency per year per customer.
- The ENS (Energy Not Supplied) is the yearly amount of energy non-supplied expressed in kWh per year.

The smaller these indicators are, the higher the reliability and the quality of service of the power system will be. More details about theses indices are provided in [*ALVA09*].

I.6.2 Electrical criteria

This criterion is taken into account through the respect of currents and voltages and the minimization of losses in the power system. These items will be described in the following section.

I.6.2.1 Permissible current

The permissible current of a device (conductor or transformer) is the maximum current in the steady state condition that can flow through it without exceeding the thermal limitation. This value depends on the gauge of the conductor and the maximum temperature of its insulation [*RAY06*]. Beyond these temperatures, insulation and/or conductor are deteriorated and this can cause fires. The bigger surface of cable section is the smaller the resistance will be. Thus, it is necessary to determine the properly size of the conductors for supplying the load so that the currents flows respect the permissible intensity over the planning horizon. A complete table of conductors used in Cambodia can be found in [*LVAB12*]. Table I-5 summarizes the main ones which will be used in this thesis.

Table I- 5 : The permissible of the conductors used in this thesis

Items	**Section of conductors (mm²)**					
	4[*CHSO15*]	**50**	**70**	**95**	**150**	**240**[*CHSO15*]
Resistance (Ω / km)	4.95	0.641	0.443	0.32	0.206	0.125
Maximum permissible intensity (A)	32	150	185	225	285	432

I.6.2.2 Voltage profile

The voltage difference between two points in an electrical circuit is defined as the voltage drop ΔV_{ij}. According to Ohm's law, the voltage drop is expressed by following equation.

$$\underline{\Delta V_{ij}} = \underline{Z_{ij}} \times \underline{I_{ij}} \tag{I-1}$$

Where,

$\underline{Z_{ij}}$: complex impedance of the conductor between point i and j

$\underline{I_{ij}}$: complex current flowing from point i to j

According to Eq. I-1, the voltage drop is linked to the current flowing through the conductor and its impedance. Moreover, this impedance increases with the length of the conductor and consequently the voltage drop too. Likewise, in case of power system with classical loads, without decentralized production, the voltage at consumers is lower than the voltage at substation. In addition, the voltage profile must also respect the constraint of operation in the power system; presently, the limit of voltage which is implemented for the low-voltage distribution in Cambodia is -10%/+6 % [*KING04*]. Therefore, it is mandatory to consider conductor length and impedance when applying the distribution planning.

I.6.2.3 Losses

The power losses are due to heating that occurs when an electrical current flows through a conductor [*GLAD15*]. For a conductor with a given resistance r in (Ω / km), a length L (km), a flowing current I (A) during a period Δt (h), the power losses at a given time t and the energy losses during a period of Δt are expressed by the following equations.

$$Power_{losses}(t) = r \times L \times I^2(t) \tag{I-2}$$

$$Energy_{losses}(t) = r \times L \times I^2(t) \times \Delta t \tag{I-3}$$

As seen in Eq. I-2 and Eq. I-3, power losses and energy losses are also linked to length and current.

I.6.3 Economic criteria

Other criteria in planning of power distribution system are economic ones; the capital expenditure (CAPEX) and the operational expenditure (OPEX) of the system design must be considered. In order to take into account the fluctuation of currency, the economic calculation uses the actualization principle. The actualization rate is a fixed value i which expresses the fact that N dollars today are worth $N \times (1+i)^t$ in the year t and so encourage to defer investment if possible. If $D(t)$ dollars are spent at the year t, the equivalent cost today is $\frac{D(t)}{(1+i)^t}$.

The actualized cost is integrated into the planning studies to choose between different strategies. The total actualized cost is defined by the following formula with $C_{total-act}$ being the current cost at year 0:

$$C_{total-act} = \sum_{t=0}^{N} \frac{C_{invest}(t) + Op(t)}{(1+i)^t} \tag{I-4}$$

Where:

- $C_{total-act}$: total actualized cost in $kUSD$
- $C_{invest}(t)$: investment cost in the year t (CAPEX) in $kUSD$

- $Op(t)$: operation cost in the year t (OPEX) in $kUSD$
- i : actualization rate in %

An example of the actualized cost calculation for different types of cable is presented in the PhD work of [*ALVA09*].

I.7 Scope of the thesis

This thesis will develop a long-term planning tool of LV distribution system for both electrified and non-electrified areas considering the technical and economic criteria previously defined and the actualized cost method over a planning period of 15 years. Compared to traditional planning studies, this PhD work will study the impact of uncertainties of load demand (i.e. growth rate, new load, and load profile) on the grid-reinforcement decisions. New solutions will be investigated such as the integration of PV generation and battery energy storage (BES) with their control in order to reduce the global cost and increase the electrification of the country. A first concept of LV microgrid architecture including PV and battery energy storage (BES) is then proposed.

In this work, some assumptions are made such as:

- The PV is characterized as a non-predicable renewable energy source in a long term perspective. Consequently, in this thesis, we assume that the power output of PV is proportional to the solar curve available on the NASA home page [*NASA11*] in Cambodia.
- The integration of DG as a grid planning option is currently strongly encouraged by the regulation. In that purpose, it is assumed that the regulation accepts the capacity of PV which are found by the developed algorithm.

I.8 Conclusion

In this chapter, we have started from the context and background of the power system in Cambodia. It was highlighted that there is about 75% of own generation and the remaining 25% are imported from neighboring countries even if Cambodia has a high potential for renewables. Presently, the main lines are distributed with single-phase and three-phase conductors along the roads for rural areas, and are almost three-phase for urban areas in Cambodia. In traditional planning, the local generation such as PV and battery energy storage (BES) are not taken into account; thus it is interesting to integrate them into planning studies as alternative solutions to gird reinforcements. The constraints taken into account for the optimal architecture are linked to the topology and the electrical variables (i.e. current, voltage and power losses). The main objectives of this thesis are to search for the optimal topology and impact of PV-BES integration in low-voltage distribution systems over the planning horizon. These problems will be considered in the next three chapters.

REFERENCES

[*Alva09*] M.-C. Alvarez-Hérault, “Architectures des réseaux de Distribution du futur en présence de Production décentralisée,” Thèse de doctorat, Institut polytechnique de Grenoble, 2009.

[*Asso10*] E. C. Associates, “The Potential of Regional Power Sector Integration: Greater Mekong Subregion(GMS),” London, 2010.

[*Beno15*] C. Benoit, “Models for investigation of flexibility benefits in unbalanced Low Voltage Smart Grids,” Thèse de doctorat, Institut polytechnique de Grenoble, 2015.

[*Chso15*] Chan and Sodavath, “Technical criteria for electrical wiring and safety for buildings and households of the kingdom of cambodia,” 2015.

[*Clim17*] Climate, “Sunshine & Daylight Hours in Phnom Penh, Cambodia Sunlight, Cloud & Day length,” 2017. [Online]. Available: http://www.phnom-penh.climatemps.com/sunlight.php.

[*Eac12*] EAC, “Report on power sector of the kingdom of Cambodia in Khmer Language,” 2012. [Online]. Available: https://eac.gov.kh/publication/report/.

[*Eac15*] EAC, “Report on power sector of the Kingdom of Cambodia,” 2015. [Online]. Available: https://eac.gov.kh/publication/report/.

[*Eac16*] EAC, “Report on power sector of the kingdom of Cambodia in Khmer Language,” 2016. [Online]. Available: https://eac.gov.kh/publication/report/.

[*Eav11*] R. Eav, “Kingdom of Cambodia,” 2011. [Online]. Available: http://eneken.ieej.or.jp/data/3840.pdf.

[*Fao11*] FAO, “Cambodia and FAO Achievements and success stories,” 2011. [Online]. Available: www.fao.org/3/a-at004e.pdf.

[*Glad15*] E. Gladkikh, “Optimisation de l ‘architecture des réseaux de distribution de l’énergie électrique,” Thèse de doctorat, Institut polytechnique de Grenoble, 2015.

[*Home15*] Homer, “HOMER - Hybrid Renewable and Distributed Generation System Design Software,” 2015. [Online]. Available: http://www.homerenergy.com/.

[*Jica06*] Jica, “The master plan study on rural electrification by renewable energy in the kingdom of Cambodia,” Phnom Penh, 2006.

[*Keir09*] Keirin, “Study on integrated coal mine and power generation plant in cambodia,” 2009. [Online]. Available: http://www.ecfa.or.jp/japanese/act-pf_jka/H21/JDI(cambodia)/english.pdf.

[*King04*] N. R. King, “General requirements of electric power technical standards of the kingdom of cambodia,” 2004. [Online]. Available: http://eac.gov.kh/wp-content/uploads/2014/08/General-Requirements-of-Electric-Power-Technical-Standards.en_.pdf.

[*King14*] N.-R.- King, “Preliminary Results of Cambodia Inter-censal Economic Survey,” 2014. [Online]. Available: http://www.nis.gov.kh/nis/CIES/CIES2014_Preliminary_Report_En.pdf .

[*Kosa12*] P. Kongchheng and T. Savong, “Energy Market Integration in East Asia: Theories, Electricity Sector and Subsidies,” 2012. [Online]. Available: http://www.eria.org/publications/research_project_reports/energy-market-integration-in-east-asia-theories-electricity-sector-and-subsidies.html.

[*Lvab12*] LVABC, “LV-ABC 0.6-1kV.pdf,” 2012. [Online]. Available: http://gelexcambodia.com.

[*Mme16*] MME, “Current Status of Renewable Energy in Cambodia,” 2016. [Online]. Available: http://www.irena.org/eventdocs/Cambodia presentation.pdf.

[*Nasa11*] Nasa, “Surface meteorology and Solar Energy,” *Solar Energy*, 2011. [Online]. Available: http://eosweb.larc.nasa.gov/sse/.

[*Nasa17*] Nasa, “ASDC _ Processing, archiving, and distributing Earth science data at the NASA Langley Research Center,” 2017. [Online]. Available: http://eosweb.larc.nasa.gov.

[*Nrel16*] NREL, “NREL Dynamic Maps, GIS Data, and Analysis Tools - Solar Maps,” 2016. [Online]. Available: http://www.nrel.gov/gis/.

[*Phok16*] C. Phok, “Contribution to electric energy generation for isolated-rural areas using 2nd life components and renewable energies modelling and control of an induction generator,” Université de Toulouse III, 2016.

[*Ray06*] S. Ray, *Electrical Power Systems: Concepts, Theory and Practice*. PHI Learning Pvt. Ltd., 2006.

[*Ref17*] REF, "Transferring the Benefits Resulting from the Development of Electricity to the Population in Rural Area," 2017. [Online]. Available: http://ref.gov.kh/page/products/category/42-Publications.

Chapter II

Planning of Low-Voltage Distribution System with Uncertainty on Load Demand

Chapter II

Planning of low-voltage distribution system with uncertainty on load demand

Summary

II.1 Introduction

The low-voltage (LV) distribution systems are reinforced and expanded in the recent years due to the load demand increase (i.e. population growth and living standard improvement); these points compel the electricity distributors to perform a planning following these issues. In a planning procedure of power distribution system, it is essential to design an appropriate topology in order to satisfy economic and technical aspects. The LV distribution systems are almost unbalanced radial system due to various single-phase and three-phase loads as shown in Figure II-1. To cope with these problems, a radial distribution system optimization has been developed in the literature to find a lowest investment cost by using either a path search algorithm in [*KUKS13*] or a direct approach in [*SSGS12*]. Also, the authors in [*SWLM12*] and [*MRMM05*] have been studied the problem of feeders routing respectively by using a mixed integer linear programming model or the dynamic programming; these methods allow to model finely the reality but are applied for transmission networks which are not radial as distribution network. To build a radial topology considering the environment, the researchers in [*BOMP02*] have been applied a dynamic programming method in order to obtain the topology. Likewise, the work of [*LITW96*] suggests some heuristics based on simple mathematics to allocate the substations and the feeders of a distribution networks. But both [*BOMP02*] and [*LITW96*] focus their studies on the medium voltage networks which phases are balanced. The authors of [*GOAR15*] studied the optimal planning of urban distribution network considering its topology by using adapted simulated annealing algorithm; this method aims at minimizing the upgrades of the existing network necessary for its expansion. But [*GOAR15*] considered only balanced three-phase medium-voltage systems.. Also, as the phase balancing gives many advantages in distribution systems, the authors in [*GRGL12*] have studied the loss reduction obtained thanks to an optimal phase balancing algorithm; this method has reduced the current of line and enhanced the unbalanced voltage factor. Furthermore, other methods such as the mixed-integer programming in [*ZHCZ98*] and the simulated annealing in [*ZHU99*] propose to switch the phase connection of single-loads to reduce power losses. In these research works, only the existing radial topology is considered. The challenge on LV distribution planning are still missing whilst finding an optimal topology with phase balancing faced to load demand uncertainty in unbalanced system.

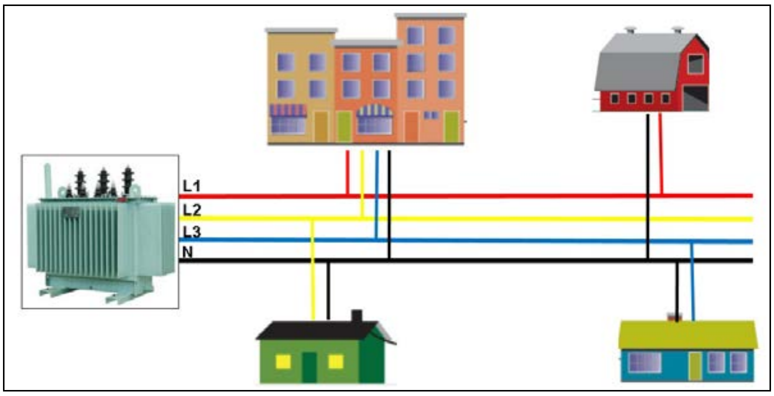

Figure II- 1 : Example of low voltage distribution system in urban areas

In this chapter, we aim at developing a long-term planning methodology to tackle the challenge of load demand uncertainty (i.e. growth rate and new load connection) in LV distribution system. We develop a novel algorithm to search for an optimal topology by finding which load connection induces the lowest costs (investment and power losses) and phase balancing improvement. In the first part, the low-voltage distribution network model is described. Then, the proposed algorithms are presented as well as the case study on which they will be applied. Finally, simulation results will be provided and analyzed.

II.2 Distribution system modeling and power flow

II.2.1 Low Voltage system modeling

II.2.1.1 Three-phase four-wire

Most of the LV distribution systems are three-phase four-wire systems, the fourth wire being the neutral except in some rural areas supplying by a single phase transformer. The four-wire system is modeled as series impedance, i.e. resistance and inductance. The shunt capacitance can be neglected in overhead line LV distribution systems since the distances of distribution systems are short [*BENO15*]. The LV system can be modeled as it follows.

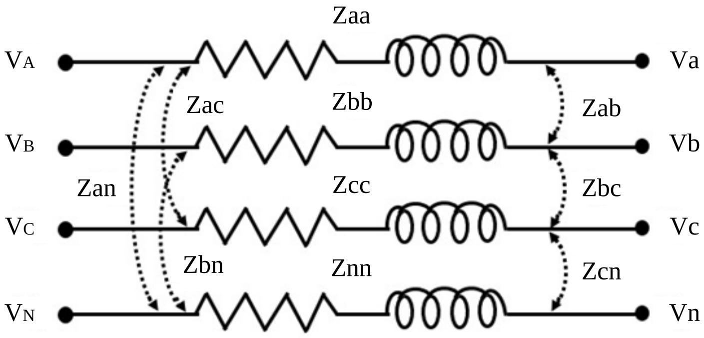

Figure II- 2 : Model of a three phase four-wire line[*TENG03*]

Figure II-2 shows a three-phase four-wire line section model between two buses. A 4x4 matrix which takes into account the self and mutual coupling effects of the unbalanced three-phase line section is expressed by:

$$[Z_{abcn}] = \begin{bmatrix} Z_{aa} & Z_{ab} & Z_{ac} & Z_{an} \\ Z_{ba} & Z_{bb} & Z_{cb} & Z_{bn} \\ Z_{ca} & Z_{cb} & Z_{cc} & Z_{cn} \\ Z_{na} & Z_{nb} & Z_{nc} & Z_{nn} \end{bmatrix} \tag{II-1}$$

If phase a does not exist in the system (i.e. single phase or two phases network), the elements of row and column of this matrix will be equal to zero as shown in Eq. II-2.

$$[Z_{bcn}] = \begin{bmatrix} 0 & 0 & 0 & 0 \\ 0 & Z_{bb} & Z_{cb} & Z_{bn} \\ 0 & Z_{cb} & Z_{cc} & Z_{cn} \\ 0 & Z_{nb} & Z_{nc} & Z_{nn} \end{bmatrix} \text{ and } [Z_{cn}] = \begin{bmatrix} 0 & 0 & 0 & 0 \\ 0 & 0 & 0 & 0 \\ 0 & 0 & Z_{cc} & Z_{cn} \\ 0 & 0 & Z_{nc} & Z_{nn} \end{bmatrix} \tag{II-2}$$

Where:

Z_{abcn} : impedance of the system in Ω / km,

Z_{ii} : self-impedance of the system, $i = a...n$ in Ω / km,

Z_{ij} : mutual-impedance of system, $i \neq j, i = a...n, j = a...n$ in Ω / km.

The impedance matrix can be computed using the method developed by Carson and Lewis [*KERS13*]. The values of self and mutual impedance of lines can be calculated from basic data such as the radius of conductor, the GMR (geometric mean radius), the distance between conductors, and the line frequency. The simplified Carson's equations [*EBBH11*] for calculating self and mutual impedance will be provided in Appendix II-A.

II.2.1.2 Neutral wire model

The current in the neutral wire is the current vector sum in the three phases. The following equations express the current in the neutral wire.

$$\forall Nodes, \quad \overline{I_{neutral}^{bus}} = \sum_{k \in phases} \overline{I_k^{bus}} \tag{II-3}$$

$$\forall Lines, \quad \overline{I_{neutral}^{line}} = \sum_{k \in phases} \overline{I_k^{line}} \tag{II-4}$$

Where:

$I_{phases,neutral}^{bus}$: phase and neutral currents injected in the bus,

$I_{phases,neutral}^{line}$: phase and neutral currents of line.

The current in the neutral wire is a huge issue in three-phase four-wire low voltage distribution systems. This current not only leads the losses, but also increases the temperature in the neutral wire [*BENO15*] and can reduce the security for labors .

II.2.1.3 Load model

The loads in distribution system are typically specified by the apparent power consumed. The voltage specified will be always the voltage at the LV terminals of the distribution substation. Iterative techniques are usually employed such as [*CIFO03*] to deal with the non-linearity of the equations to be solved. The loads on a distribution system can be modeled as [*KERS13*]:

- Constant power: $I_{bus} = \left(\frac{S}{V_{bus}}\right)^*$
- Constant impedance: $I_{bus} = \frac{V_{bus}}{Z_{bus}}$
- Constant current: I_{bus}
- Any combination of the above

However, the households usually are a mix of constant power, impedance and current loads, but are classically considered as constant power, since power is the common measurement [*BENO15*]. Therefore, the constant active and reactive power loads model is chosen in this thesis.

The specified apparent powers and voltages of loads are defined as it follows:

Phase A : $|S_a| \underline{/\theta_a} = P_a + jQ_a$ and $\underline{V_{an}} = |V_{an}| \underline{/\delta_a}$ (II-5)

Phase B : $|S_b| \underline{/\theta_b} = P_b + jQ_b$ and $\underline{V_{bn}} = |V_{bn}| \underline{/\delta_b}$ (II-6)

Phase C : $|S_c| \underline{/\theta_c} = P_c + jQ_c$ and $\underline{V_{cn}} = |V_{cn}| \underline{/\delta_c}$ (II-7)

Further, the line currents for constant active and reactive power loads are given by:

$$\underline{I_a} = \left(\frac{S_a}{V_{an}}\right)^* = \frac{|S_a|}{|V_{an}|} \underline{/\delta_a - \theta_a} \quad \text{(II-8)}$$

$$\underline{I_b} = \left(\frac{S_b}{V_{bn}}\right)^* = \frac{|S_b|}{|V_{bn}|}\underline{/\delta_b - \theta_b}$$

$$\underline{I_c} = \left(\frac{S_c}{V_{cn}}\right)^* = \frac{|S_c|}{|V_{cn}|}\underline{/\delta_c - \theta_c}$$

Where:

I_{a-b-c}: phase current injection (a, b, c),

$V_{an-bn-cn}$: phase voltage (a, b, c),

S_{a-b-c}: phase apparent power (a, b, c),

δ_{a-b-c}: phase voltage angles (a, b, c),

θ_{a-b-c}: power factor angles (a, b, c).

In this model, the terminal voltages will change during each iteration until the convergence is achieved [*KERS13*].

II.2.2 Power Flow Analysis

II.2.2.1 Classical Power Flow

The classical power flow equations are written using the admittance matrix Y and constant power loads:

$$\forall i \in Nodes, \quad \underline{S_i} = P_i + jQ_i = \underline{V_i} \times \underline{I_i^*} = \underline{V_i} \times \sum_{j \in bus} \underline{Y_{ij}^*} \times \underline{V_j^*} \tag{II-9}$$

After separation of real and imaginary parts ($S = P + jQ$ and $Y = G + jB$), and V expressed in its polar form ($V = |V| \cdot e^{j \cdot \delta}$), the active and reactive powers are defined as follows.

$$P_i = \sum_{j \in bus} |\underline{V_i}| \cdot |\underline{V_j}| \cdot (G_{ij} \cdot cos(\delta_i - \delta_j) + B_{ij} \cdot sin(\delta_i - \delta_j)) \tag{II-10}$$

$$Q_i = \sum_{j \in bus} |\underline{V_i}| \cdot |\underline{V_j}| \cdot (G_{ij} \cdot sin(\delta_i - \delta_j) - B_{ij} \cdot cos(\delta_i - \delta_j)) \tag{II-11}$$

Where

P_i: net active power injection to the i^{th} bus,

Q_i: net reactive power injection to the i^{th} bus,

V_i: voltage magnitude of i^{th} bus,

$\delta_{ij} = \delta_i - \delta_j$: voltage angle between the bus i and j,

G_{ij} : conductance between the bus i and j,

B_{ij} : susceptance between the bus i and j.

II.2.2.2 Selected Power Flow

Instead of the usual admittance matrix $\underline{Y}$, the matrix of lines impedance $\underline{Z_{system}}$ is used, in which each line has the impedance defined in Eq. II-1 and Eq. II-2. The backward/forward sweep load flow[*CIFO03*] will be used for unbalanced power flow analysis for this work. The current line and voltage drop are expressed by:

$$\underline{J_l} = -\underline{I_{lr}} + \sum \underline{J_{lr}} \quad \text{(II-12)}$$

$$\underline{\Delta V} = \underline{V_{ls}} - \underline{V_{lr}} = \underline{Z_l} \times \underline{J_l} \quad \text{(II-13)}$$

Where

J_l : current flow in branch l

I_{lr} : current injection of node lr

$\sum J_{lr}$: currents in branches downstream node lr

ΔV : voltage drop of branch l

V_{ls} : sending end voltage of branch l

V_{lr} : receiving end voltage of branch l

Z_l : series impedance of branch l

Furthermore, more details of four-wire unbalanced load flow are further provided in Appendix II-B.

II.2.2.3 Voltage Unbalance Factor (VUF)

In a perfectly balanced system, the currents in the three phases are equal and shifted by $2\pi/3$. Therefore, these currents combine in the neutral wire, whose current is equal to zero. However, when the system is unbalanced, they do not cancel themselves, and a neutral current appeared.

The unbalance is defined at every bus by the magnitude of the ratio of the negative sequence voltage $\underline{V_{neg}}$ by the positive sequence voltage $\underline{V_{pos}}$ [*PIMA01*]:

$$\text{Unbalance}(i \in Nodes) = \left| \frac{\underline{V}_{i,neg}}{\underline{V}_{i,pos}} \right| = \left| \frac{\underline{V}_{i,a} + a^2 \underline{V}_{i,b} + a \underline{V}_{i,c}}{\underline{V}_{i,a} + a \underline{V}_{i,b} + a^2 \underline{V}_{i,c}} \right|, \text{ with } a = e^{j\frac{2\pi}{3}} \qquad \text{(II-14)}$$

Where

$V_{i,neg,pos}$: negative and positive sequences of voltages of the i^{th} bus

$V_{i,a-b-c}$: voltage magnitude of phase $a-b-c$ of the i^{th} bus

II.3 Uncertainty on load demand

The loads growth rate and the apparition of new loads are increasing with unpredictability year by year in the LV distribution network. In this chapter, we thus propose to study the three cases of uncertainty defined as it follows.

II.3.1 Case 1: Evolution of the growth rate of the existing loads

This case considers uncertainty on the growth rate of the existing loads only. In this chapter, its value is assumed to be between 2% and 4%[1] per year since there is currently no relevant information available on this growth rate. As depicted in Figure II-3, the difference of colors of households highlights that the demands of each household are increased during the planning study with a different growth rate.

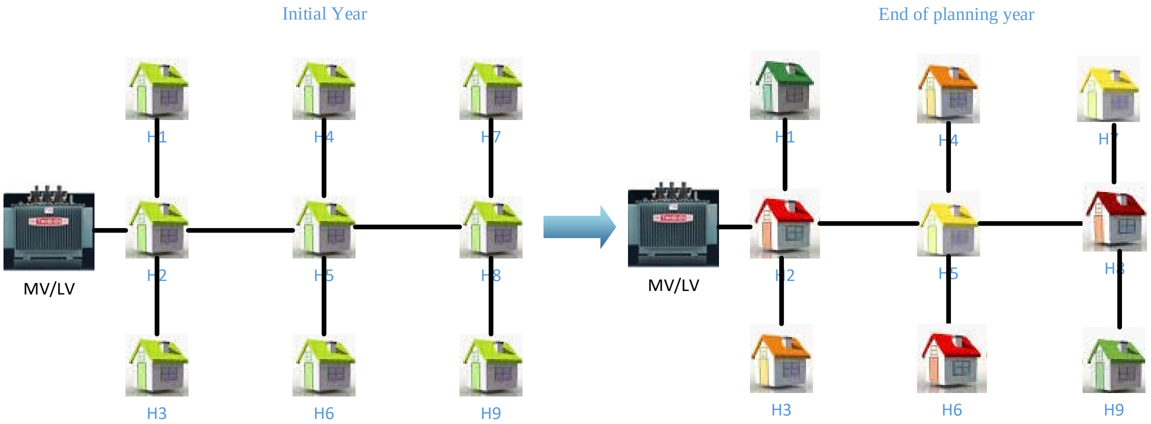

Figure II- 3 : Uncertainty on load demand of case study 1

II.3.2 Case 2: Only new connected loads

The demand of existing loads is assumed to be constant and new loads appear in the network with uncertainties on their locations and powers. The new households will be connected to the LV distribution system by fixing randomly the location (x, y) and peak

[1] This assumption is made for testing the algorithms. The sensitivity of this parameter will have to be made in further studies.

demand during the planning period study. Figure II-4 shows the demonstration of case 2. In this example, at the end of the planning period, there are three new households (H10-H11-H12) connected to the LV grid.

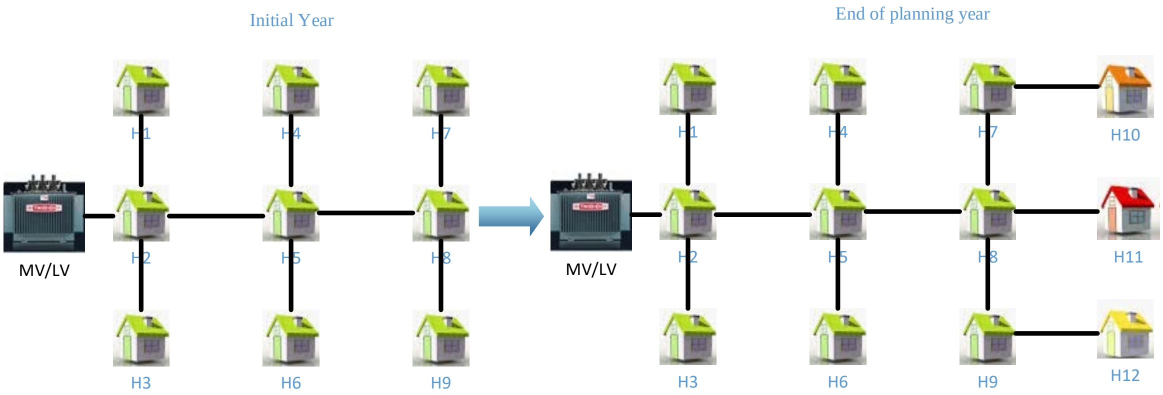

Figure II- 4 : Uncertainty on load demand of case study 2

II.3.3 Case 3: Evolution of the growth rate of existing loads and connection of new loads

For the last case, it is taken into account the uncertainty on both the growth rate of existing loads and the apparition of new connected loads; it means a combination of case 1 and case 2. As shown in Figure II-5, there are three households (H10-H11-H12) that will be connected to LV grid and the demands of all existing households are also increased during the planning study.

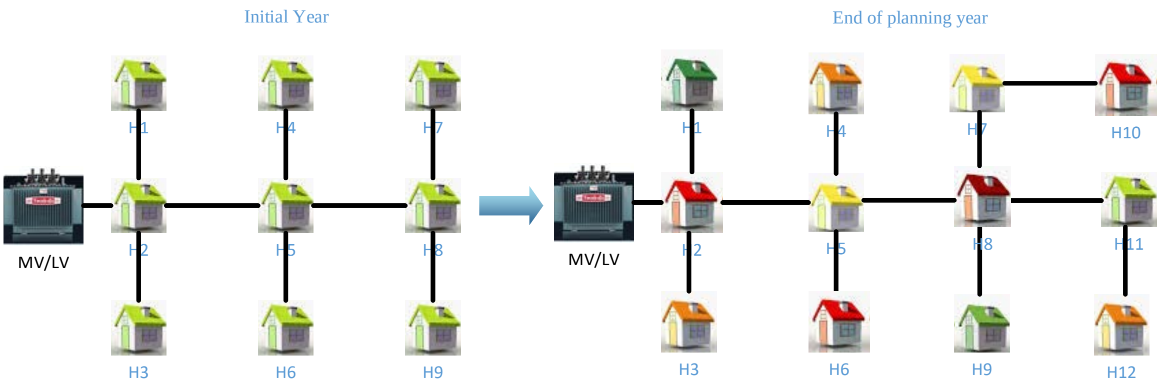

Figure II- 5 : Uncertainty on load demand of case study 3

II.4 Proposed method

II.4.1 Type of areas

Urban areas are characterized by a high load density. Then finding the optimal radial architecture (number of feeders and optimal paths) is not directly visible and optimization algorithms are required. In this section, two strategies for finding the optimal topology of LV urban networks are explained. Rural areas are characterized by a low load density and the main line path can be usually drawn by hand. In urban area, there are two different cases. If the MV/LV transformer is single phase, then the main line follows the road and the customers are connected to the closest pole. In case of a three phase transformer, an optimization algorithm is required to find which loads will be allocated to which phase so as to balance the network. In this case a First Fit Bin Packing algorithm (FFBP) also used in strategy 1 for urban network is applied. In that purpose, in this chapter, the planning tool only for the urban network will be detailed.

II.4.2 Detailed description of the methodology for planning the urban network

As presented in the context and the literature review of planning issues in LV distribution systems (see II.1), the objective of this part aims at developing a method to cope with designing the optimal topology under uncertainty on load demand. The objective is to minimize the length of the radial topology to deliver electricity to all the end users while ensuring phase balancing and considering technical and economic criteria in the low voltage distribution system. Figure II-6 shows a flowchart of the proposed method to automatically optimize the radial topology in low-voltage distribution system. The different steps of this Monte Carlo [*HACR10*] based algorithm are:

1) The input data are the location and peak demands of the loads and the MV/LV substation corresponding to a non-electrified area and the planning period. In addition, prevision, of new loads and the minimal, maximal and average load growth of the studied area are assumed.

2) The optimal architecture at the initial year is built as a starting solution. First, all the possible lines locations are created using the Delaunay triangulation algorithm [*FAPI93*] in order to minimize the length of lines and reduce the search space. Then mixed integer quadratically constrained programming-MIQCP [*CHSA12*] in ILOG-CPLEX [*IBM16*] (Eq. II-15) enables to find the optimal radial topology at the initial year (Strategy 1) and at the end of the planning year with the average load growth (Strategy 2) which minimizes the total length of the network while ensuring the phase balancing.

3) The three case studies of uncertainties previously defined are computed (i.e. uncertainty on growth rate and new connected loads). 1000 Monte Carlo (N_{MCS}) simulations are done in which the variables are the peak load growth of the existing loads every year, the locations of new loads, their peak power and the year of apparition. Many guides have focused on the simple random sampling, but only one common rule was found

from the literature [MATA08] saying that the larger the sample size is, the more information we get. The sample size required may depend on the distribution, number of variables or something else. The only way to see if the number of samples is enough is to make more simulations and see if the result stays similar. In our case, it seems that 1000 random samplings is enough for convergence.

4) The two strategies are compared for the three cases studied. The first one (Strategy 1) consists in making the network evolve year by year without anticipating in the long term. If new loads appear, they are connected to the architecture using a two stages algorithm (shortest path [*CORA14*] and first-fit bin packing [*RARA07*] algorithms). The second strategy (Strategy 2) consists in imagining the target network at the end of the planning period and directly building it as explained in 2). This optimal architecture is kept without any change all over the planning period. Reinforcements can occur if constraints appear.

5) An unbalanced load flow enables to evaluate current and voltage constraints and to reinforce the network.

6) The total actualized cost during the planning study with uncertainty on load growth rate and new connected loads is evaluated for each Monte Carlo simulation.

7) The optimal topology will be selected according to the lowest total actualized cost of each low-voltage system design.

Furthermore, more information on each step will be provided in the following sections.

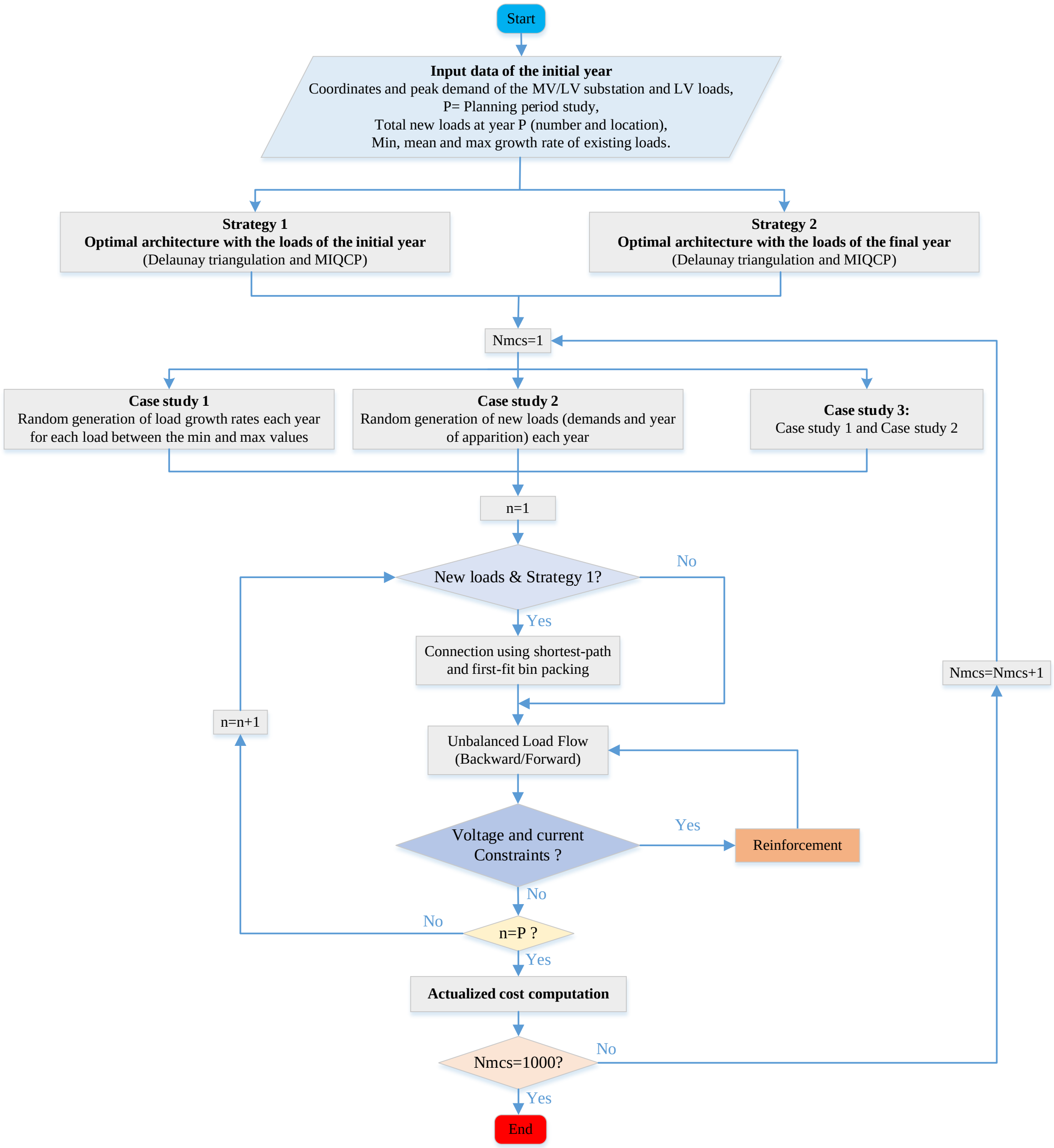

Figure II- 6 : Flowchart of proposed method

II.4.3 Mixed Integer Quadratically Constrained Programming-MIQCP[*VGBA17*]

A graph [*WEST05*] can be used to characterize an electrical grid which is defined as a pair of sets $G \equiv G(V,E)$, where $V = \{1.2...N\}$ is a set of N vertices of the graph representing the LV loads and $E \subseteq V \times V = \{e_{ij}\}(i,j) \in V\}$, $\{e_{ij}\}$ is a set of edges between vertices i and j representing the lines of the network. Figure II-7 illustrates the topological graph which represents the distribution system.

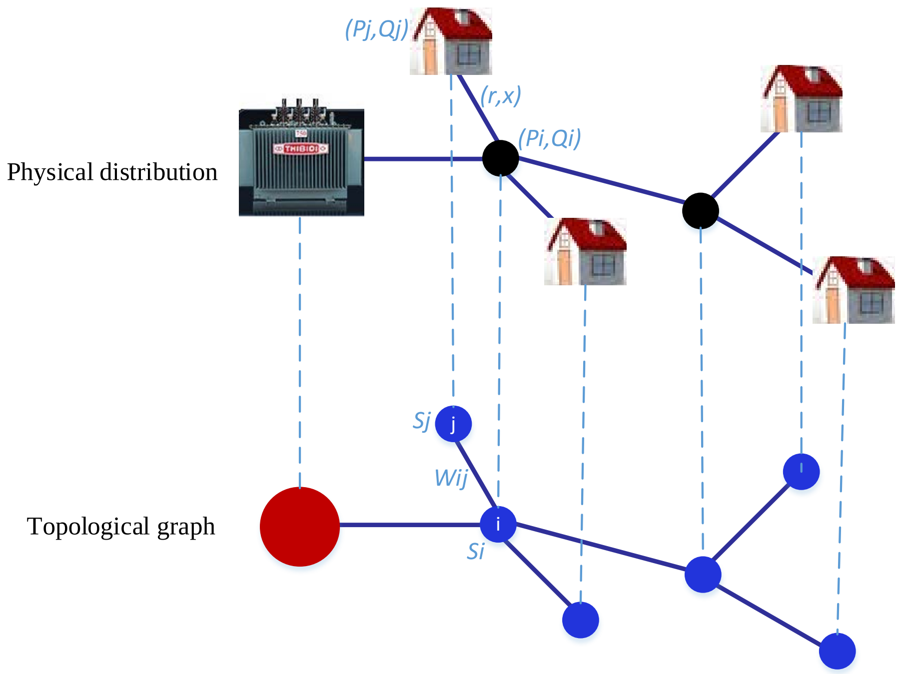

Figure II- 7 : Example of a graph representation of a distribution system

The optimization problem of minimizing the conductor length is modelled as a MIQCP and given by:

$$\text{Minimize:} \quad \sum_{(i,j)\in E} d_{ij} \cdot (x_{ij} + x^{A}_{ph\_ij} + x^{B}_{ph\_ij} + x^{C}_{ph\_ij}) \tag{II-15}$$

Where:

$x_{ij}, x^{A}_{ph\_ij}, x^{B}_{ph\_ij}, x^{C}_{ph\_ij} \in \{0,1\}$: state of connection between two buses i and j

A, B, C : phases of system

(0: bus i and bus j are not linked and 1: bus i and bus j are linked)

$d_{ij} \in \{\Re^{+}\}, \forall (i,j) \in E$: distance between two buses

Subject to the following constraints:

- Arborescence

$$\begin{aligned}
&\sum_{(i,j)\in\delta^{in}(j)} x_{ij} = 1, \forall j \in V \setminus S, S \text{ is source} \\
&\delta^{in}(j) : \text{set of incomming edge for } j^{th} \text{ vertex} \\
&x_{ij} + x_{ji} \le 1, \forall (i,j) \in E \\
&x^{A}_{ph_ij} \le x_{ji}, \forall (i,j) \in E \\
&x^{B}_{ph_ij} \le x_{ji}, \forall (i,j) \in E \\
&x^{C}_{ph_ij} \le x_{ji}, \forall (i,j) \in E
\end{aligned} \tag{II-16}$$

- Load balancing

$eps \in \{\Re^+\}$, maximal power difference between two phases
p_i: active power of loads i
$load\_ph_i^\alpha \in \{0,1\}$: phase connection of loads i , $\alpha = A, B$ or C

$$\left(\sum_{i=1}^{n} p_i load\_ph_i^A - \sum_{i=1}^{n} p_i load\_ph_i^B\right)^2 \le eps^2$$
$$\left(\sum_{i=1}^{n} p_i load\_ph_i^A - \sum_{i=1}^{n} p_i load\_ph_i^C\right)^2 \le eps^2 \qquad \text{(II-17)}$$
$$\left(\sum_{i=1}^{n} p_i load\_ph_i^B - \sum_{i=1}^{n} p_i load\_ph_i^C\right)^2 \le eps^2$$

- Thermal capacity limit of lines

$\forall (i, j) \in E$:
$P_{ij}, p_{ij}^{\max}$: active power flow and maximal active power flow on line ij
$Q_{ij}, q_{ij}^{\max}$: reactive power flow and maximal reactive power flow on line ij (II-18)

$$P_{ij}^A \le p_{ij}^{\max} x_{ph\_ij}^A, P_{ij}^B \le p_{ij}^{\max} x_{ph\_ij}^B, P_{ij}^C \le p_{ij}^{\max} x_{ph\_ij}^C$$
$$Q_{ij}^A \le q_{ij}^{\max} x_{ph\_ij}^A, Q_{ij}^B \le q_{ij}^{\max} x_{ph\_ij}^B, Q_{ij}^C \le q_{ij}^{\max} x_{ph\_ij}^C$$

- Load phase allocation

$\forall i \in V \setminus S, S$ is source
$load\_ph_i^\alpha \in \{0,1\}$: phase connection of loads i , $\alpha = A, B$ or C

$$load\_ph_i^A + load\_ph_i^B + load\_ph_i^C = \begin{cases} 1, \text{if 1 phase} \\ 3, \text{if 3 phase} \end{cases} \qquad \text{(II-19)}$$

- Power flow without loss

$\forall i \in V \setminus S, S$ is source
p_i: active power of loads i
q_i: reactive power of loads i
$load\_ph_i^\alpha \in \{0,1\}$: phase connection of loads i , $\alpha = A, B$ or C

$$\sum_{(j,i)\in E} P_{ji}^\alpha - \sum_{(i,j)\in E} P_{ij}^\alpha = \begin{cases} p_i load\_ph_i^\alpha, \text{if i connect to 1 phase} \\ \dfrac{p_i load\_ph_i^\alpha}{3}, \text{if i connect to 3 phases} \end{cases} \qquad \text{(II-20)}$$
$$\sum_{(j,i)\in E} Q_{ji}^\alpha - \sum_{(i,j)\in E} Q_{ij}^\alpha = \begin{cases} q_i load\_ph_i^\alpha, \text{if i connect to 1 phase} \\ \dfrac{q_i load\_ph_i^\alpha}{3}, \text{if i connect to 3 phases} \end{cases}$$

This modelled is used for finding the optimal network at the initial stage and for strategy 2.

II.4.4 Shortest Path and First Fit Bin Packing (SP-FFBP)

In case 2 and 3, new loads appear in the network from the year 1 to the end of the planning period and have to be connected to the LV grid with the objective of minimizing the conductor usage and optimizing the phase balancing. In that purpose, the shortest path (SP) and first-fit bin-packing (FFBP) algorithms will be applied. In graph theory, the SP problem consists in finding a path between two vertices (or nodes) in a graph such that the sum of the weights (here the length of lines) of its edges is minimized. The FFBP problem consists in packing all items into defined number of bins, while minimizing the difference of total weight of each bin. In this work, the items are the load demands (P, Q) and the bins are the phases (A-B-C) of the power system, respectively. Figure II-8 shows the pseudocode algorithm and concept of the SP-FFBP algorithms applied to this work. Firstly, the SP algorithm is run to find the closest node to connect the new load and then the first-fit bin packing is used to balance the phases of those new connected loads.

P: planning period study
B: bus of existing loads
M: bus of new and existing loads
L: closest existing loads from the new loads
d: distance between two buses
for $i = 1:P$
  for $j = M - B : M$
    for $k = 1 : B$
      $d^i = d^i_{jk}$
      $d_j = \min(d^i)$
      $p = find(d^i = d_j)$
      $L_i = [p \quad j]$
    end
  end
end

P: planning period study
P_n^α: load demand at year n, α = A, B or C
y_n^α: phase connection at year n, α = A, B or C
for $i = 1:P$
  if load is one phase
  if $(sum(P_{n-1}^A) < sum(P_{n-1}^B)$ & $sum(P_{n-1}^A) < sum(P_{n-1}^C))$
    $[y_n^A, y_n^B, y_n^C] = [1, 0, 0]$
  elseif $(sum(P_{n-1}^B) < sum(P_{n-1}^A)$ & $sum(P_{n-1}^B) < sum(P_{n-1}^C))$
    $[y_n^A, y_n^B, y_n^C] = [0, 1, 0]$
  elseif $(sum(P_{n-1}^C) < sum(P_{n-1}^A)$ & $sum(P_{n-1}^C) < sum(P_{n-1}^B))$
    $[y_n^A, y_n^B, y_n^C] = [0, 0, 1]$
  else
    ph = [1,0,0]
    idx = randperm (numel(ph))
    $[y_n^A, y_n^B, y_n^C] =$ ph(idx)
  end
  end
  if load is three phase
    $[y_n^A, y_n^B, y_n^C] = [1,1,1]$
  end
end

Figure II- 8 : Pseudocode algorithm of the SP (left) and the FFBP (right) algorithms

II.4.5 Actualized cost

The actualized cost of the networks over *P* years for different topologies and planning strategies will be computed. This calculation takes into account the capital expenditure (CAPEX) and the operation expenditure (OPEX) due to power losses. The actualized cost [*APCR11*] thus can be expressed by:

$$C_{total\_act} = \sum_{t=0}^{P} \frac{C_{invest}(t) + C \times Ploss(t)}{(1+i)^t} \qquad \text{(II-21)}$$

Where:

- C_{total_act}: total actualized cost in $kUSD$
- $C_{invest}(t)$: investment cost in the year t in $kUSD$
- C: cost of 1 kW peak losses in $kUSD/kW$
- $Ploss(t)$: power losses at the year t in $kUSD$
- i: actualization rate in $\%$

II.4.6 Monte-Carlo simulation

To cope with the problem of uncertainty on load demand during the planning study, the Monte-Carlo (MC) simulation will be employed to compute the probability distribution of the overall actualized cost (see II.4.3) by taking into account these uncertainties. The random parameters are the peak load growth rate which is randomly chosen using a uniform law between two extreme values and that location of new loads which is also uniformly randomly chosen. The MC results of the total actualized cost for both strategies with different topologies (see II.6.4.2) will enable to select the best solution.

II.4.7 Load connection phase and reinforcement

Two load categories are taken into account in this work: single phase load (A, B, C) and three phase load (ABC). The loads higher than 10 kW [*VGBA17*] are classified as three-phase loads and single phase loads otherwise. The reinforcements of cables type-LV-ABC (Aerial bundled cable) from 50-70-95-150-240 mm^2[*VGBA17*] to avoid the current constraints have been considered in this chapter.

II.5 Strategy of planning

As presented in section II.3, in case of load demand uncertainty, we thus proposed to study two strategies of planning: reinforcing year by year waiting the constraints appear or reinforcing at the initial stage intending to minimize power losses.

II.5.1 Strategy 1: Upgrades year by year

This strategy consists in designing the topology with the initial load demand and all loads will be increased every year over the planning study. The topology will be found by applying a MIQCP algorithm for the initial year. The SP and FFBP algorithms are used from year 1 to the end of the planning study for case 2 and case 3 when new loads have to be connected. Figure II-9 illustrates the principle of this strategy. It can be seen that the loads have been increased from the initial year (light green color) to year 1 (dark green color and other); at that time, it can be noticed that the current constraint has appeared (over the admissible capacity of the cables) for lines (MV/LV-H2 and H2-H5), but not for voltage due to the case of urban area. To avoid these current constraints, the lines have been reinforced (red color of line), e.g. 50 mm2 to 70 mm2. Additionally, this process is applied until the end of the planning study (year P) as shown in the figure.

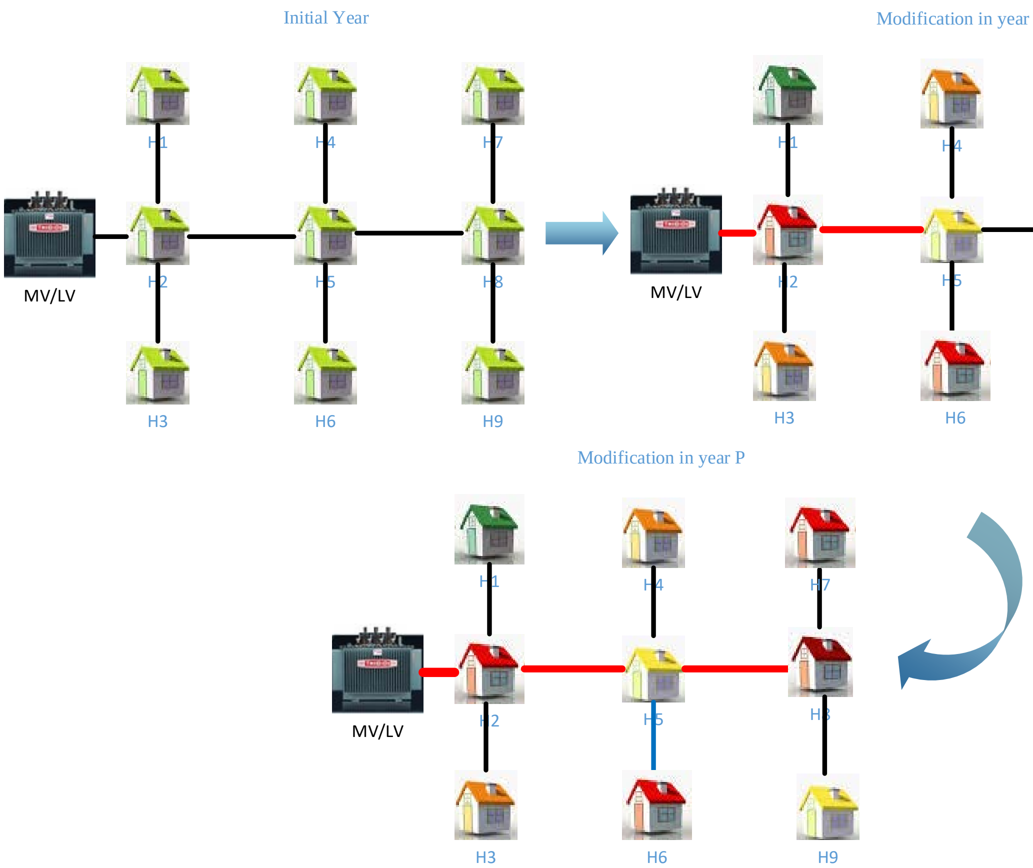

Figure II- 9 : Strategy 1-upgrades year by year

II.5.2 Strategy 2: Upgrades at initial year

For this strategy, the loads have been predicted for the end of the planning horizon. All the existing lines are removed and the topology is rebuilt with these predicted loads by using MIQCP algorithm and a default section of 240 mm². Then the conductor sections are chosen to respect the electrical voltage and current profile at the end of the planning horizon. Figure II-10 illustrates an example of new topology considering the loads consumption of the end of the planning horizon. The current flows in each section are computed for the whole system and the cables are reinforced (red color of lines) completely in initial year to avoid the constraint.

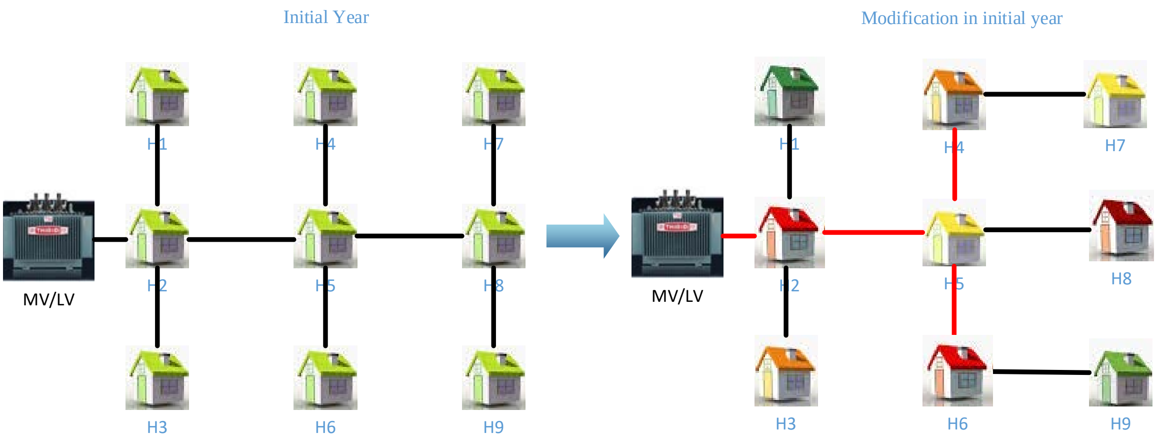

Figure II- 10 : Strategy 2-upgrades at initial year

II.6 Test system and simulation

II.6.1 Topology and peak demand

This case study is designed for an urban area; there is thus a high density of energy consumption. The low-voltage of the test system is delivered from the 22-kV/0.4-kV Transformer at bus 1 to 32 buses of loads as shown in Figure II-11. This LV test system is developed randomly in order to validate the proposed method.

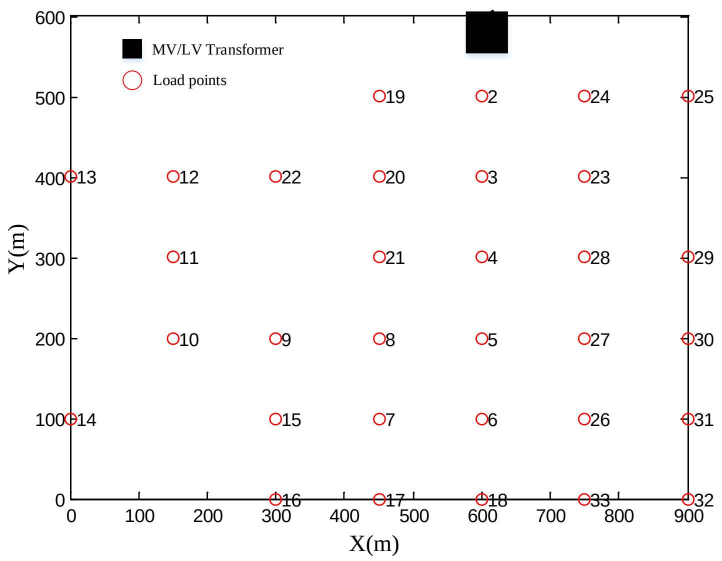

Figure II- 11 : LV Test system representing an urban area

The total active and reactive power is respectively 147 kW and 48.32 kvar (power factor of 0.95) randomly generated for the initial planning year. The details of peak demand for the LV customers and their locations are given in Table II-1. We assumed that fifteen loads will be connected to the LV grid by fixing randomly the location (x, y) and the peak demand (P, Q) as provided in Table II-2. In addition, these new connected loads will randomly appear from year 1 to the end of the planning study.

Table II- 1 : Existing load specification at the initial year

No. Bus	**Peak active and reactive power**		**No. Bus**	**Peak active and reactive power**		**No. Bus**	**Peak active and reactive power**	
	P(kW)	**Q(kvar)**		**P(kW)**	**Q(kvar)**		**P(kW)**	**Q(kvar)**
1	0	0	12	3	0.99	23	3	0.99
2	4	1.31	13	3	0.99	24	6	1.97
3	10	3.29	14	6	1.97	25	4	1.31
4	6	1.97	15	3	0.99	26	3	0.99
5	3	0.99	16	3	0.99	27	3	0.99
6	3	0.99	17	3	0.99	28	3	0.99
7	6	1.97	18	4	1.31	29	4	1.31
8	6	1.97	19	4	1.31	30	6	1.97
9	3	0.99	20	6	1.97	31	10	3.29
10	10	3.29	21	6	1.97	32	4	1.31
11	3	0.99	22	3	0.99	33	3	0.99

Table II- 2 : New connected loads

Coordinates		**Peak real and reactive power**		**Coordinates**		**Peak real and reactive power**	
X	**Y**	**P(kW)**	**Q(kvar)**	**X**	**Y**	**P(kW)**	**Q(kvar)**
480	390	4	1.31	510	360	2	0.66
510	390	3	0.99	540	360	3	0.99
540	390	4	1.31	570	360	4	1.31
570	390	10	3.29	600	360	6	1.97
600	390	4	1.31	630	360	10	3.29
630	390	4	1.31	660	330	3	0.99
660	390	10	3.29	600	330	4	1.31
480	360	3	0.99				

II.6.2 Economic parameters

The actualized cost is computed to make an investment decision. The total time study for the analysis is set to 15 years and the actualization rate is 12 % [*VGBA17*]. The list of the parameters for the economic analysis is shown in Table II-3.

Table II- 3 : Parameters of the economic analysis [*VGBA17*]

Parameters	**Value**
Planning period study	15 years
Discount rate	12 %
Annual peak power losses cost	1.58 kUSD/kW
50 mm² cable cost	0.8 kUSD/km
70 mm² cable cost	1 kUSD/km
95 mm² cable cost	1.5 kUSD/km
150 mm² cable cost	2 kUSD/km
240 mm² cable cost	2.5 kUSD/km

II.6.3 Electrical parameters of cable

In this work, the cable type LV-ABC is used for simulation. The cable topology of LV-ABC-4Cores is shown in Figure II-12. The impedances 4x4 matrix of cable (Ω / km, 50Hz) are provided in Appendix II-C.

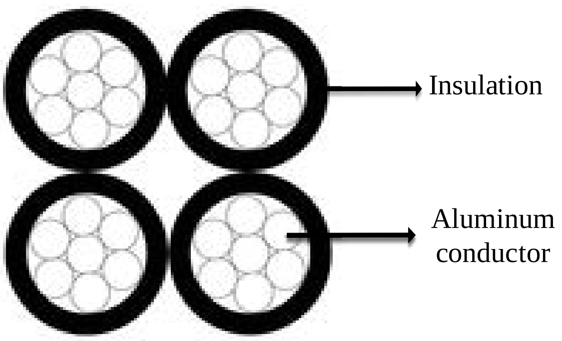

Figure II- 12 : LV-ABC-4Cores Cable

II.6.4 Simulation result and discussion

All simulation and graphical results have been obtained by using ILOG-CPLEX and MATLAB software.

II.6.4.1 Available paths

The MIQCP algorithm needs all the available paths to be defined as constraints. Figure II-13 shows the available paths of this distribution system found using Delaunay Triangulation algorithm.

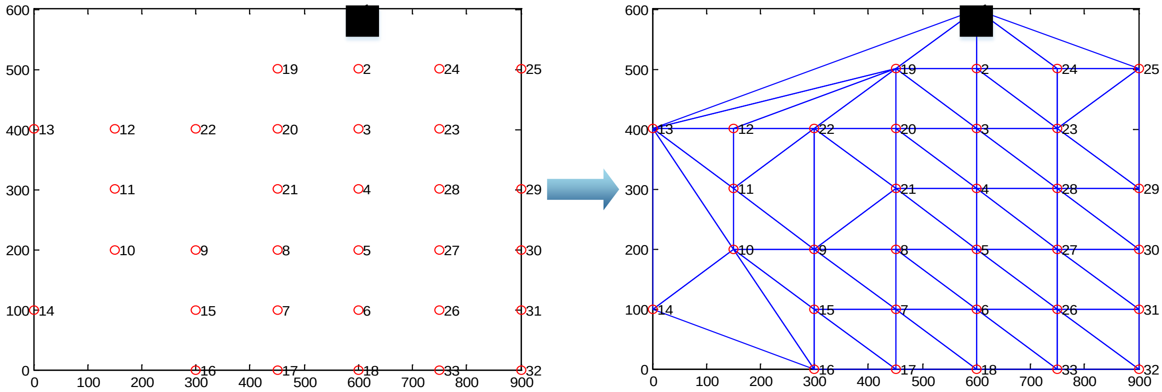

Figure II- 13 : Available paths of the distribution system with Delaunay Triangulation

II.6.4.2 Optimal radial topology

The optimal radial topologies obtained with strategy 1 (using the SP and the FFBP algorithms) and strategy 2 (MIQCP algorithm) are illustrated with Figure II-14 to Figure II-16 representing case 1 to 3 for the 1st iteration of the Monte Carlo simulation.

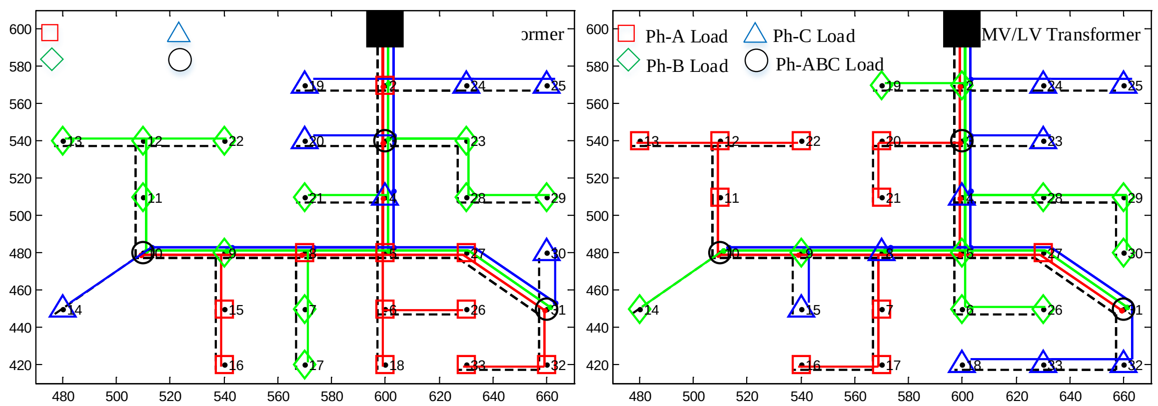

Figure II- 14 : Optimal topology of case 1: 1st strategy (left) and 2nd strategy (right)

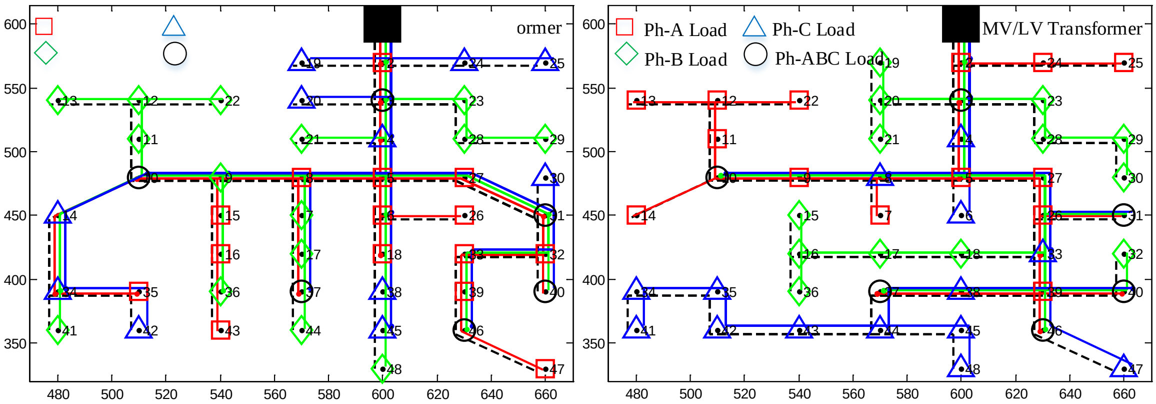

Figure II- 15 : Optimal topology (N1-MC) of case 2: 1st strategy (left) and 2nd strategy (right)

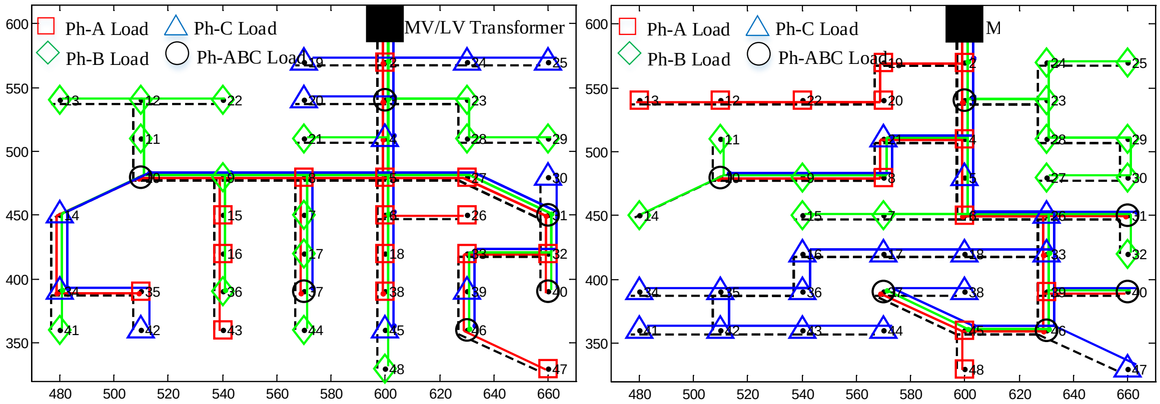

Figure II- 16 : Optimal topology (N1-MC) of case 3: 1st strategy (left) and 2nd strategy (right)

II.6.4.3 Actualized cost

In this part, the total actualized costs for the two different strategies of each case have been computed. Figure II-17 to Figure II-19 show the averaged actualized costs for the three case studies and the two strategies. Table II-4 lists the summary results of the average actualized costs of each case study.

Table II- 4 : Average actualized cost of each case

Strategy	**Case study**		
	Case study 1	Case study 2	Case study 3
1st strategy (S1)	146 kUSD	150 kUSD	183 kUSD
2nd strategy (S2)	93 kUSD	170 kUSD	195 kUSD
Difference between S2 and S1	+36.30 %	-13.33 %	-6.55 %
Chosen strategy	*S2*	*S1*	*S1*

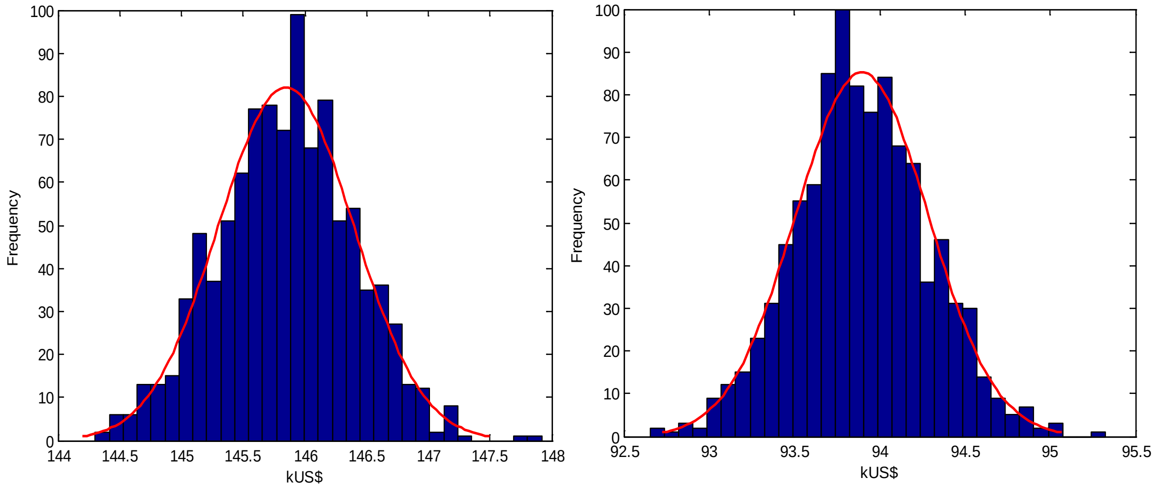

Figure II- 17 : Histogram of total actualized of case study 1-1st strategy (left) and 2nd strategy (right)

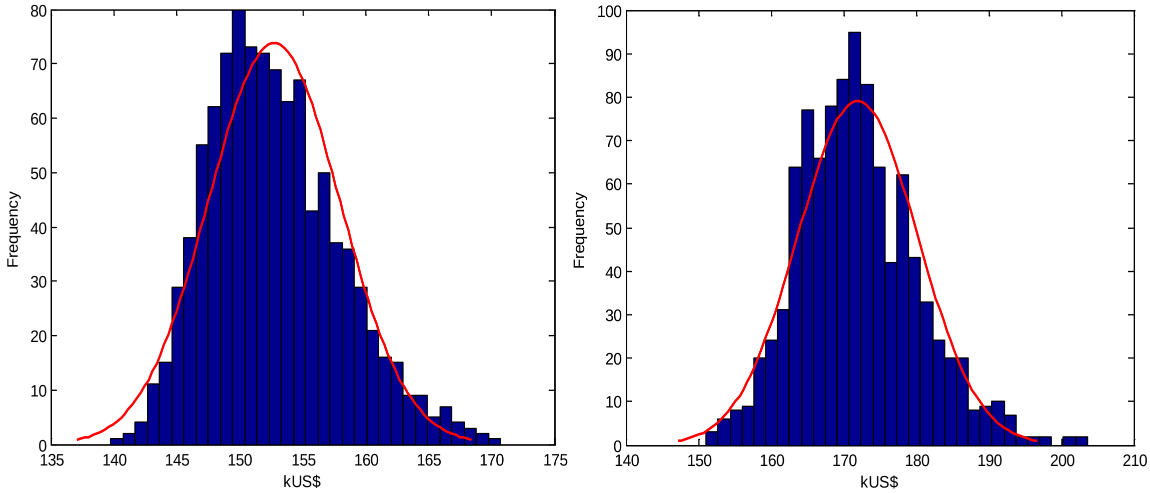

Figure II- 18 :Histogram of total actualized of case study 2-1st strategy (left) and 2nd strategy (right)

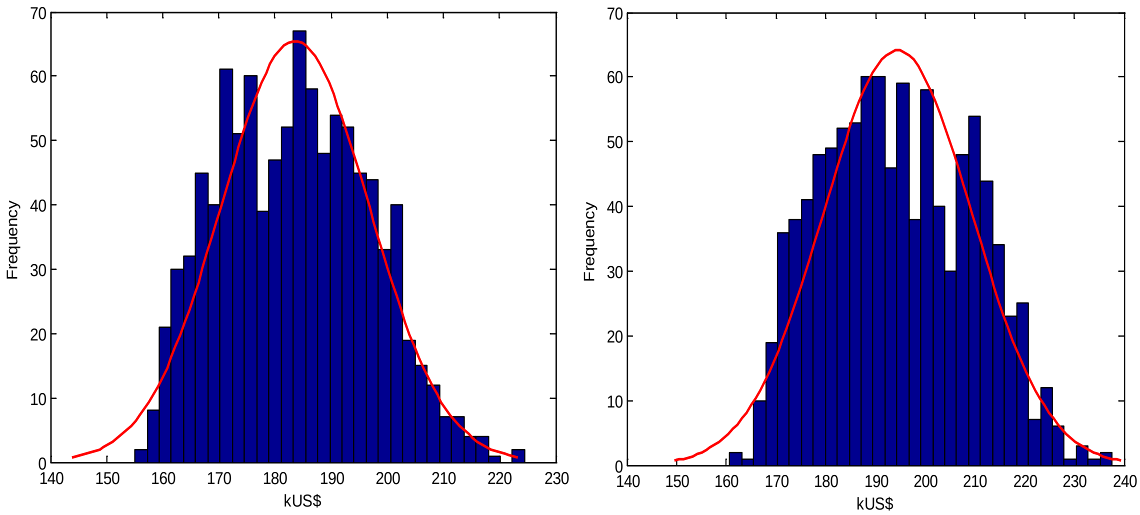

Figure II- 19 : Histogram of total actualized of case study 3-1st strategy (left) 2nd strategy (right)

According to these results, we can conclude that the 2nd strategy (S2) is selected for the case study 1 (about 36% less expensive) and the 1st strategy (S1) for the case studies 2 and 3 (between 7 and 14% less expensive).

Figure II-20 shows the CAPEX and OPEX for each year of both strategies 1 and 2 for case 1. In this case, only the existing loads are evolving and no new loads appear during all the planning period. In that case, building directly the optimal structure in the initial year is more economic for two reasons. First, the objective of this strategy is to minimize the total length of conductors while respecting a set of constraints. In the 2nd strategy, the total length of the final architecture is 2.53 km while the total length of the conductor to reinforce is 3.25 km for the 1st strategy. As the cost of conductor is proportional to its length, the CAPEX in the 2nd strategy is lower. In addition, the power losses are reduced over all the planning studies because the size of the conductor is bigger in the 2nd strategy. Then the OPEX is also lower in the 2nd strategy.

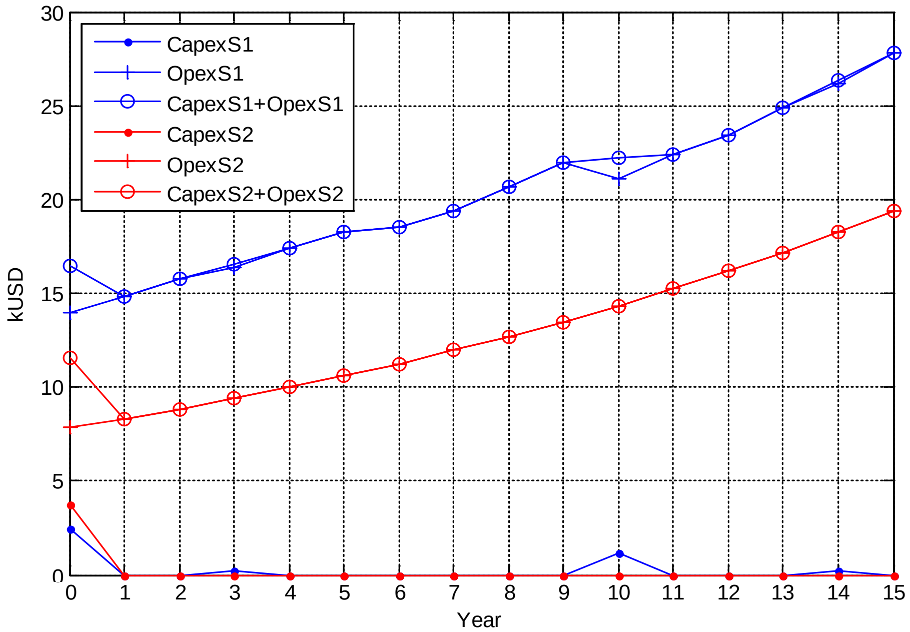

Figure II- 20 : Evolution of the OPEX, CAPEX and their sum for case study 1

For case studies 2 and 3, new loads will appear during the planning period. Figure II-21 and Figure II-22 show the evolution of the OPEX, CAPEX and their sum over the planning period of strategy 1 and 2 for case study 2 and case study 3 for one given Monte Carlo iteration. It can be seen that the global cost of strategy 2 is lower than strategy 1 from year 1 to year 9 (resp. year 6) for case study 2 (resp. case study 3) and higher after year 9 (resp. 6). The network found by strategy 2 has more single phase lines because it aims at minimizing the total conductor length. Then, when the number of new loads reaches a certain level, the power losses of strategy 2 becomes higher than strategy 1. It can be concluded that in case of new load appearing over the planning study, the 1st strategy will be more economic because the uncertainties on new loads have a big impact on the topology.

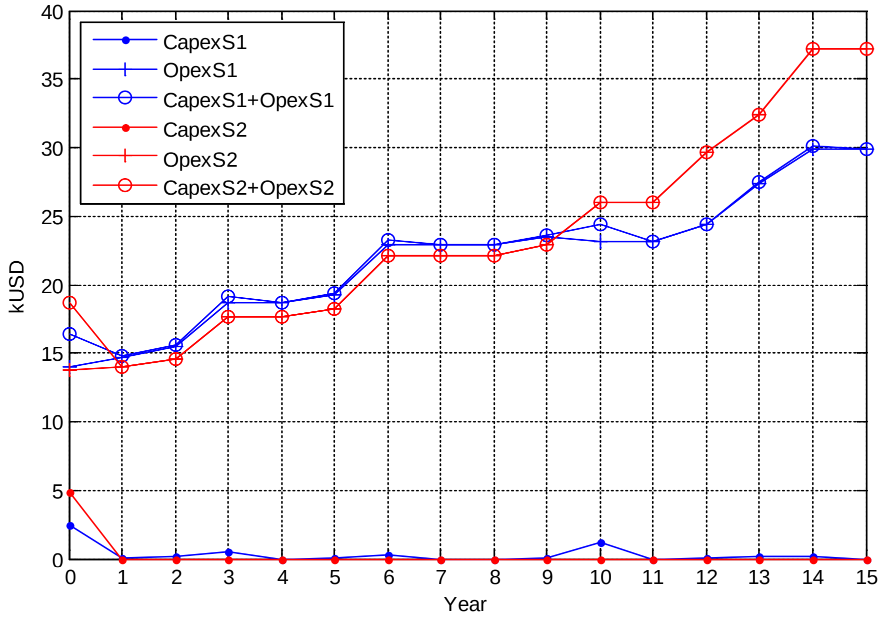

Figure II- 21 : Evolution of the OPEX, CAPEX and their sum for case study 2

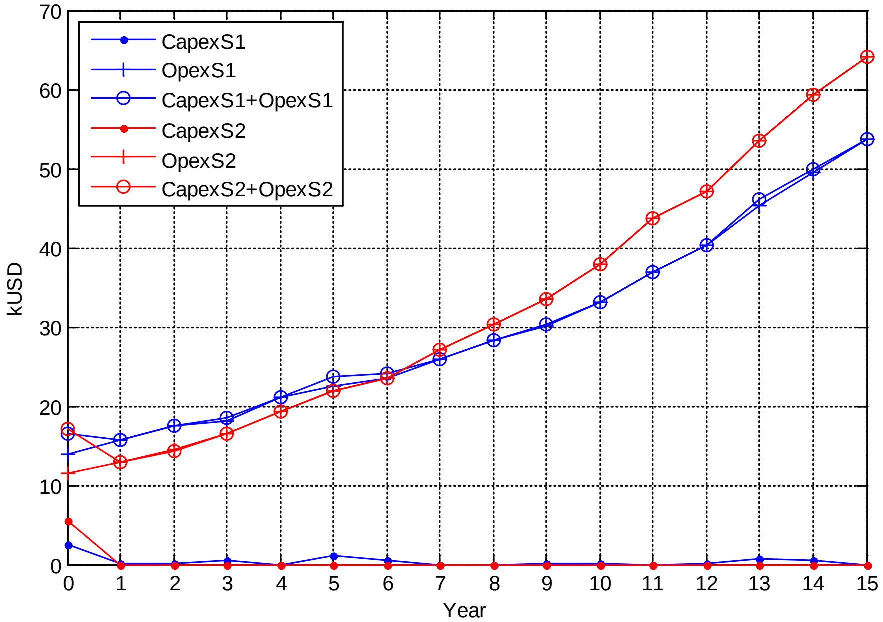

Figure II- 22 : Evolution of the OPEX, CAPEX and their sum for case study 3

Therefore, the conclusion of this chapter is that the 2nd strategy will be chosen for areas having a very low probability to have new customers (for example very dense neighborhood), otherwise the 1st strategy will be applied for areas in development (new districts or new shops). Nevertheless, it is necessary to run theses simulations on other data before generalizing the results.

II.7 Conclusion

This chapter proposed methodologies and tool to plan the LV distribution network considering uncertainties on the load evolution (increasing of the consumption of loads present at the year 1 and new loads appearing during the planning period). Two types of optimization methods were used. The 1st strategy consists in making the LV network evolve as constraints or new loads appear. In that purpose, the shortest path and fit bin packing algorithms were used. The 2nd strategy consists in finding the optimal architecture at the end of the planning period and building it at the year1 thanks to a MIQCP algorithm. These 2 strategies have been integrated in a Monte Carlo simulations were the peak load growth per year and per customers, the location, power and year of appearance of new loads are randomly generated. An average actualized cost enable to conclude that the 1st strategy enable to reach more economic solutions in case of new loads while the 2nd strategy enable to reach more economic solutions otherwise. These tools enable the planers to design optimal LV grids for non-electrified areas with the objective of minimizing the total length of lines, maximizing the load balancing and respecting a set of technical constraint. In this chapter, only topological options have been considered as planning solutions (reinforcement of cables and optimal design of network). In this tool, the presence of renewable sources has not been considered. Nevertheless, in non-electrified areas, some customers are equipped with PV (SHS) to have access to the electricity but are not connected to the main grids. The next chapter proposes to integrate the presence of PV in the LV planning tool.

REFERENCES

[*Apcr11*] M.-C. Alvarez-Herault, D. Picault, R. Caire, B. Raison, N. HadjSaid, and W. Bienia, "A Novel Hybrid Network Architecture to Increase DG Insertion in Electrical Distribution Systems," *IEEE Trans. Power Syst.*, vol. 26, no. 2, pp. 905–914, 2011.

[*Beno15*] C. Benoit, "Models for investigation of flexibility benefits in unbalanced Low Voltage Smart Grids," Thèse de doctorat, Institut polytechnique de Grenoble, 2015.

[*Bomp02*] N. G. Boulaxis, S. Member, and M. P. Papadopoulos, "Optimal Feeder Routing in Distribution System Planning Using Dynamic Programming Technique and GIS Facilities," *IEEE Trans. Power Deliv.*, vol. 17, no. 1, pp. 242–247, 2002.

[*Chsa12*] R. Chang and T. K. Saha, "Application of MIQCP based SVC allocation method to a complex real-world grid," *IEEE Power Energy Soc. Gen. Meet.*, pp. 1–6, 2012.

[*Cifo03*] R. M. Ciric, A. P. Feltrin, and L. F. Ochoa, "Power flow in four-wire distribution networks-general approach," *IEEE Trans. Power Syst.*, vol. 18, no. 4, pp. 1283–1290, 2003.

[*Cora14*] A. F. Contreras and G. A. Ramos, "Fault location algorithm based on shortest path optimization problem for Distribution networks with DG," *2014 IEEE PES T&D Conf. Expo.*, pp. 1–5, 2014.

[*Ebbh11*] R. Ebrahimi, A. Babaee, and M. Hoseynpoor, "Evaluation and Calculation of Overhead Line Impedance in Distribution Networks," *Aust. J. Basic Appl. Sci.*, vol. 5, no. 8, pp. 1278–1284, 2011.

[*Fapi93*] T. P. Fang and L. A. Piegl, "Delaunay Triangulation Using a Uniform Grid," *IEEE Comput. Graph. Appl.*, vol. 13, no. 3, pp. 36–47, 1993.

[*Goar15*] V. Gouin, M.-C. Alvarez-Hérault, and B. Raison, "Optimal planning of urban distribution network considering its topology," in *International Conference on Electricity Distribution*, 2015, no. June, pp. 1–5.

[*Grgl12*] M. Granada Echeverri, R. A. Gallego Rendón, and J. M. López Lezama, "Optimal phase balancing planning for loss reduction in distribution systems using specialized genetic algoritm," *Ing. y Cienc. - ing.cienc.*, vol. 8, no. 15, pp. 121–140, 2012.

[*Hacr10*] N. Hadjsaid, M. C. Alvarez-Hérault, R. Caire, B. Raison, J. Descloux, and W. Bienia, "Novel architectures and operation modes of Distribution Network to increase DG integration," *IEEE PES Gen. Meet. PES 2010*, pp. 1–6, 2010.

[*Ibm16*] IBM, "IBM CPLEX Optimizer - United States," 2016. [Online]. Available: https://www-01.ibm.com/software/commerce/optimization/cplex-optimizer/%5Cnhttp://www-01.ibm.com/software/commerce/optimization/cplex-optimizer/.

[*Kers13*] W. H. Kersting, *Distribution system modelling and analysis*. 2013.

[*Kuks13*] V. Kumar, R. Krishan, and Y. R. Sood, "Optimization of Radial Distribution Networks Using Path Search Algorithm," *Int. J. Electron. Electr. Eng.*, vol. 1, no. 3, pp. 182–187, 2013.

[*Litw96*] W. Lin, M. Tsay, and S. Wu, "Application of geographic information system for substation and feeder planning," *Electr. Power energy Syst.*, vol. 18, no. 3, pp. 175–183, 1996.

[*Mrmm05*] C. Monteiro *et al.*, "GIS Spatial Analysis Applied to Electric Line Routing Optimization," *IEEE Trans. Power Deliv.*, vol. 20, no. 2, pp. 934–942, 2005.

[*Pima01*] P. Pillay and M. Manyage, "Definitions of Voltage Unbalance Call for Short Papers," no. May, pp. 50–51, 2001.

[*Rara07*] S. V. K. Raja and P. H. Raj, "Balanced traffic distribution for MPLS using bin packing method," *Proc. 2007 Int. Conf. Intell. Sensors, Sens. Networks Inf. Process. ISSNIP*, pp. 101–106, 2007.

[*Ssgs12*] A. Samui, S. Singh, T. Ghose, and S. R. Samantaray, "A Direct Approach to Optimal Feeder Routing for Radial Distribution System," vol. 27, no. 1, pp. 253–260, 2012.

[*Swlm12*] J. Shu, L. Wu, Z. Li, S. Member, and M. Shahidehpour, "A New Method for Spatial Power Network Planning in Complicated Environments," *IEEE Trans. Power Syst.*, vol. 27, no. 1, pp. 381–389, 2012.

[*Teng03*] J. H. Teng, "A direct approach for distribution system load flow solutions," *IEEE Trans. Power Deliv.*, vol. 18, no. 3, pp. 882–887, 2003.

[*Vgba17*] V. Vai, E. Gladkikh, L. Bun, M.-C. Alvarez-Hérault, and B. Raison, "Planning of low-voltage distribution systems with uncertainty on load demand in urban areas," in *IEEE-EEEIC / I&CPS Europe*, 2017, pp. 1–6.

[*Vgba17*] V. Vai, E. Gladkikh, L. Bun, M.-C. Alvarez-Hérault, and B. Raison, "Study of low-voltage distribution system with integration of PV-battery energy storage for urban area in developing country," in *IEEE-EEEIC / I&CPS Europe*, 2017, pp. 1–6.

[*Vgba17*] V. Vai, E. Gladkikh, L. Bun, M.-C. Alvarez-Hérault, and B. Raison, "Low-Voltage Distribution System Planning under Load Demand Uncertainty : Growth Rate with Connection of New Loads," in *IEEE International Electrical Engineering Congress (iEECON)*, 2017, pp. 1–4.

[*West05*] D. B. West, "Introduction To Graph Theory Notice Second Edition (2001) Solution Manual," *Read*, no. 2001, 2005.

[*Zhcz98*] J. Zhu, M. Y. Chow, and F. Zhang, "Phase balancing using mixed-integer programming," *IEEE Trans. Power Syst.*, vol. 13, no. 4, pp. 1487–1492, 1998.

[*Zhu99*] J. Zhu, "Phase balancing using simulated annealing," *IEEE Trans. Power Syst.*, vol. 14, no. 4, pp. 1508–1513, 1999.

Chapter III

Integration of Photovoltaic using Battery Energy Storage in Low-Voltage Distribution System

Chapter III

Integration of Photovoltaic using Battery Energy Storage in Low-Voltage Distribution System

Summary

III.1 Introduction

In chapter II, a LV tool has been proposed to find the optimal LV topology in non-electrified areas. Only the loads and the uncertainties on them have been considered and the effects of PVs have not been studied. Nevertheless, if the production occurs in a moment of low consumption (which is the case for the PV), all the electricity produced is not locally consumed. Over-voltages, over-currents and even reverse power flows at the MV/LV substation (i.e. current going from the LV network to the MV network) can occur and could lead to high investment in the MV network. In Cambodia, the SHS used by customers are small size units and their number is low enough not to cause potential voltage and current constraints. But there is a desynchronization between the time when the peak load occurs (between 19h and 20h regarding the type of areas) and the time when the peak production occurs (between 12h and 13h) in an electrified LV Cambodia system. Then, in an LV network with PVs, reverse power flows are likely to happen. Then the new planning problem becomes: how to connect non-electrified customer while canceling reverse power flows due to PV? In this chapter, a centralized BES has been connected to the MV/LV substation so as to cancel the power flows. For the particular case of rural areas, if under-voltage constraints appear due to the load, decentralized battery energy storage will also be used to prevent from reinforcing the network (no under-voltage constraints in urban areas). Consequently, this chapter proposes algorithms to locate and size BES in order to integrate PV into the distribution network planning. This novel planning methodology leads to the creation of LV microgrids which could be disconnected to the main grids during some moments of the year enabling to reduce the investment in the MV network. The methodology will be described for the rural case in order to present the two kind of BES strategies used. It will be applied on a simple rural case study (single phase MV/LV transformer) as depicted in Figure III-1.

Figure III- 1 : Low-voltage distribution system in Bavel-Battambang-Cambodia [13°18'28.8"N,102°52'54.4"E]

It consists on the extension of an existing LV rural electrified grid to integrate non-electrified customers. Two solutions will be compared. The first solution is the traditional planning method consisting in building new lines so as to provide electricity for the maximal consumption case. The second solution will consist in combining grid extension with the integration of Photovoltaic (PV) and Battery Energy Storage (BES) so as to reduce the global cost and to cancel the reverse power flows. Figure III-2 provides a summary of the planning problem.

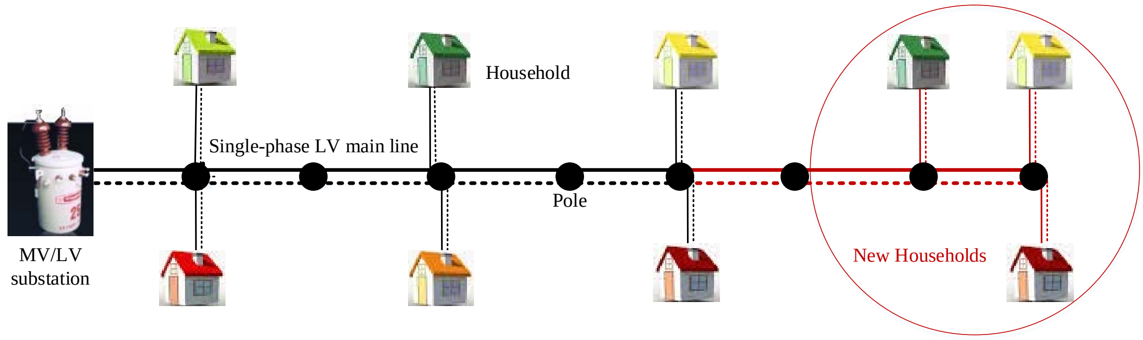

Figure III- 2 : Problem of the extension of electricity coverage area in LV distribution system

III.2 Integration of PV and BES in distribution network planning

In rural areas, the main technical constraints encountered in the LV distribution network are voltage constraints at the end of the distribution lines [*MURA09*]. One alternative solution to the classical reinforcement to solve this problem is the integration of PV-BES into the grid. The association of PV with BES enables to better control power flows as we know that the energy of PV is only available during the day and depends on the solar radiation received. Thus the BES integration is interested when power is required but cannot be provided by PV. In this chapter, we assume that a single-phase PV unit will be installed at some households. Besides, two possibilities of BES integration (i.e. decentralized BES and centralized BES) will be investigated in the following section and their performance and costs will be compared. A technical and economic study will compare the interest of the association of PV and BES to reduce the global cost of the network (i.e. the CAPEX and OPEX).

III.2.1 Decentralized BES

The Decentralized Battery Energy Storage (DeBES) is integrated at some households' nodes in the LV distribution system. The objective of PV-DeBES integration is to improve the voltage profile in the whole system without deploying a communication system along the network.

III.2.2 Centralized BES

When the PV production is very high and the consumption low, reverse power flows can go from the LV network to the MV network. Then, the integration of Centralized Battery Energy Storage (CeBES) at the MV/LV substation could be added to store these excesses of power. Another interest of CeBES would be to reduce the power requirement from the MV grid by providing electricity to the customers when the PV production is not enough. The CeBES combined with PV could enable the creation of an LV microgrid with some autonomous operation times which could be potentially disconnecting from the main grid.

III.3 Methodology

The general algorithm proposed to extend the existing LV network to the non-electrified area is depicted by the flowchart of Figure III-3.

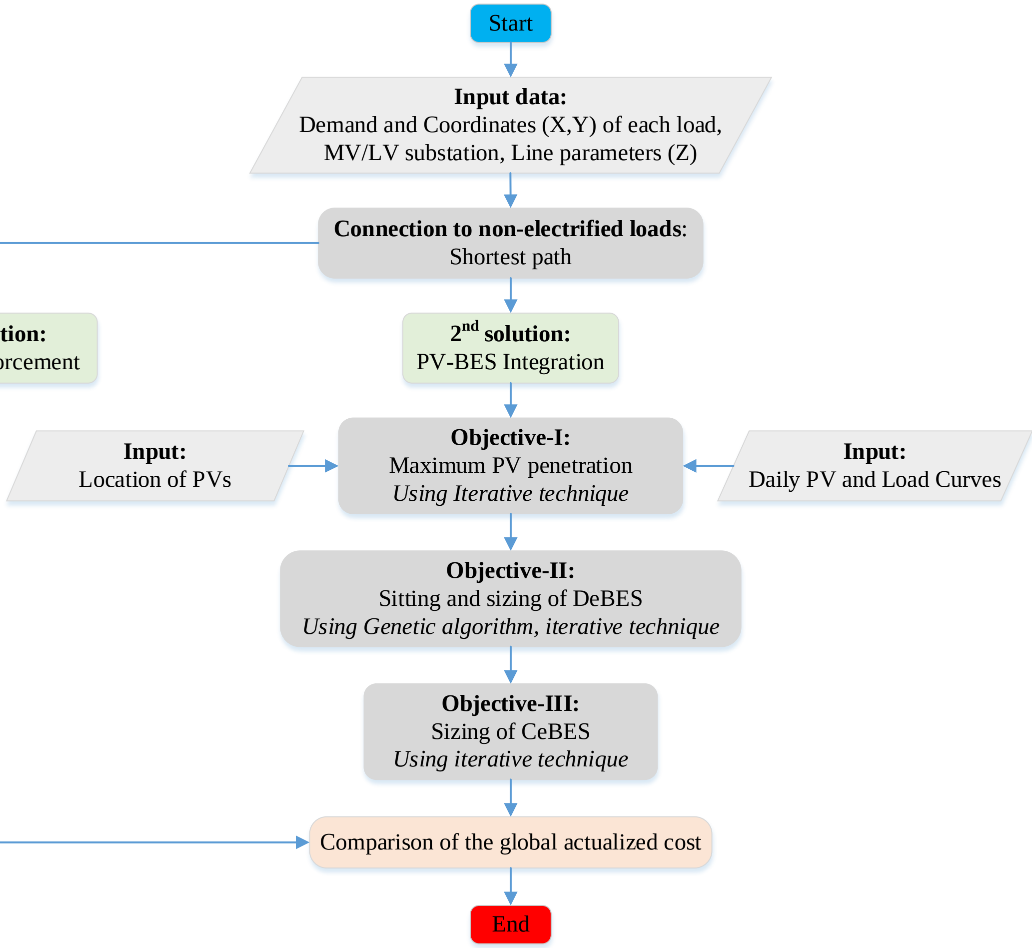

Figure III- 3 : Flowchart of proposed method

As shown in Figure III-3, the data of loads demand, their locations and the lines parameters of the LV distribution system are requested as input as well as information on non-electrified loads (location and peak power). For the 1st proposed solution, the expansion/reinforcement of existing grid will be studied in order to solve the under voltage problem by sizing the minimum cable which respects the voltage and current constraints. For this 2nd proposed solution, we define the amount and location of the single-phase PV integration at households; in this chapter it is assumed that PVs will be connected to some customers having the highest load demand. Then the maximum power penetration of PVs will be sized according to PV-load curves and using an iterative technique which is described in section III.3.1.1. One decentralized BES is connected in the optimal location of the LV grid defined by a Genetic algorithm [*IBA93*] (see section III.3.2.1). The minimum capacity of the battery is found with an iterative technique. Then, the centralized BES at the MV/LV substation is sized to remove the reverse power flow and also to increase the autonomous operation time by using a sizing strategy development (see III.3.2.3). Finally, the two strategies are compared by computed their global actualized cost.

The following section will provide the developed algorithms listed above.

III.3.1 Strategy 1: grid reinforcement

Once the non-electrified customers are connected to the existing LV grid, the grid reinforcement procedure enables to size the lines so as to avoid under voltage and current problems. The cable size will be reinforced considering the peak load of 19h00 (see III.4.3). Figure III-4 details the process of grid reinforcement.

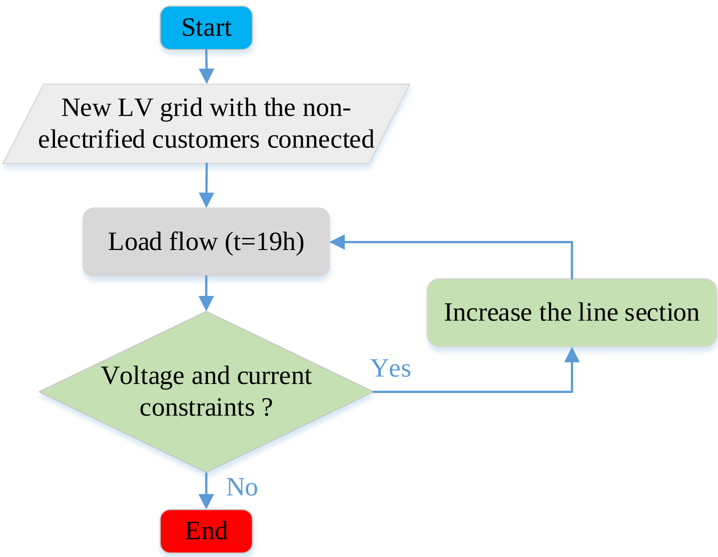

Figure III- 4 : Concept of grid reinforcement

III.3.2 Strategy 2: integration of PV-Battery Energy Storage

III.3.2.1 Sizing of Decentralized PVs

There are a lot of uncertainties regarding the PVs locations and powers in the future. Therefore, the location of PVs is assumed among the households. The objective here is to find out a maximum PV peak power which can be integrated into the LV grid while respecting voltage and current constraints. This problem is solved by using an iterative technique. Figure III-5 shows the flowchart for the determination of the decentralized PVs sizing. Firstly, we insert the system data (i.e. lines parameters, MV/LV substation, loads demand and locations) and daily PV-load curve. Then, PV units having the same size are placed at the customers having the highest peak power. The maximal power of these PV units is defined using the iterative technique presented in Figure III-5. The power of PV is incremented until the maximum voltage limits and/or the maximal current limit where de

PVs are connected are reached for each hour of the day. The maximal powers of each hours are saved and finally, the maximum PV penetration of system is the minimum of these maximum powers.

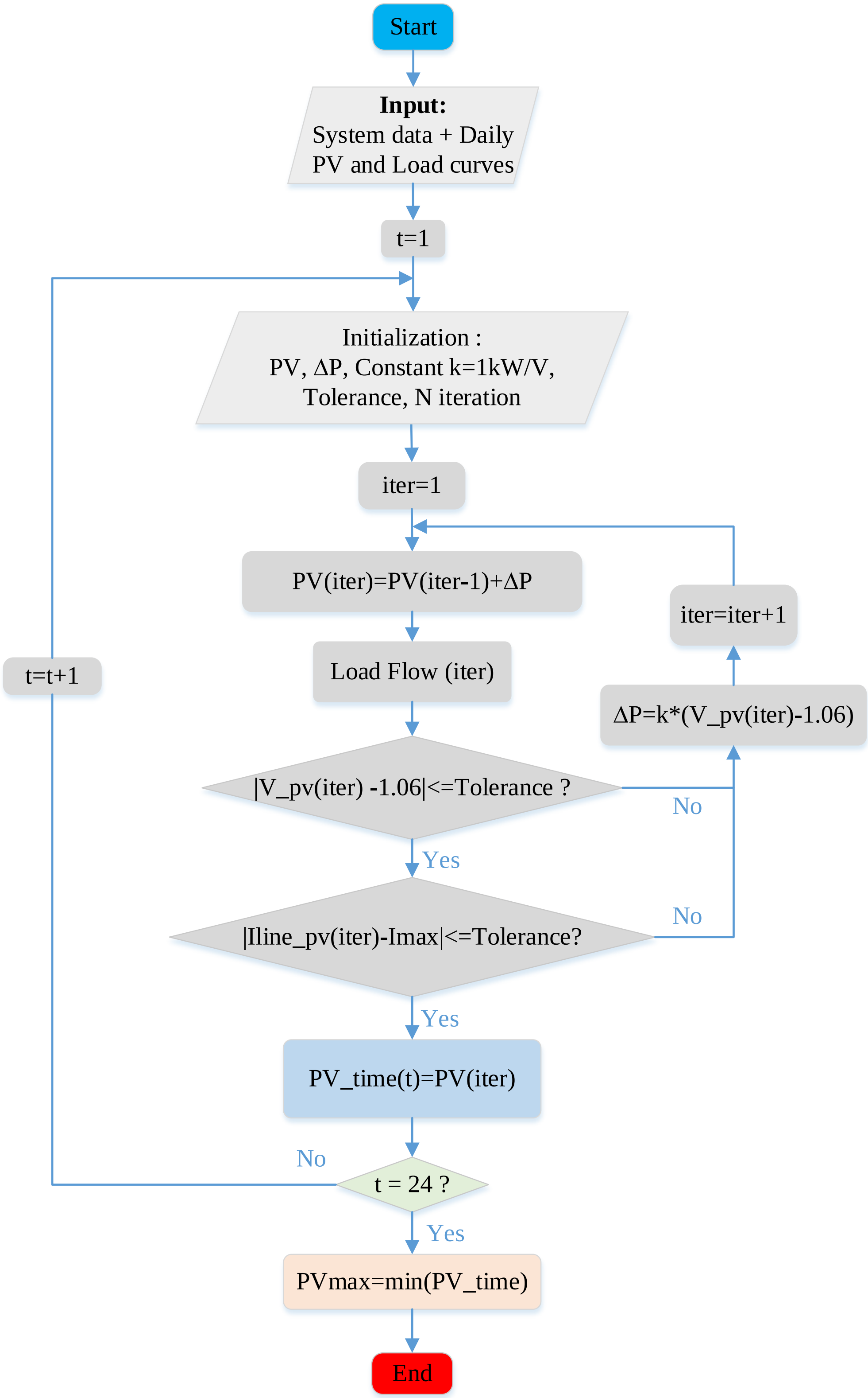

Figure III- 5 : Flowchart of sizing of PVs integration

III.3.2.2 Location and Sizing of Decentralized BES-DeBES

III.3.2.2.1 Location of DeBES

The under voltage problem is almost always at the furthest connected household with and without the presence of PV. Indeed, the maximal consumption occurs in general when the PV production is low. Then the case of low-voltage constraint is the same with and without PV connected. The DeBES is located in the network in order to remove the low-voltage constraint. However, the integration of the DeBES at the furthest household is not always the optimal location. Therefore, the optimal location of the DeBES is computed using a genetic algorithm. The advantage of the genetic algorithm here is its ability to avoid being trapped in local optima. Also, this algorithm is able to search a problem with mixed-integer constraint. The objective is to search for the optimal location and power of the DeBES which minimize the power injection at 19h00 (hour when it is maximal). The objective function is formulated as it follows:

$$\text{Objective:} \qquad \min Pbes_k^t \tag{III-1}$$

Where:

$Pbes_k^t \in \{\Re^+\}$, power injection of DeBES, $\forall k \in$ electrical poles' node at $t = 19h00$

Subject to following constraints:

- Voltage constraint [*KING04*]

$$0.9\,pu \le V_{\text{limit}} \le 1.06\,pu \tag{III-2}$$

- Current constraint

$$I_{line} \le I_{max} \tag{III-3}$$

Moreover, the implementation of the GA will be done with generations consisting of 50 individuals of location and sizing. The maximum number of generations is set to be 200. The fitness of each individual is given by the objective function, and it also considers a penalization if the voltage goes outside the allowed interval, plus another penalization if the current exceeds admissible capacity of cable. The fitness value f for any individual x is

$$f(x) = Pbes(t) + C_1\delta_1 + C_2\delta_2 \tag{III-4}$$

Where $Pbes(t)$ is computed from Eq. III-1; $\delta_1 = \max(0, 0.9 - V_{node}) + \max(0, V_{node} - 1.06)$ with a penalty C_1 of 10e+5 if the voltage lies outside the limits; $\delta_2 = \max(0, I_{line} - I_{\max})$ with a penalty C_2 of 10e+5 if the current exceeds $I_{\max}$. After several simulations, the settings of the algorithm (number of individuals, number of generations and penalty coefficients) have been chosen to be a trade-off between simulation time and convergence.

III.3.2.2.2Sizing of DeBES

This part is dedicated to the sizing of the minimum DeBES capacity integrated into the grid in order to solve the under voltage problem. In a first step, we find the maximum and minimum power (i.e. charge, discharge) of the DeBES (see III.4.4.2.2) over 24h which corresponds to the reference voltage requirement at DeBES (Vset, see III.3.2.2.3) by using an iterative technique as explained in Figure III-6. Additionally, this sizing of DeBES will be upgraded to 20% bigger in order to satisfy the minimum state of charge of the battery (which have to be higher than 20%)[*MJCX14*].Then, the sizing of the DeBES is equal to the sum of all the negative (discharge) values of power as follows.

$$DeBES\_Capacity\ (kWh) = \sum_{t=1}^{24} P\_DeBES_i(t) \qquad \text{(III-5)}$$

Where $P\_DeBES_i(t)$: negative power, power injection of DeBES in kW at bus *i*

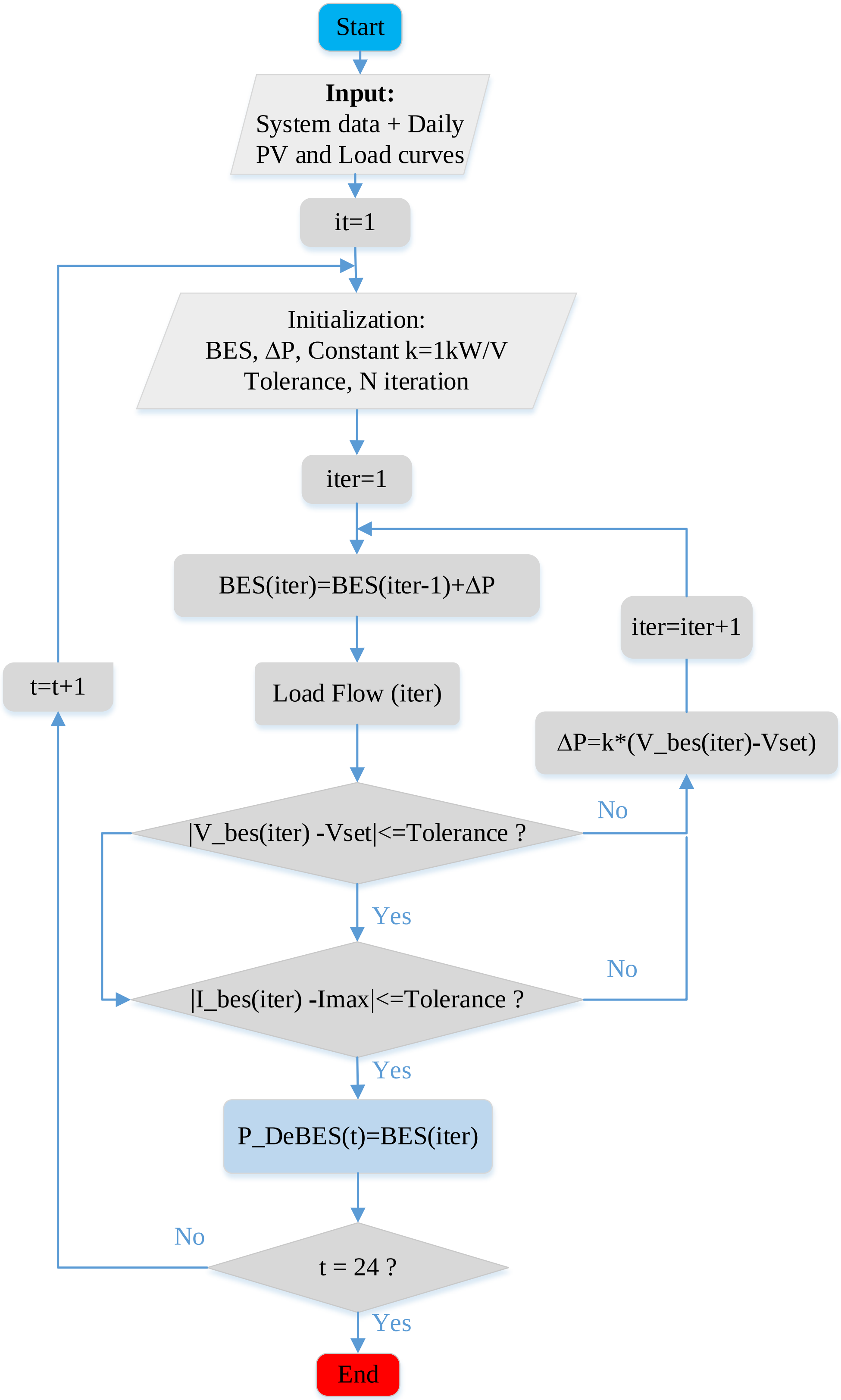

Figure III- 6 : Flowchart of the minimal discharge and maximal charge of DeBES

III.3.2.2.3Decentralized control of BES

In rural LV distribution grids, particularly in developing countries, there are almost no information communication technology (ICT) components used to receive the data (current, voltage) in distance from the substation. In this primary study, we thus proposed a decentralized strategy to control the DeBES without using a large ICT system as depicted in Figure III-7. A simple measure of the voltage at the node where the DeBES is connected enable will control the charge and discharge of the battery provided that its state of charge remains between SoCmin and SoCmax. In section III.3.2.2.1, the DeBES has been located and size so as to solve the constraint of low-voltage. In that purpose, the maximal power injected by the battery has been determined at 19h, time where the worst low-voltage constraint appear. A load flow at 19h with this maximal discharge power enables to get the voltage at the battery node under which a low-voltage constraint will appear in the network. This voltage will be the set point voltage of the decentralized control of the battery called V_{set}. In other words, if the voltage at the DeBES node is higher or equal to V_{set}, the under voltage problem will not occur on whole system.

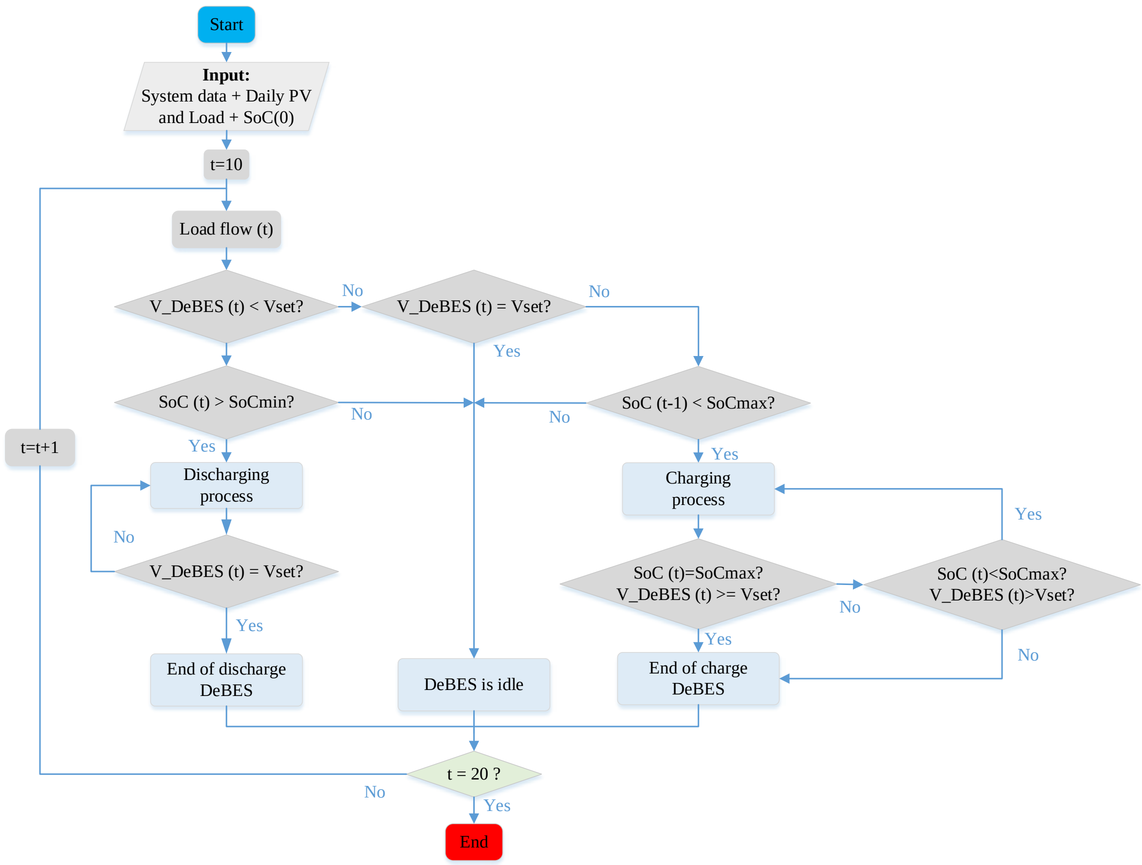

Figure III- 7 : Flowchart of decentralized control of DeBES from 10h00 to 20h00

III.3.2.3 Sizing of the centralized BES(CeBES)

The objective of the CeBES is to charge the energy during reverse power flows from the LV grid to the MV grid and to discharge when the grid must supply the LV loads provided that the state of charge of the battery remains between SoCmin and SoCmax.

Figure III-8 shows the flowchart of the sizing strategy. In other words, the CeBES will be the primary source and the MV grid the secondary source when possible. For each hour of the year, the power of charge and discharge of the battery is computed so as to remove the reverse power flows at the MV/LV substation. Then maximal value between the sum of the power charged and the sum of power discharger during a day gives the SoC of the battery.

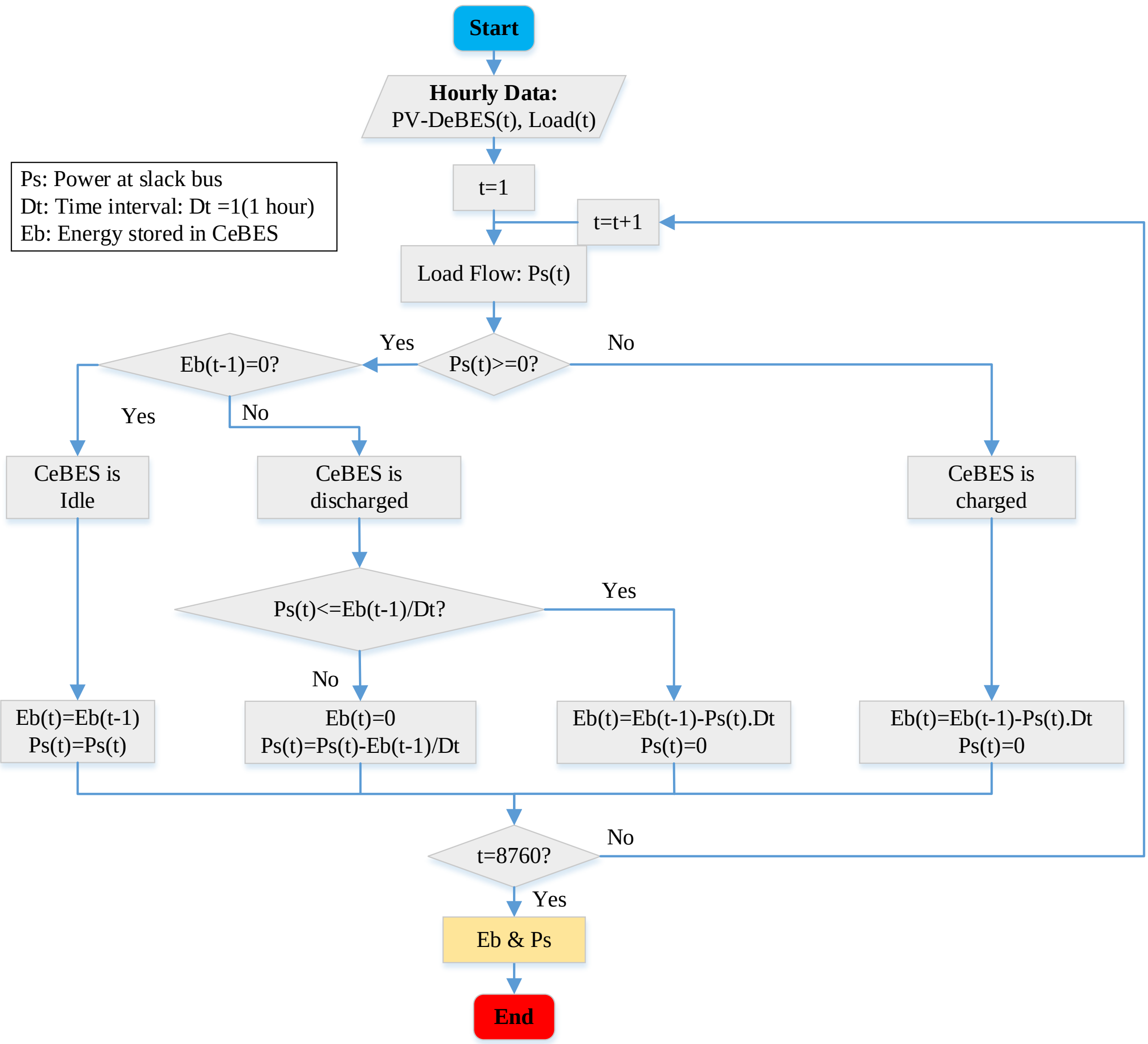

Figure III- 8 : Flowchart of the sizing strategy of the centralized BES

Figure III-9 gives the control of the CeBES which has the same principle than the algorithm to size the battery. The power at the MV/LV substation is measured and if it is negative then the battery will charge and if it is positive then the battery will discharge if the state of charge of the battery remains in the limits.

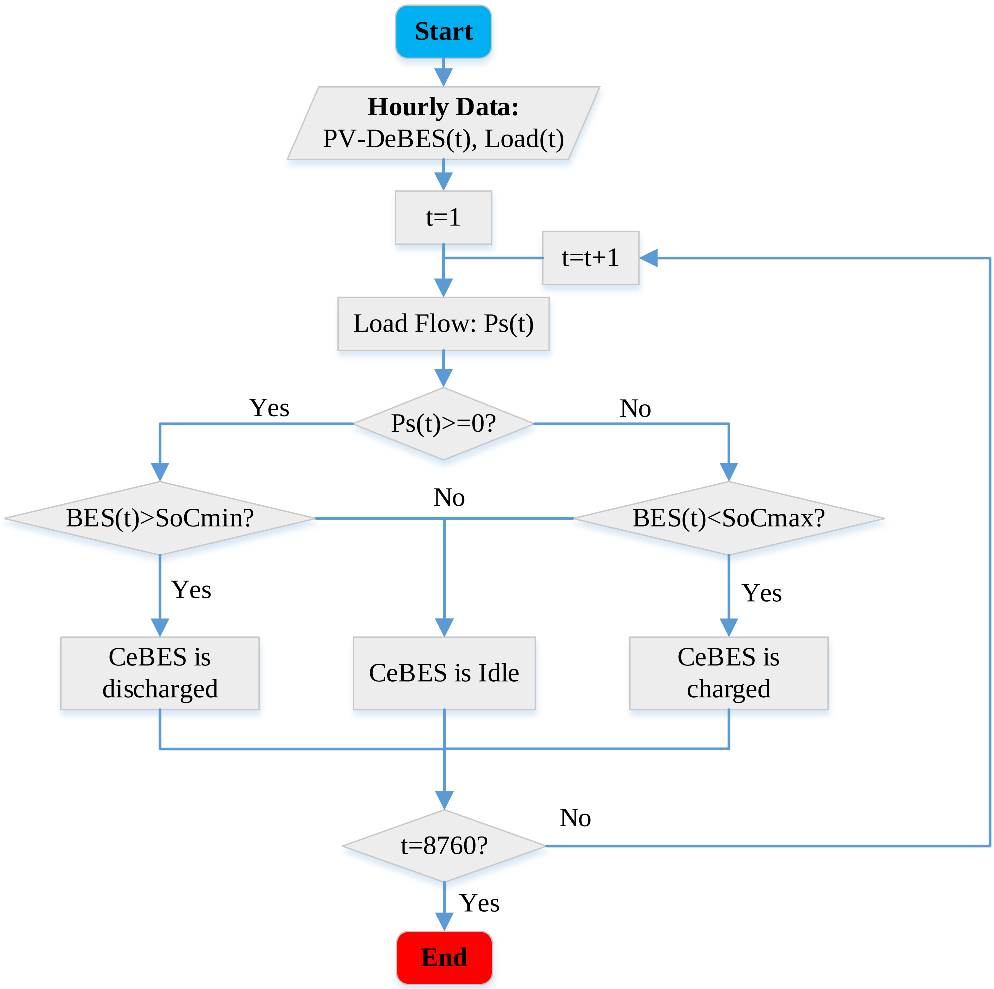

Figure III- 9 : Control algorithm of CeBES

III.4 Test system

III.4.1 Topology of system

In this chapter, a village in Bavel in the province of Battambang in Cambodia is selected to be the case study as seen in Figure III-10 in order to validate the proposed method. In developing countries, the households are almost all single-phase, located along the road in rural area. The LV system is supplied from a single-phase 22-kV/0.23-kV transformer at bus 1. Since there is no available information for all loads, we proposed to use random process of normal distribution with mean of 0.35 kW and standard deviation of 0.05 kW in order to obtain the peak demand of loads. The values chosen for the mean and de standard deviation are representative of loads in rural area. The total active power is 24 kW with a power factor (pf) of 0.95. The peak demand and location of loads are presented in Appendix

III-A. The poles are numbered from 1 to 22 with a distance between poles of 40m. In LV rural distribution area in Cambodia, a typical conductor size used for the main lines is 50 mm^2 (Imax=150A) and for poles to each household is $4mm^2$ (Imax=32A).

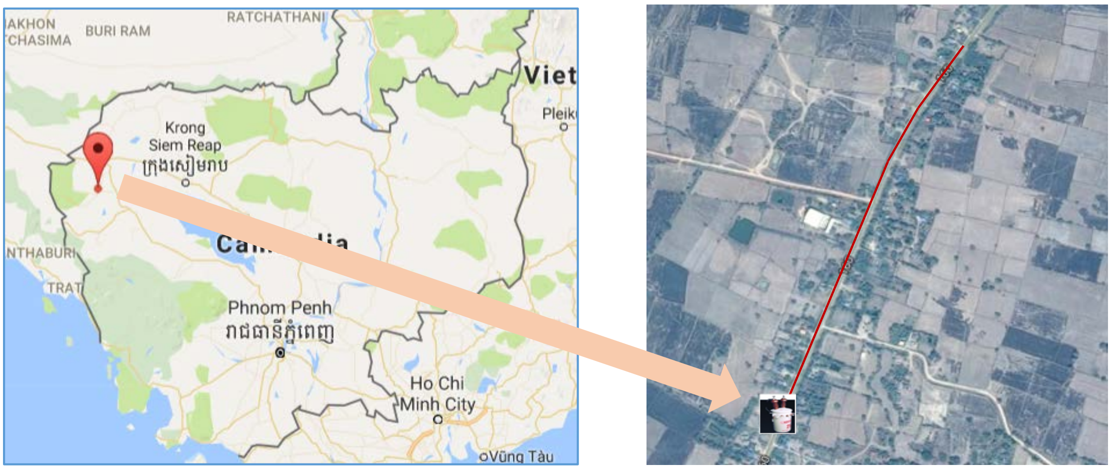

Figure III- 10 : The test system topology of low voltage distribution in Bavel-Battambang-Cambodia [13°18'28.8"N,102°52'54.4"E]

Figure III-11 shows the existing LV network and the non-electrified loads which required to be connected to the LV network.

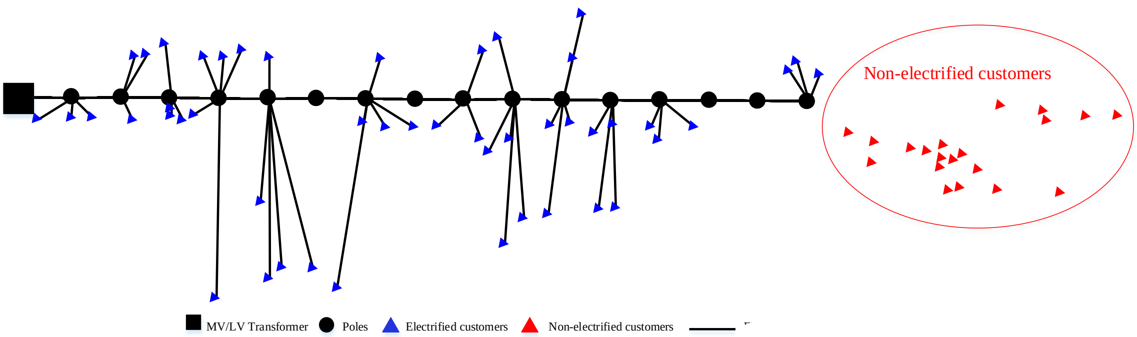

Figure III- 11 : Case study in rural village

III.4.2 Impedance of the system

The impedance of the distribution overhead lines is determined by using Carson's equations [*EBBH11*]. Further, the LV-ABC-2Cores topology and 2x2 matrix of single-phase low-voltage distribution are shown in Figure III-12 and Eq. II-6.

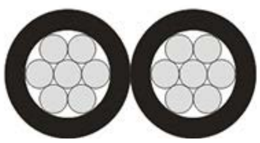

Figure III- 12 : LV-ABC-2Cores cable

$$Z_{an} = \begin{bmatrix} Z_{aa} & Z_{an} \\ Z_{na} & Z_{nn} \end{bmatrix} \qquad \text{(III-6)}$$

Besides, the self-impedance and mutual-impedance of test system are shown in Appendix III-B.

III.4.3 Load and PV curve

A simplified daily load which is taken from local measurement (see Appendix III-C) of two households and the PV curves presented in [*VGBA17*] in Cambodia have been used and given in Figure III-13. The load profile is repeated for one-year simulation in this chapter. This strong hypothesis is made because no data are available for the moment. It has to be mentioned that during summer, the consumption peak can increase due to fans due to the high outside temperature.

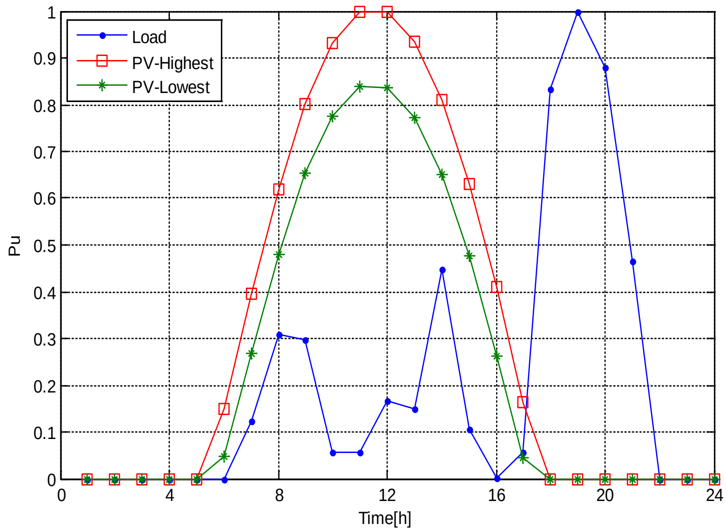

Figure III- 13 : Daily PV(highest-lowest) and load curves in rural area

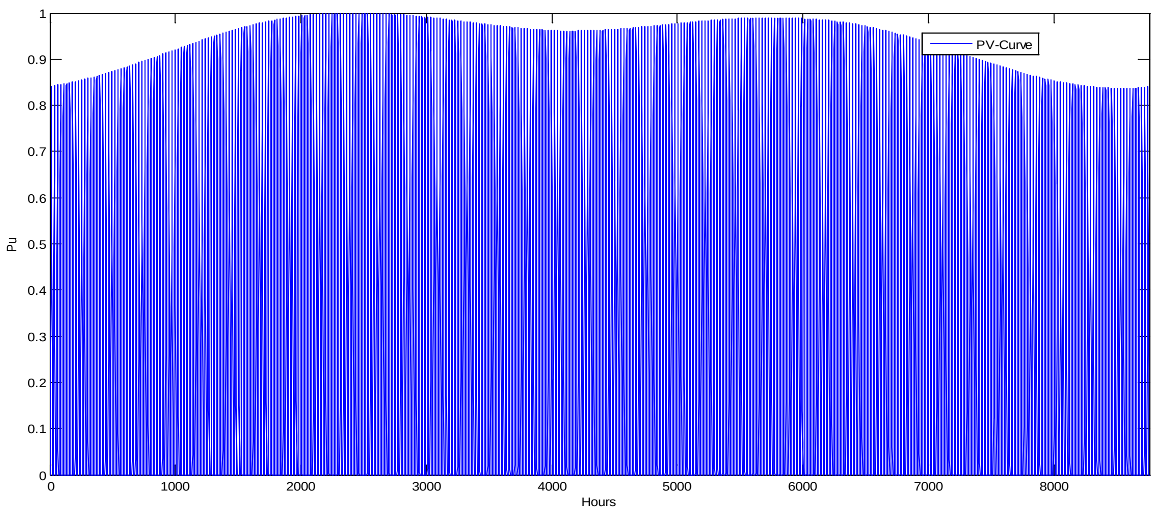

Figure III- 14 : Annual PV curve in Cambodia [*VGBA17*][*NASA17*]

III.4.4 Simulation results and discussion

In in this part, we focused on the simulation results and discussion. Moreover, the backward/forward load flow algorithm [*CIFO03*] is used when a power flow analysis is required.

III.4.4.1 Strategy 1: Grid reinforcement

Figure III-15 shows the voltage at each node of the test system for several cable sizes used in Cambodia at 19h where the peak load occurs.

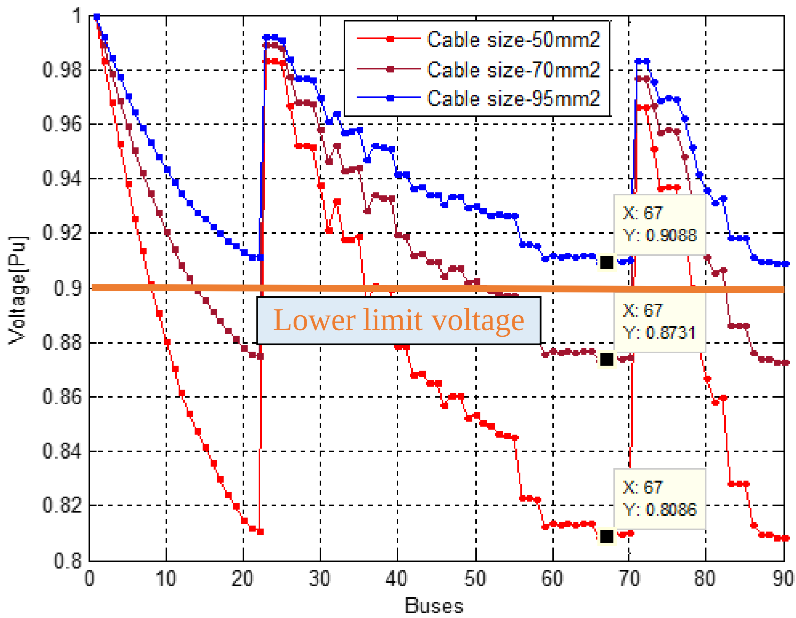

Figure III- 15 :Voltage profile of different cable sizes (50mm2-70mm2-95mm2)

The minimal voltage and maximal current are listed in Table III-1.

Table III- 1 : Minimal voltage and maximal current with several cable sizes.

Cable size	**Min voltage (pu)**	**Max current (in % of the maximal admissible current)**	**Decision**
ABC-2x50mm2	0.8086 pu	86.7 %	NO
ABC-2x70mm2	0.8731 pu	66.5 %	NO
ABC-2x95mm2	0.9088 pu	53.3 %	**YES**

According to these results, we can conclude that the cable size of 95mm2 is selected for the grid reinforcement since there is no voltage and current constraints in our test system.

III.4.4.2 Strategy 2: PV-BES

III.4.4.2.1PV integration

Currently, there are no information about the percentage of PV use on households (solar home system) and also integrated into the LV distribution system in Cambodia. In this chapter, we will assume that the six households who have the highest load demand will have a single PV unit with an identical maximal power connected to the grid and located at bus 38, 48, 56, 61, 77 and bus 85. The size of the PV is found by using the iterative technique (see section III.3.2.1). Figure III-16 shows the voltage profile with PV integration at 11h00 (when it is maximal). As seen in Figure III-16, the maximal voltage is reached (1.06 pu) with 1.54 kWp for each PV. Therefore, the sizing of each PV unit which will be integrated to the grid is 1.54 kWp. Then the total PV penetration is about 38.5 % of the maximal load.

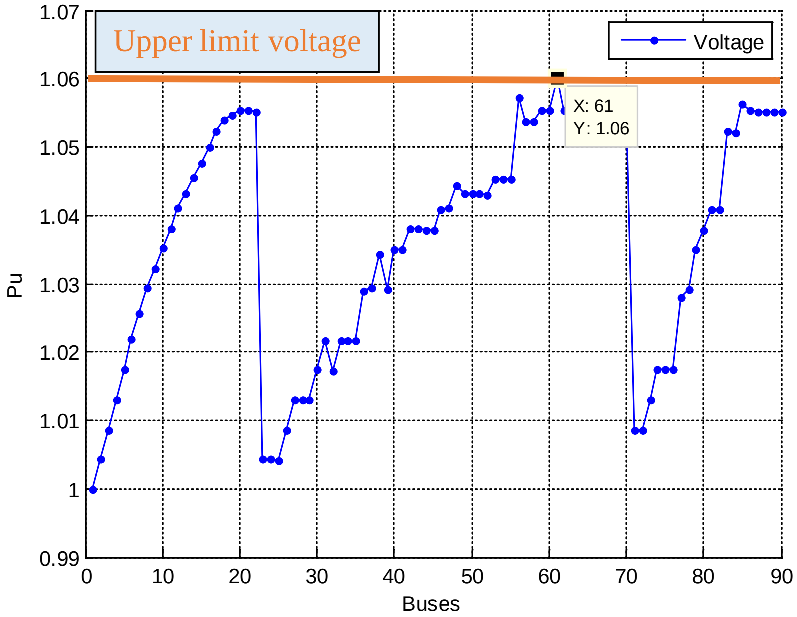

Figure III- 16 : Voltage profile with PV integration at 11h00

III.4.4.2.2DeBES integration

In our work, we propose to use only one DeBES which is integrated to the LV distribution system. By applying the genetic algorithm, the optimal sitting of DeBES has been obtained. That optimal location of DeBES is at point 21 (see Figure III-18) which corresponds to a minimum power injection of 5.92 kW. The fitness evolution of the applied GA to find a location and sizing of DeBES is shown in Figure III-17. In the implementation of GA, we set 50 individuals, 200 generations, 10e-10 of tolerance constraint (TolCon) and 10e-10 of tolerance penalty fitness (TolFun) as inputs in optimization. As seen in Figure

III-17, the algorithm converged at the 190th generation due to the average change in the penalty fitness value less than TolFun and constraint violation is less than TolCon.

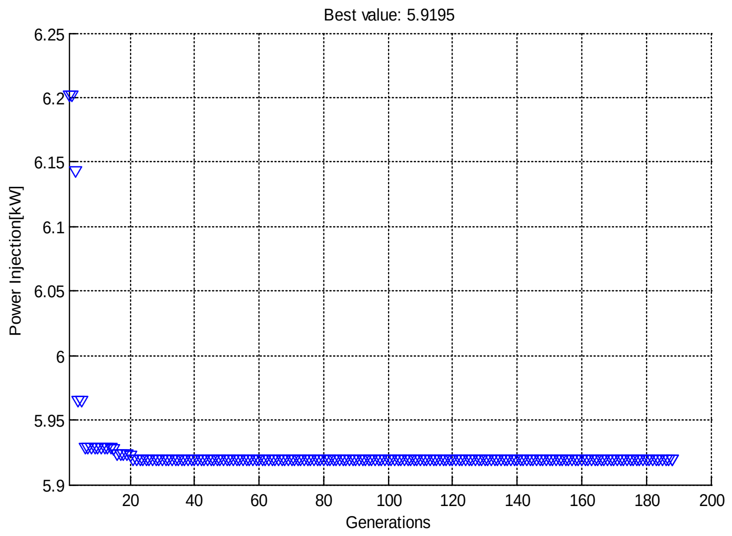

Figure III- 17 : Evolution of the best DeBES location (21) and Sizing at 19h00 over 200 generations setting

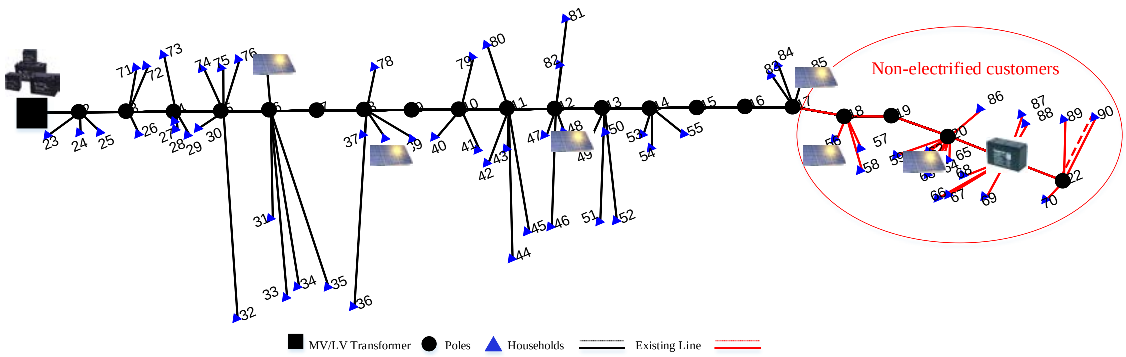

Figure III- 18 : The test system of low voltage distribution with PV-BES integration

According to the optimal location of DeBES (see Figure III-18), the sizing of that battery will be provided by using an iterative technique (see Eq. III-5). Figure III-19 shows the maximal charging and minimal discharging of DeBES at bus 21. So, the sizing of the DeBES is determined by the sum of discharge power from 18h00 to 20h00 and supplemented by 20%; therefore, the sizing of DeBES is 17.4 kWh.

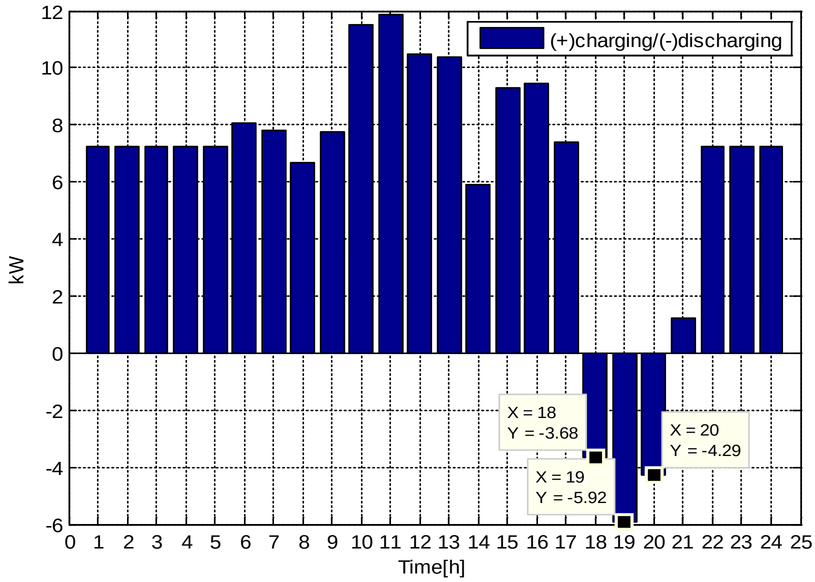

Figure III- 19 : Max charging (+) and min discharging (-) of DeBES power

Figure III-20 shows the voltage profile of the complete feeder at 19h00 (peak demand) with and without PV-DeBES integration. According to that figure, it is identified that the system does not respect the voltage constraint in case of non-integrated DeBES. However, this constraint has been removed thanks to DeBES.

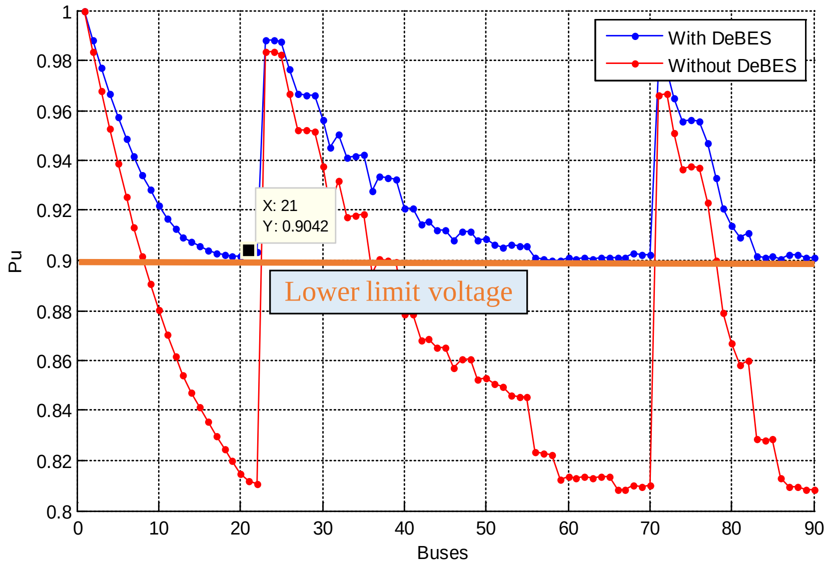

Figure III- 20 : Voltage profile with/without DeBES at time=19h00 (peak load)

Furthermore, Figure III-21 and Figure III-22 show the result of the power absorbed or injected by the battery and the state of charge of the DeBES by applying the decentralized control of DeBES described in section III.3.2.2.3 over two days of different solar radiation. It can be seen that the results are identical showing that the low-voltage constraint always appear when the PV production is low. The V_{set} (0.9042 pu) of the DeBES controller is found from Figure III-20 at bus of 21 (optimal location). In this work, we assumed that a

6kW battery inverter (bi-directional inverter)[*SMAS17*] which is available in Cambodia, is used for simulation. Also, the same schedule will be repeated in over a year of simulation.

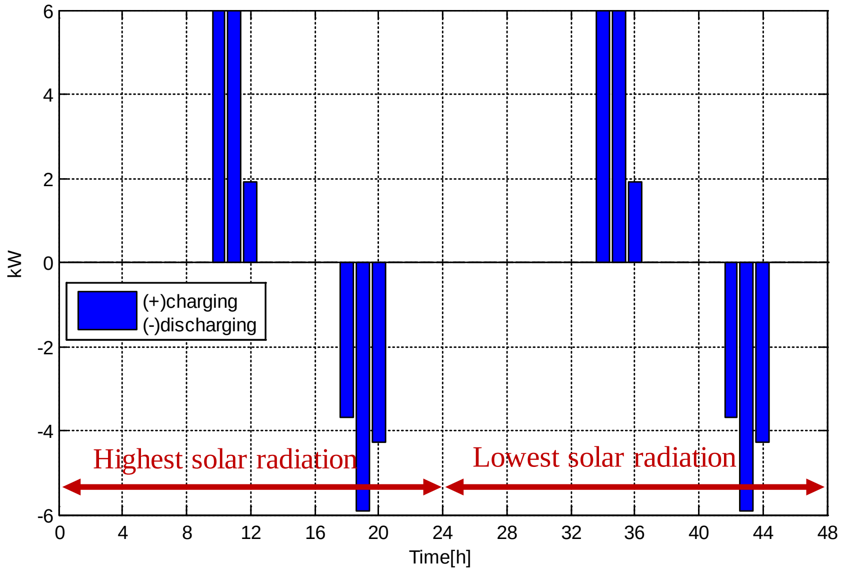

Figure III- 21 : Operation of DeBES over two days of different solar radiation using the decentralized control

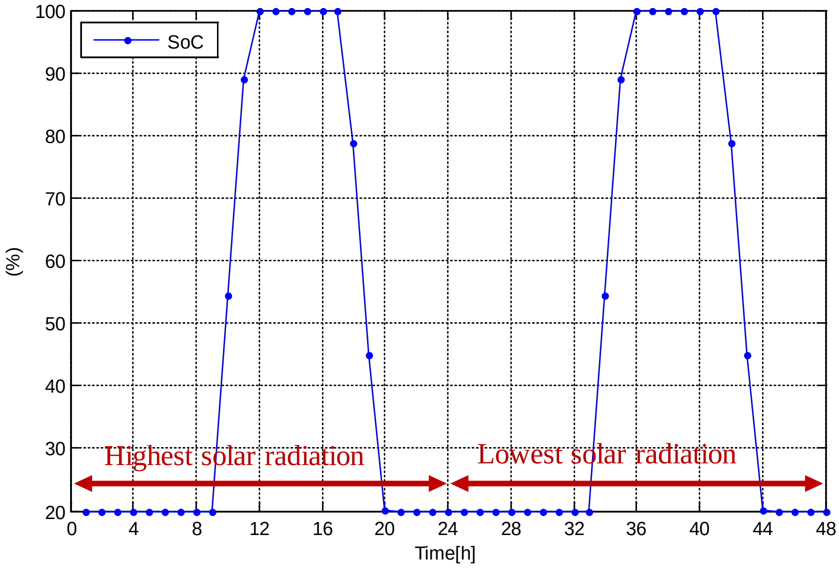

Figure III- 22 : State of charge of DeBES over two days of different solar radiation

With the operation of the DeBES by the controller, the minimal voltage profile of the system and the voltage profile at the DeBES nodes are shown in Figure III-23. According to this figure, we can say that the decentralized controller is running well and no under voltage problems has been occurred.

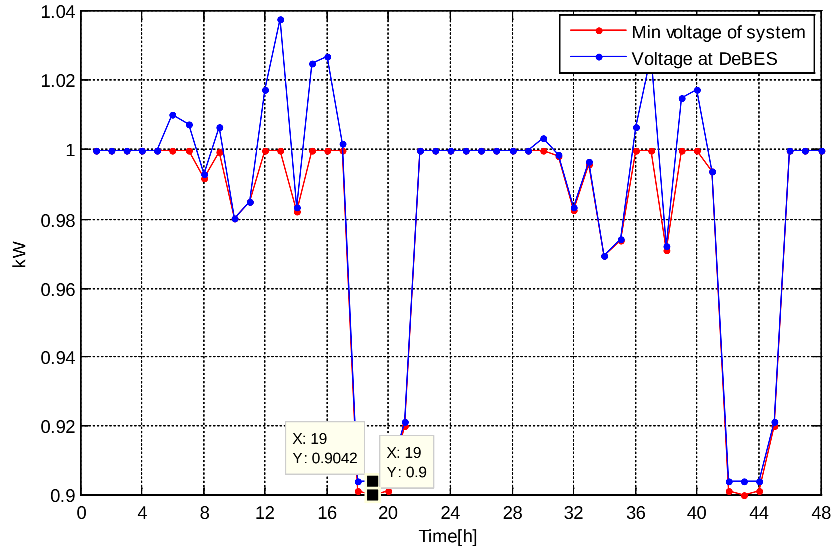

Figure III- 23 : Minimal voltage profile of the system and voltage at the DeBES node over two days of different solar radiation

Moreover, a daily active power flow at the MV/LV substation over two days is also depicted in Figure III-24; there are some negative values due to the PVs integration and the fact that the DeBES cannot store more energy but they will be removed with the use of the CeBES (more details will be provided in section III.4.4.2.3).

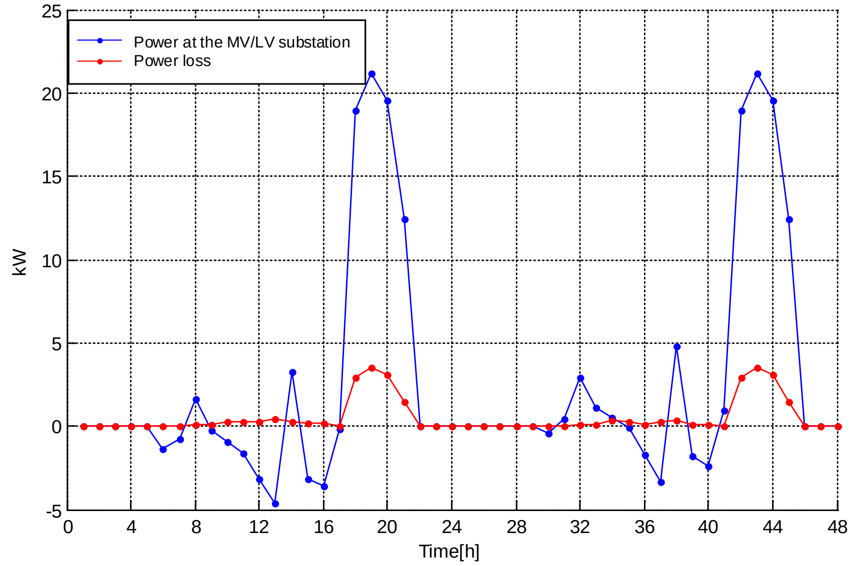

Figure III- 24 : Active powers at the MV/LV substation and power losses over two days of different solar radiations

III.4.4.2.3CeBES integration

The CeBES is installed at the MV/LV substation (1st bus) and the sizing strategy of the centralized BES is applied to find out its capacity. Figure III-25 shows the histogram of the annual power at the MV/LV substation without PV-BES integration; the maximal active power at the MV/LV substation is about 32 kW. This maximal value is not reduced by the

PVs integration since it happens at 19h00 when PVs are not available; but there are some negative values (reverse power flows) at the MV/LV substation as depicted in Figure III-26. However, this maximum active power has been reduced to 21 kW thanks to DeBES integration as given in Figure III-27.

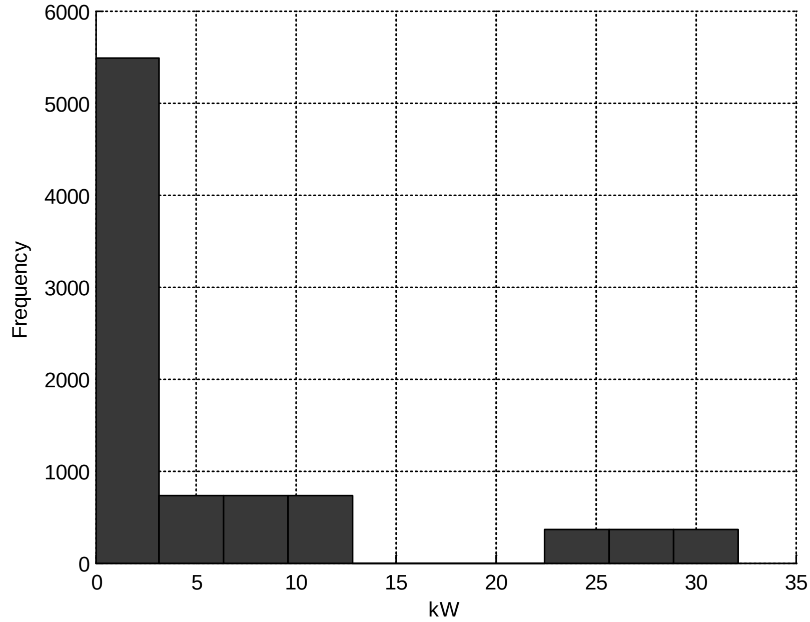

Figure III- 25 : Histogram of the annual active power at the MV/LV substation without PV-DeBES-CeBES

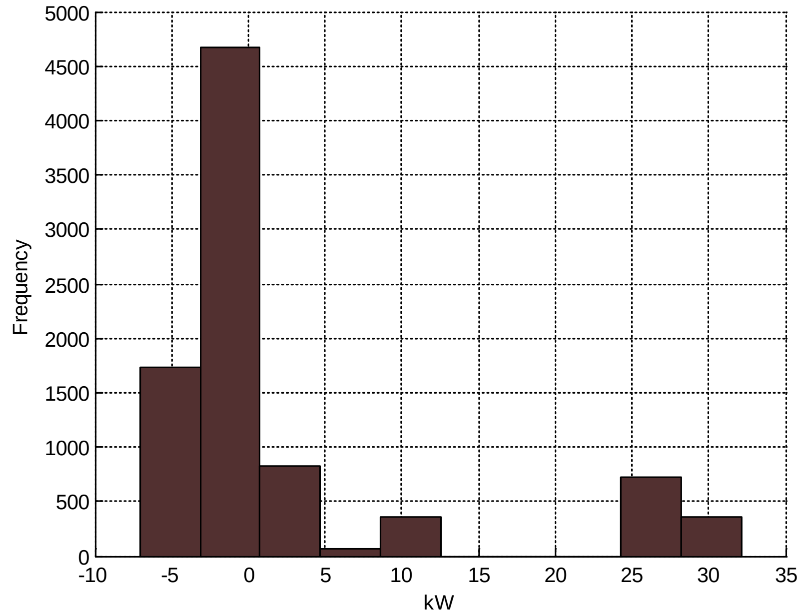

Figure III- 26 : Histogram of the annual active power at the MV/LV substation bus with PVs integration

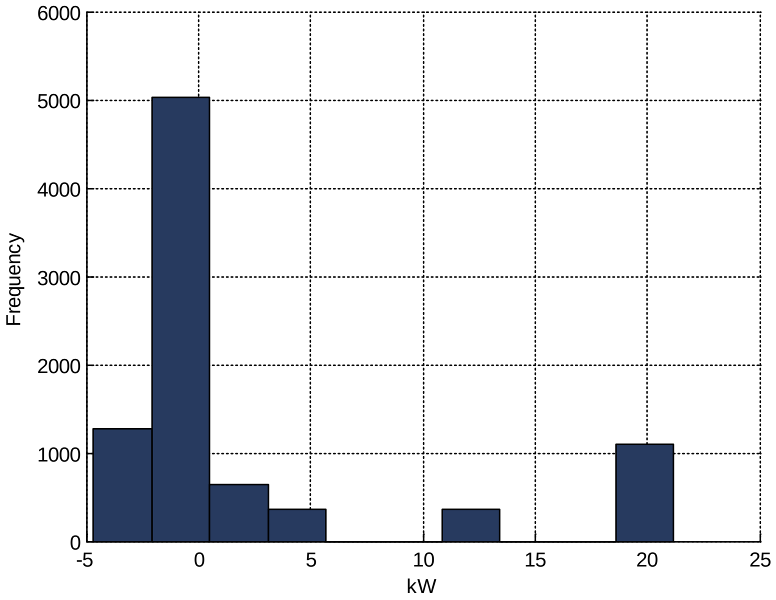

Figure III- 27 : Histogram of the annual active power at the MV/LV substation with PVs-DeBES integration

Moreover, to remove the reverse power flow from the LV grid to the MV grid, the centralized CeBES is used at the MV/LV substation. As shown in Figure III-28, the negative amounts have been stored in the CeBES by applying the strategy described in section III.3.2.3. Also, the active power from coming from the MV grid has thus been reduced to 19 kW. The sizing of the CeBES is 19.25 kWh as seen in Figure III-29.

Besides, the autonomous operation time of the LV system has been increased with the integration of the CeBES and the end users have been supplied with the electricity coming from the PV-DeBES-CeBES in some period without energy from the MV grid.

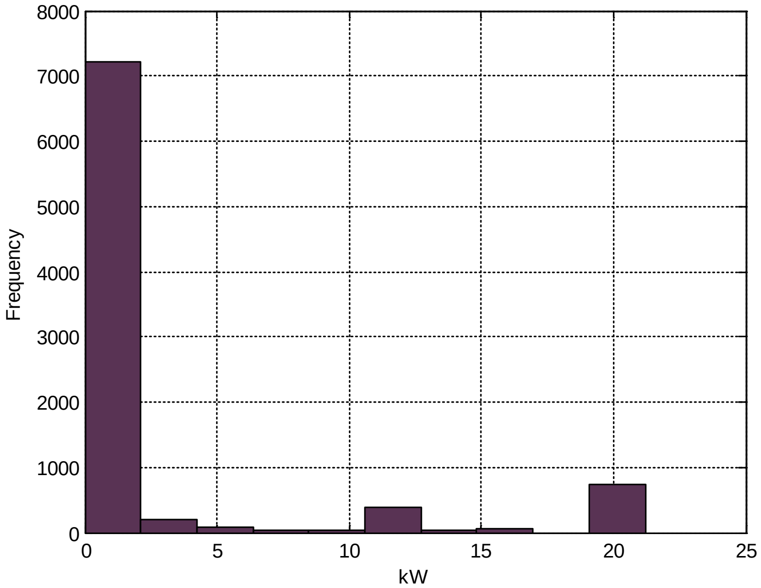

Figure III- 28 : Histogram of the active power per year at the MV/LV substation with PV-DeBES-CeBES

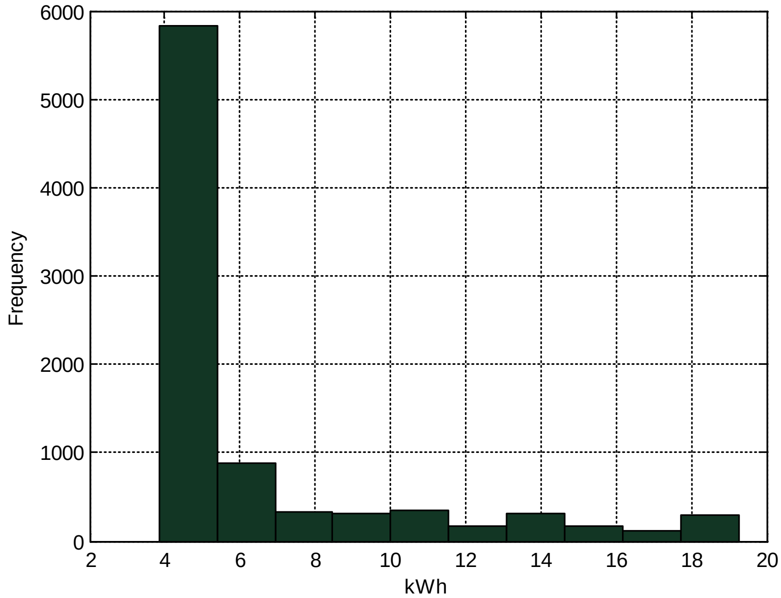

Figure III- 29 : Histogram of the annual energy of centralized battery energy storage-CeBES

Furthermore, Table III-2 summarized the main results of this case study.

Table III- 2 : Simulation results of PV-BES integration

Parameters	**Without-PV-DeBES-CeBES**	**With-PV**	**With-PV-DeBES**	**With-PV-DeBES-CeBES**
6PV [kWp]	0	1.54	1.54	1.54
Decentralized BES [kWh]	0	0	17.4	17.4
Centralized BES [kWh]	0	0	0	19.25
Maximal power at the MV/LV substation [kW]	32.12	32.12	21.20	21.20
Energy supplied from grid [MWh/year]	51.69	37.70	28.74	22.82
Autonomous time [%hours/year]	37.5 (no load)	70.15	69.12	78.26
Number of hours with voltage problem (V<0.9pu)/day	3	3	0	0

According to the above table, the active power requirement from grid has been decreased drastically by the PV-DeBES-CeBES integration from 32.12 kW to 21.20 kW. Likewise, the energy supplied from grid has been also decreased from 51.69 MWh to 22.82

MWh representing about 55 % reduction. Moreover, the LV distribution system could be operated as an isolated microgrid with an autonomous operation time of 78 % per year. Additionally, the under voltage problem has been completely removed thanks to DeBES integration and its decentralized control.

III.4.4.3 Comparison between grid reinforcement and PV-BES integration

In this work, the actualized cost method is employed to evaluate the two different proposed solutions over *N* years. This actualized cost takes into account the capital expenditure (CAPEX) and the operation expenditure (OPEX) of the energy losses in the LV distribution system. In addition, the reduction of the energy consumed by the loads thanks to the Ce-BES has been added in the cost computation. Then the energy used is defined as the energy consumed by the loads plus the energy losses.

The actualized cost [*APCR11*] thus can be expressed by:

$$C_{total\_act} = \sum_{t=0}^{N} \frac{C_{invest}(t) + C \times En_{used}(t)}{(1+i)^t} \quad \text{(III-7)}$$

Where:

- C_{total_act} : total actualized cost in $kUSD$
- $C_{invest}(t)$: investment cost in the year t in $kUSD$
- C : electricity price in $kUSD/kWh$
- $En_{used}(t)$: energy used in the year t in $kUSD$
- i : actualization rate in $\%$

The planning period for the analysis is 15 years and the actualization rate is estimated to be 12 % [*VGBA17*]. The list of the parameters for the economic analysis is shown in Table III-3.

Table III- 3 : Parameters for the economic analysis [*VGBA17*]

Parameters	**Value**
Planning period	15 years
Actualization rate	12 %
Electricity cost	0.3 USD/kWh[*EAC15*]
ABC-2x50 mm^2 cable cost	1.6 kUSD/km
ABC-2x95 mm^2 cable cost	3 kUSD/km
PV panel cost	1.2 kUSD/kWp[*ECOS17*]
Battery energy storage cost	0.13 kUSD/kWh[*ECOS17*]

PV inverter cost	0.72 kUSD/kW[*NIPO05*]
Bi-directional inverter cost	1.155 kUSD/kW[*NIPO05*]

The CAPEX at the year 1 of the two strategies is detailed in Table III-4. For this primary study, since there is no available information about the construction cost of the LV distribution grid in Cambodia, the actualized cost takes into account only the components costs (i.e. cable, PV, BES and converter).

Table III- 4 : CAPEX of the two strategies

Items	**Proposed solution**			
	1st : Grid reinforcement		*2nd : PV-BES integration*	
	Values	Cost(kUSD)	Values	Cost(kUSD)
2x50 mm^2 cable	0 m	0	211 m (extension)	0.338
2x95 mm^2 cable	955 m	2.866	0 m	0
PV	0 kWp	0	1.54x6 kWp	11.088
DeBES	0 kWh	0	17.4 kWh	2.262
CeBES			19.25 kWh	2.50
Grid connected inverter	0 kW	0	1.6x6 kW	6.91
BES Bi-directional inverter	0 kW	0	6kW (DeBES) and 16kW(CeBES)	20.79
Total cost		**2.866 kUSD**		**43.888 kUSD**

It can be seen that the initial CAPEX for the second solution is about 15 times higher than the first solution. When the OPEX costs are integrated and the total actualized cost is computed, the tendency is reversed. The OPEX cost consists in the cost of the energy the DSO will have to pay. The 2nd strategy enables to increase the autonomy of the LV grid by decreasing the energy coming from the MV grid. In this case, the energy required without the PV-DeBES-CeBES to supply all the customers is about 47.1 MWh and with this system about 22.8 MWh, i.e. 2 times lower.

The actualized cost of the 1st proposed solution is about 94 kUSD and 92 kUSD for 2nd proposed solution. The cost is almost the same for both strategies however the cost of the 1st strategy is expected to increase with the planning period. Also, two advantages which cannot be quantified are the cancelation of the reverse power flows and the ability of the LV network to be operated independently from the MV network during a high period (78% of the year) thanks 2nd solution. Therefore, we can conclude that the 2nd proposed solution with

PV-BES integration is selected our test system in case without taking into account the line construction and maintenance costs.

III.5 Conclusion

In this chapter, a new way of planning non-electrified LV distribution grid has been proposed. It consists of integrating PV and storage as an alternative to grid reinforcement. In rural LV distribution network, the load density is low leading to long lines with problems of under-voltage. The traditional solution consists in reinforcing the network. The introduction of a decentralized battery (DeBES) enables to solve the problem of low-voltage constraint. PV is also introduced so as to increase the local production and decrease the power coming from the MV grid). Finally, a centralized storage (CeBES) enables to prevent the electricity produced by the PV to be injected in the MV network and also to bring the LV network as autonomous as possible. This system PV-DeBES-CeBES aims at creating a microgrid as autonomous as possible from the main grid. Several algorithms have been described to size this microgrid and applied on a real case study. The conclusion was the followings:

- The creation of the microgrid requires a high CAPEX investment at the first year,

- The OPEX reduce by twice and on the long term this solution is more economic than the reinforcement.

- Other property not quantified have to be pointed out: the microgrid can be autonomic 70% of the year and the peak power has been reduced by two. In other words, potential cost of reinforcement on the MV size would be drastically reduced or avoided.

- The control of the microgrid is simple and based on a two sensors (one for the centralized battery and another for the decentralized battery) so as to prevent from having to develop a complex and expensive ICT system.

REFERENCES

[*Apcr11*] M.-C. Alvarez-Hérault, D. Picault, R. Caire, B. Raison, N. HadjSaid, and W. Bienia, "A Novel Hybrid Network Architecture to Increase DG Insertion in Electrical Distribution Systems," *IEEE Trans. Power Syst.*, vol. 26, no. 2, pp. 905–914, 2011.

[*Cifo03*] R. M. Ciric, A. P. Feltrin, and L. F. Ochoa, "Power flow in four-wire distribution networks-general approach," *IEEE Trans. Power Syst.*, vol. 18, no. 4, pp. 1283–1290, 2003.

[*Eac15*] EAC, "Report on power sector of the Kingdom of Cambodia," 2015. [Online]. Available: https://eac.gov.kh/publication/report/.

[*Ebbh11*] R. Ebrahimi, A. Babaee, and M. Hoseynpoor, "Evaluation and Calculation of Overhead Line Impedance in Distribution Networks," *Aust. J. Basic Appl. Sci.*, vol. 5, no. 8, pp. 1278–1284, 2011.

[*Ecos17*] EcoSun, "EcoSun Solar Appliance Products," 2017. [Online]. Available: http://ecosun-products.webs.com/.

[*Iba93*] K. Iba, "Reactive power optimization by genetic algorithm," *Conf. Proc. Power Ind. Comput. Appl. Conf.*, pp. 1–6, 1993.

[*King04*] N. R. King, "General requirements of electric power technical standards of the kingdom of cambodia," 2004. [Online]. Available: http://eac.gov.kh/wp-content/uploads/2014/08/General-Requirements-of-Electric-Power-Technical-Standards.en_.pdf.

[*Mjcx14*] M. Mao, P. Jin, L. Chang, and H. Xu, "Economic analysis and optimal design on microgrids with SS-PVs for industries," *IEEE Trans. Sustain. Energy*, vol. 5, no. 4, pp. 1328–1336, 2014.

[*Mura09*] K. V. S. R. Murthy and M. R. Raju, "Electrical Energy Loss in Rural Distribution Feeders- a Case Study," vol. 4, no. 2, pp. 33–37, 2009.

[*Nasa17*] Nasa, "ASDC _ Processing, archiving, and distributing Earth science data at the NASA Langley Research Center," 2017. [Online]. Available: http://eosweb.larc.nasa.gov.

[*Nipo05*] K. Nipon, "Photovoltaic Hybrid Systems for Rural Electrification in the Mekong Countries," University of Kassel, 2005.

[*Phok16*] C. Phok, "contribution to electric energy generation for isolated-rural areas using 2nd life components and renewable energies: modelling and control of an induction generator." Toulouse, 2016.

[*Refe13*] REFEDC, "Program for the development of rural electrification of Electricité Du Cambodge (EDC) through department of Rural Electrification Fund (REF)," 2013. [Online]. Available: http://ref.gov.kh/page/home.

[*Smas17*] S. SMA Solar Technology AG, "Battery Inverters," 2017. [Online]. Available: http://www.sma.de/en/products/battery-inverters.html.

[*Vgba17*] V. Vai, E. Gladkikh, L. Bun, M.-C. Alvarez-Hérault, and B. Raison, "Study of low-voltage distribution system with integration of PV-battery energy storage for urban area in developing country," in *IEEE-EEEIC / I&CPS Europe*, 2017, pp. 1–6.

[*Vgba17*] V. Vai, E. Gladkikh, L. Bun, M.-C. Alvarez-Hérault, and B. Raison, "Low-Voltage Distribution System Planning under Load Demand Uncertainty: Growth Rate with Connection of New Loads," in *IEEE International Electrical Engineering Congress (iEECON)*, 2017, pp. 1–4.

[*Vgba17*] V. Vai, E. Gladkikh, L. Bun, M.-C. Alvarez-Hérault, and B. Raison, "Planning of low-voltage distribution systems with uncertainty on load demand in urban areas," in *IEEE-EEEIC / I&CPS Europe*, 2017, pp. 1–6.

Chapter IV

Planning the LV Distribution System with Photovoltaic and Battery Energy Storage – Case Studies

Chapter IV

Planning the LV Distribution System with Photovoltaic and Battery Energy Storage – Case Studies

Summary

IV.1 Introduction

In chapter III, a new way of planning the LV distribution grids using PV and storage as well as the required algorithms have been presented. In this chapter, we propose to apply it on two cases studies, an urban and a rural area. In both case, the first step will be to design the network and the second step will be to size the PV (for both areas), to locate, size and control the decentralized storage (only for the rural area) and to size the centralized storage (for both areas). Figure IV-1 gives an example of LV distribution grid with the new planning method. In the case of the rural network, the uncertainty on the hourly load profile on the adjustment of V_{set} is studied.

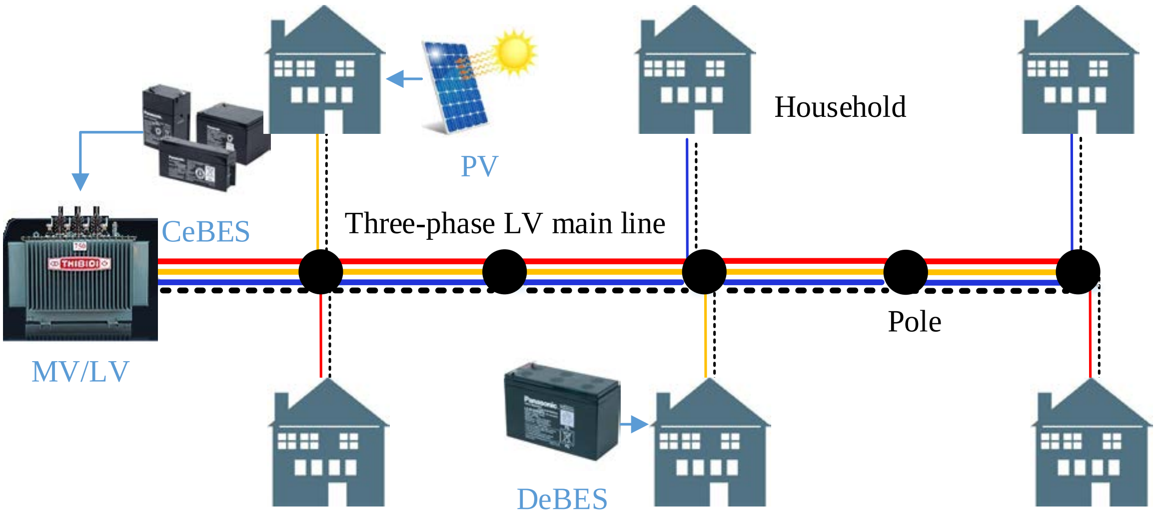

Figure IV- 1: Example of a low-voltage distribution grid with integrated PV-BES

IV.2 Methodology

The proposed method consists in planning both urban and rural area by integrating the Decentralized PV (DePV), Decentralized BES (DeBES) and Centralized BES (CeBES) in the LV distribution system using a sequential approach. The approaches used for planning an urban area and a rural area are different. Indeed, in urban area, the load density is high with short conductor lengths whereas in rural area conductor lengths are long. Current constraints thus will almost always occur in urban area whereas the voltage constraints will appear in rural area. In this context, planning solutions will be different regarding the type of constraints. The global algorithm proposed will be then different for rural and urban areas and are described in the following section. The main difference is the integration of the DeBES in the case of rural area and not in the case of urban area since the objective of DeBES in this work is to solve under voltage problems.

IV.2.1 LV urban network planning

The proposed method aims at finding the optimal topology as well as sizing the DePV and CeBES while satisfying the bus voltage constraints ($0.9pu \le V \le 1.06pu$) and the current flowing through the lines constraints (maximal admissible current of conductors). In this planning study, the four following objectives will be sequentially achieved:

- Optimal radial topology using the two strategies presented in chapter 1(shortest path fit bin packing and MIQCP),

- Maximization of the DePV penetration,

- Optimal sizing of the CeBES

A flowchart showing the various steps of the proposed algorithm is shown in Figure IV-2. The planning period is 15 years with an annual growth rate arbitrary equal to 3%. Then, we size the single-phase PV units which are integrated into the grid at the households' nodes. Then, the CeBES is also sized in order to solve a potential problem of reverse power flow and also to increase the autonomous operation of the LV network to relieve the MV network. The comparison between the two strategies is discussed thanks to the computation of the actualized cost in the last part of this work.

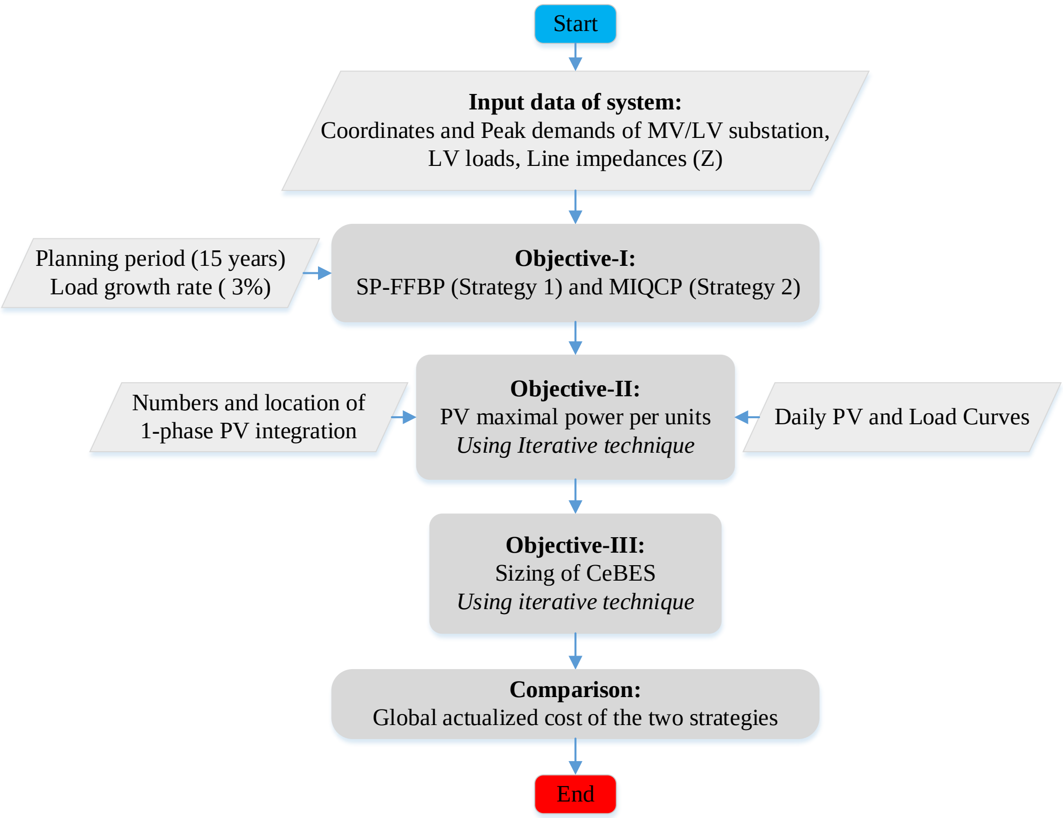

Figure IV- 2 : Flowchart of the planning algorithm in urban area

IV.2.1.1 Actualized cost

The actualized cost of the systems will be computed over *N* years for different topologies. It computation is given in section III.4.4.3 of chapter III.

IV.2.1.2 Sizing of PVs

There are a lot of uncertainties regarding the PVs locations and power production in the future. Therefore, it is assumed that the consumer having a high demand is interesting to use PV. Then the highest load consumption per phase of each feeder is equipped with a single-phase PV unit. The objective is to find the maximum PV penetration in initial year which can be integrated into grid while respecting voltage and current constraints on each feeder. This PV penetration level is defined as the ratio between the peak power of PV and the peak consumption of grid. It is expressed as:

$$PV\,penetration(\%) = \frac{Peak\ Power\ of\ \ PV(kW)}{Peak\ Consumption\ of\ \ Grid(kW)} \qquad \text{(IV-1)}$$

In this equation, the denominator stands for a maximum value of the total demand of the grid consumers. The power of the PV units is determined using the flowchart of Figure III-5 explained in chapter III.

IV.2.1.3 Sizing of CeBES

The centralized battery is sized and controlled using the methods explained in section III.3.2.3 of chapter III. We remind that the objective of the battery is to avoid reverse power flow while optimizing the autonomy of the LV network.

IV.2.2 LV rural network planning

For planning a rural area, the proposed method will address an optimal topology with load balancing and minimizing power loss using the Shortest Path (SP) and First-Fit Bin-Packing (FFBP) method and size the PV, DeBES and CeBES to respect the voltage and current constraints. The MIQCP method is not used because the problem is simple in this case. The four following objectives will be achieved in this planning study of a rural area:

- Optimal radial topology with load balancing using SP and FFBP (see chapter II)

- Maximization of the DePV penetration,

- Optimal sizing of the DeBES as well as the decentralized control algorithm

- Optimal sizing of the CeBES

Figure IV-3 presents a flowchart of proposed method for planning in rural area.

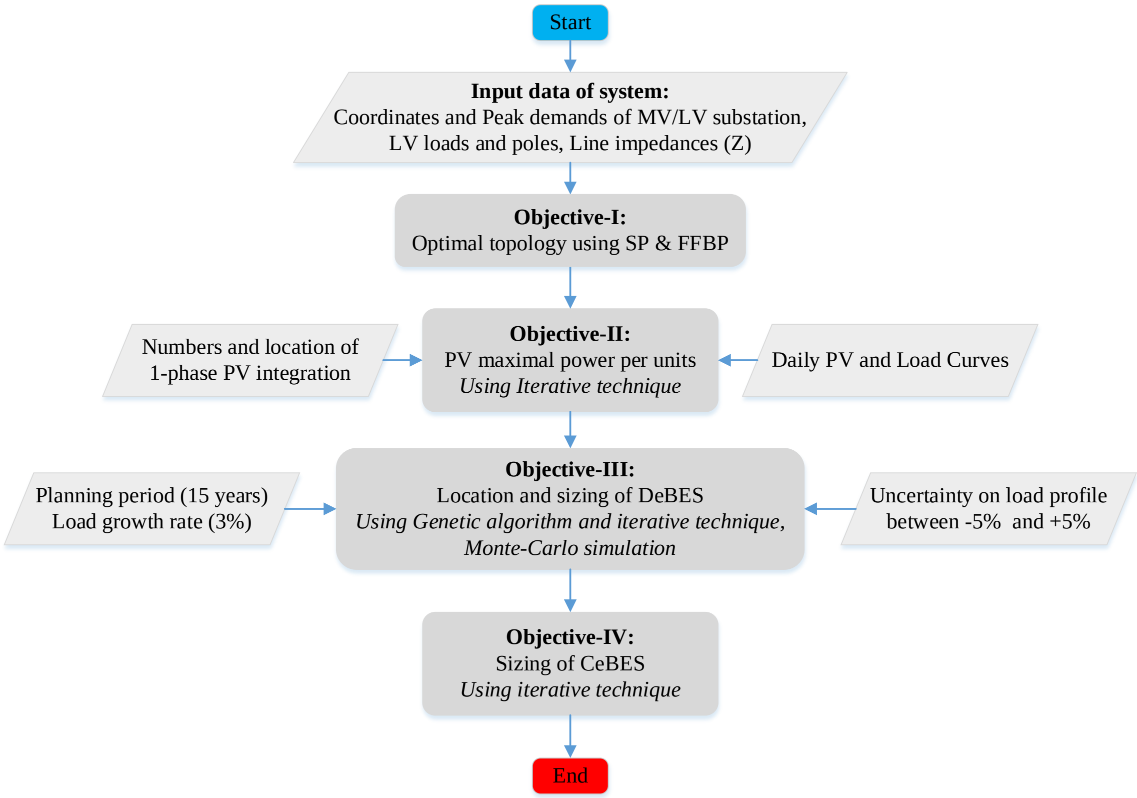

Figure IV- 3 : A flowchart of proposed method in rural area

As shown in Figure IV-3, the data of loads demand and their locations are requested as input at first. Then, a radial topology is obtained by shortest-path [*CORA14*][*VGBA17*]. Next, we search the optimal topology with load balancing by using first-fit bin-packing [*RARA07*][*VGBA17*] on each pole; that means the households are powered from energy meters at pole. After having obtained the optimal topology, we need to define the amount and the location of single-phase PV units and then to find their maximum power penetration according to PV-load curves by using the same iterative technique as the one described in chapter III. After having got the sizing of PVs, we find the optimal location of DeBES by using a genetic algorithm (see in chapter III) [*IBA93*]. Then, we size its minimum capacity by using an iterative technique at the end of the planning year with a growth rate of 3 %[1].

IV.2.2.1 Location, sizing and control of the DeBES

The method used to locate, size and control the DeBES is the same as the one developed in chapter III except that it is repeated for the three phases in this case. We remind that the objective of this storage is to relieve the low-voltage constraint due to the load.

[1] This is an assumption as hypothesis testing

IV.2.2.1.1 Integration of the uncertainties on load

To cope with the problem of uncertainty on load profile during the planning study, a Monte-Carlo (MC) simulation is employed to get the statistical distribution of the voltage at the DeBES. For each Monte Carlo simulation, uncertainties on the load profile are integrating by introducing a variation of +/-5% around the profile. The mean value of these simulations will be used to obtain V_{set}.

IV.2.2.2 Sizing of CeBES

The sizing strategy of the CeBES is the same as the one presented in chapter III.

IV.3 Test systems

IV.3.1 In urban area

IV.3.1.1 Site study

The village located in Sangkat Veal Sbov, Phnom Penh (Cambodia) is selected as a case study in this work. The LV distribution system is supplied from the 22-kV/0.4-kV Transformer at bus 1. The total active and reactive power is respectively 200 kW and 66 kvar for the initial year. Since there is no information available on the load demand for all the households at that site, these data are obtained by using a random draw following a normal distribution with a mean of 5 kW and a standard deviation of 0.5 kW. Figure IV-4 presents the site study and its detailed information (load demands and their coordinates) is provided in Appendix IV-A.

Figure IV- 4 : Site study in Phnom Penh [11°32'04.9"N 104°58'06.1"E]

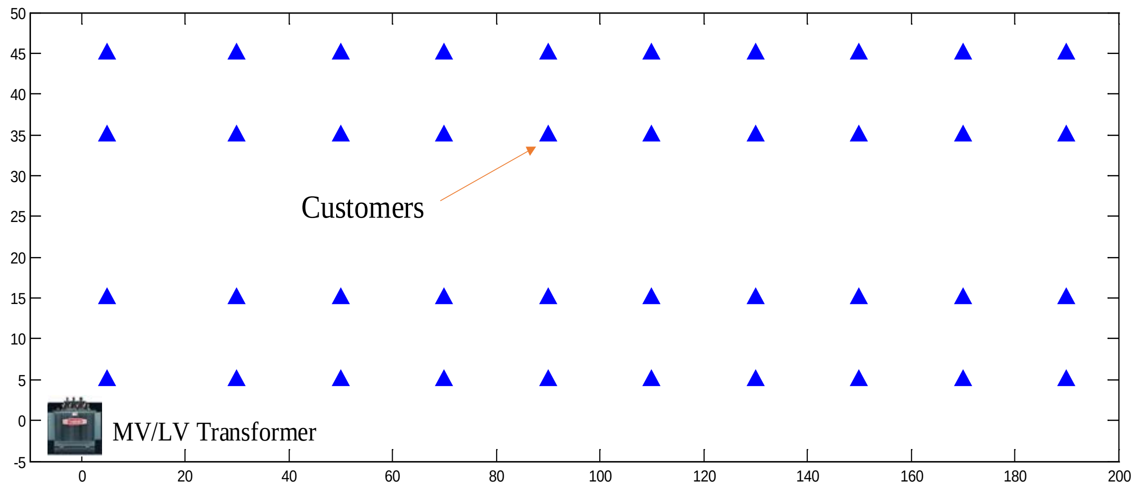

Figure IV- 5 : Urban area case study

IV.3.1.2 Simulation results and discussion

IV.3.1.2.1 Topology

This part will provide two different radial topologies by using SP and FFBP (strategy1) and MIQCP (strategy 2) separately as illustrated in Figure IV-6 and Figure IV-7. In both cases, four feeders supply the customers. In case of the 1st strategy, all the feeders are three-phase whereas in strategy 2, feeders are single and two-phase. The reason is due to the fact that strategy 2 aims at minimizing both the conductor and the load balancing but strategy only tries to optimize the load balancing.

Furthermore, a classical cable size of 70 mm^2 (I_{max}=185A) is used for the main line and 16 mm^2 (I_{max}=66A) from main line to each energy meter which is presently the standards in Cambodia. Figure IV-8 shows the voltage profile for the peak load (see Appendix III-B) of the two strategies. The voltage drop of strategy 2 is higher than strategy 1 but it remains within the limits at the end of planning period. Indeed, in strategy 2 voltage constraints are not integrated in the set of constraints of the objective function.

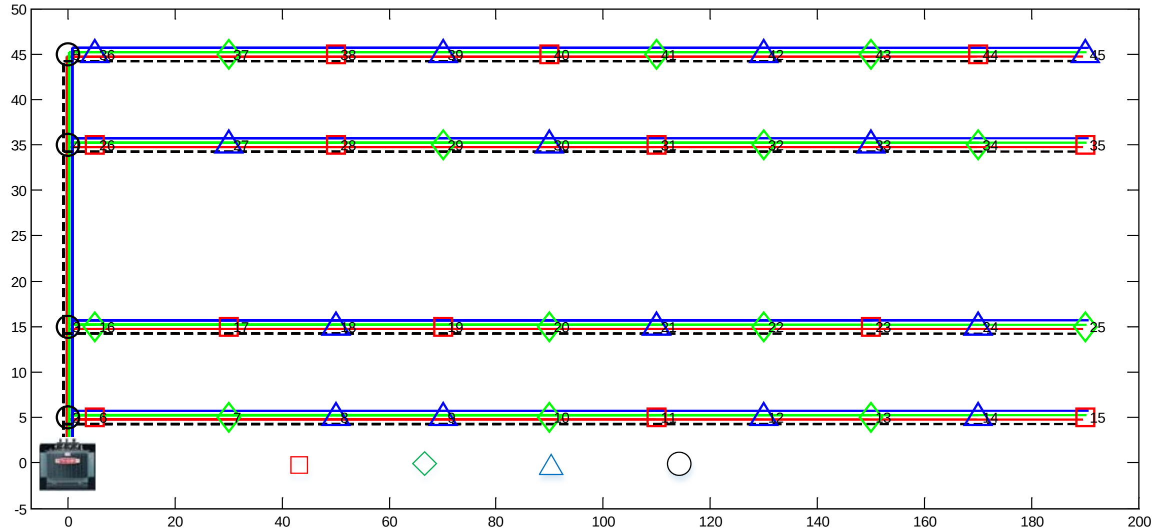

Figure IV- 6 : Optimal topology by SP and FFBP algorithm (Strategy 1)

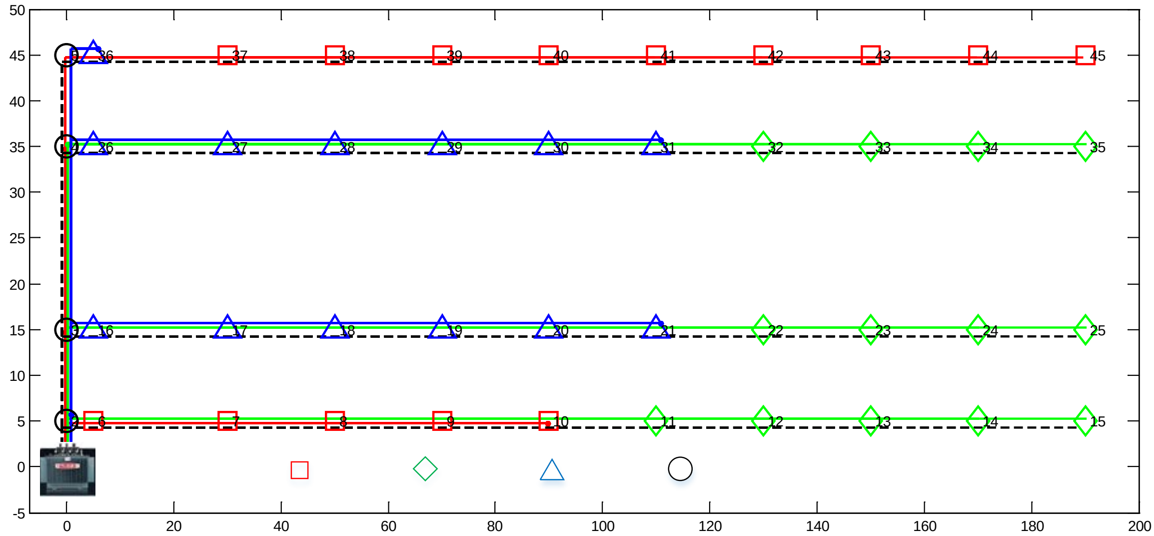

Figure IV- 7 : Optimal topology by MIQCP algorithm (Strategy 2)

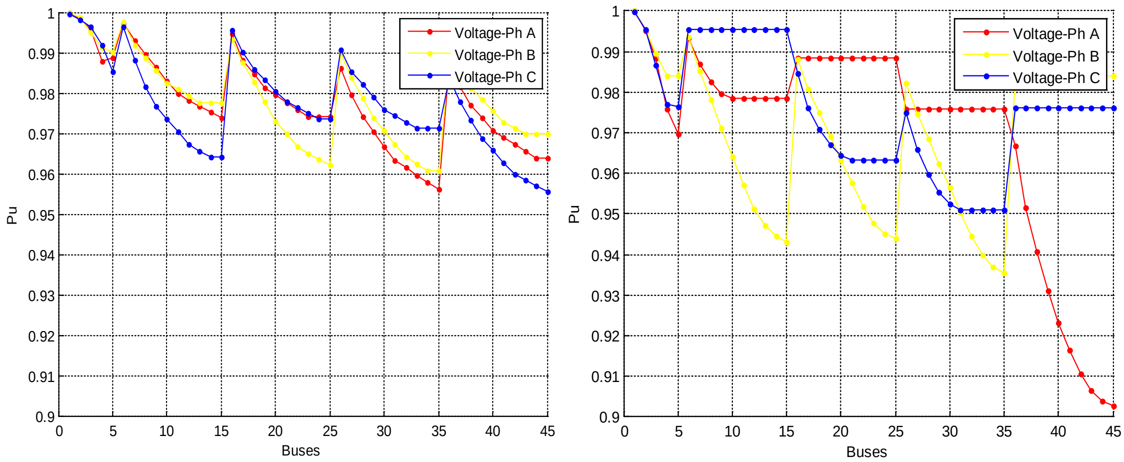

Figure IV- 8 : Voltage profile for the peak load for year 15 using two different strategy (Strategy 1-left, Strategy 2-right)

IV.3.1.2.2 PV penetration

As mentioned above, a single-phase PV per feeder will be installed at the households having the highest demand consumption. A simulation result of PV penetration is given in Table IV-1 for strategy 1. It can be seen that the sizing of all the single-phase PVs are nearly identical in the whole system and the total PV penetration is about 32% of 200kW total loads. As the phases of the network built are balanced, it is logical that the maximal PV penetration on each phase is equal. In order to compare, strategy 1 and strategy 2, the PV scenarios found for strategy 1 will be applied to strategy 2.

Table IV- 1 : Simulation of PV Penetration in urban area

Feeders	Buses of installed PV	Max PV (kWp)	PV Penetration (%)
F1	9	15.90	31.76
F2	22	15.86	
F4	31	15.85	
F4	36	15.91	

IV.3.1.2.3 Sizing of CeBES

Figure IV-9 shows the histogram of the annual power at the MV/LV substation without PV-CeBES integration for each topology for the initial year; the maximum active power at the MV/LV substation is about 206 kW (strategy 1) and 216 kW (strategy 2). This maximum power is not reduced by the PVs integration but there are some reverse power flows (-19.4 kW{strategy 1}/-19.1 kW{ strategy 2}) at the MV/LV substation as depicted in Figure IV-10 since the peak loads happened when the PV production is very low.

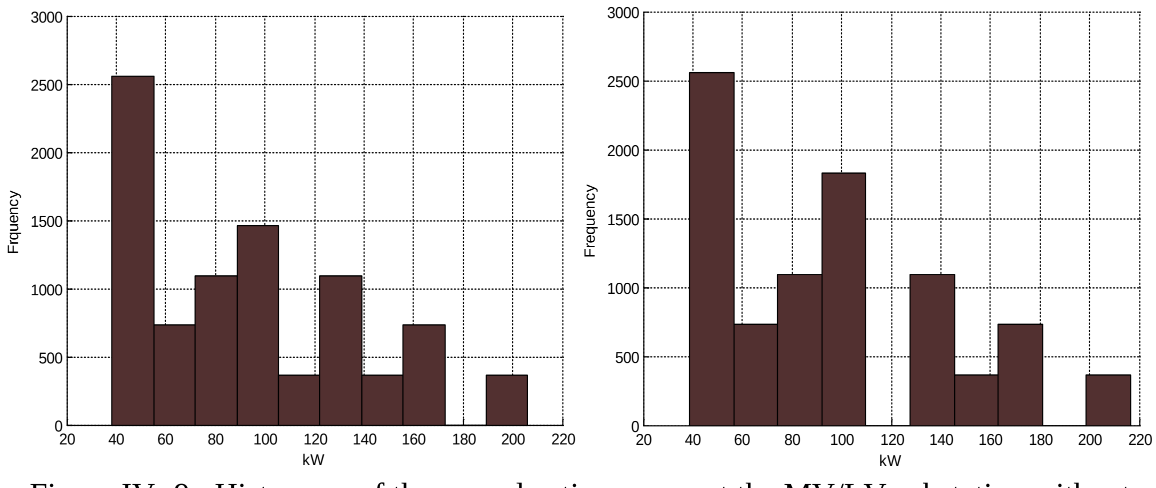

Figure IV- 9 : Histogram of the annual active power at the MV/LV substation without PV-CeBES (strategy 1-left, strategy 2-right) for the initial year

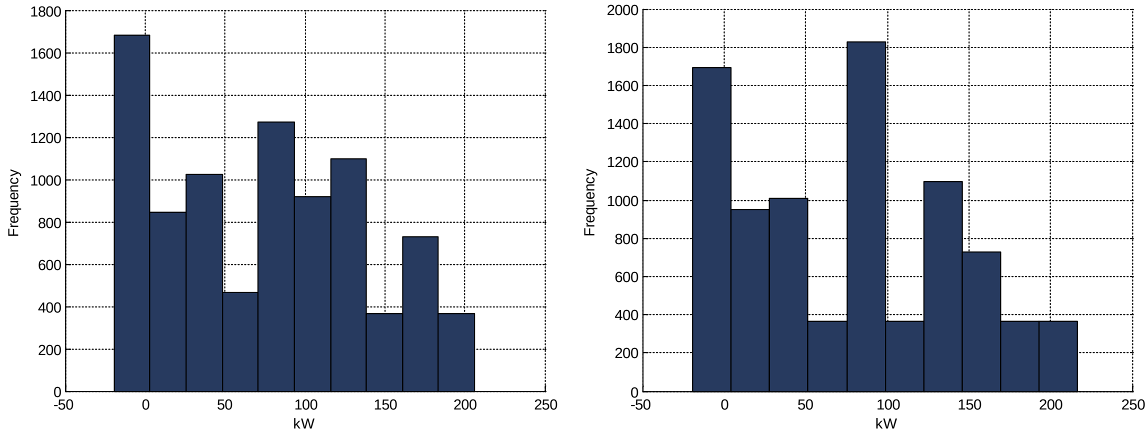

Figure IV- 10 : Histogram of the annual active power at the MV/LV substation with PVs integration (strategy 1-left, strategy 2-right) for the initial year

However, the reverse power flow is removed as well as a reduction of the electricity coming from the MV network thanks to the CeBES deployment as seen in Figure IV-11. Furthermore, a histogram of the energy in the CeBES is shown in Figure IV-12; and we found that the sizing of CeBES is about 90 kWh for each topology.

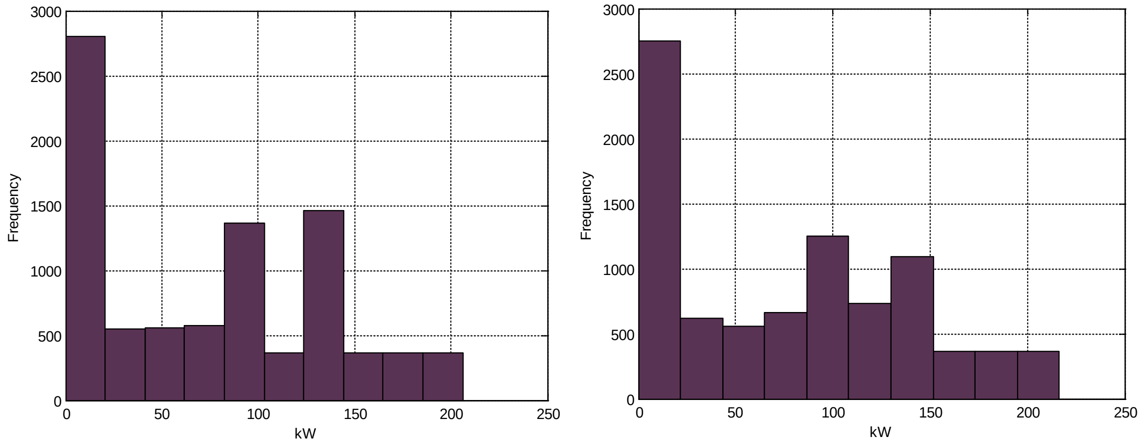

Figure IV- 11 : Histogram of the active power per year at the MV/LV substation with PV-CeBES (strategy -left, strategy 2-right) for the initial year

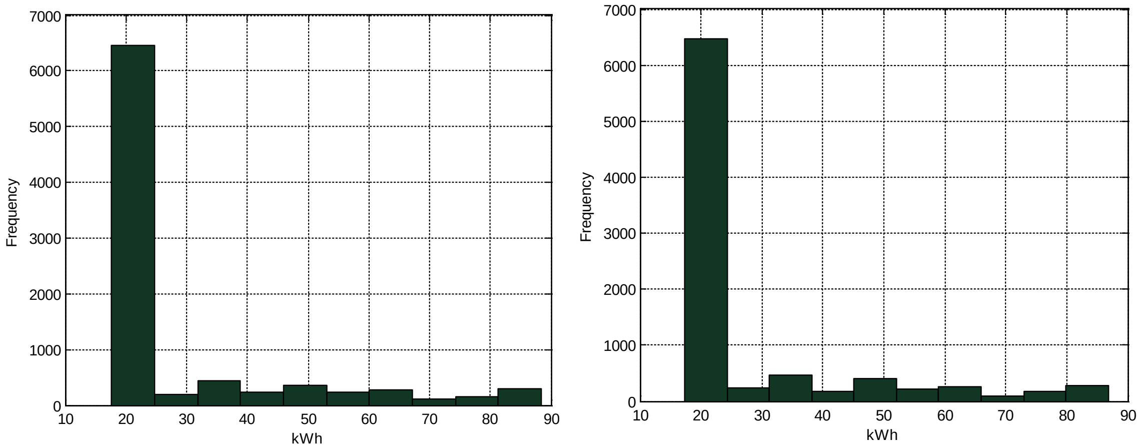

Figure IV- 12 : Histogram of the annual energy of CeBES (strategy 1-left, strategy 2-right) for the initial year

In addition, Table IV-2 provides the simulation results of two different proposed algorithms for the initial year in the urban area.

Table IV- 2 : Summary of simulation results for the initial year in the urban area

Items	***Without-PV-CeBES* (strategy *1*/ strategy *2)***	***With-PV* (strategy *1*/ strategy *2)***	***With-PV-CeBES* (strategy *1*/ strategy *2)***
4 single-phase PV [kWp]	0/0	15.85-15.86-15.90-15.91	15.85-15.86-15.90-15.91
Centralized 3ph-BES [kWh]	0/0	0/0	88.37/ 86.80
Energy used [MWh/year]	818.98/ 841.38	673.81/ 695.20	653.13/ 674.97
Active power from grid [kW]	206.14/ 216.48	206.14/ 216.48	206.14/ 216.48
Autonomous operation time [%/year]	0/0	16.67/ 16.67	26.69/ 26.54

As seen in Table IV-2, the energy supplied from the grid has been decreased from 818 MWh to 653 MWh for strategy 1 and from 841 MWh to 674 MWh per year thanks to PV-CeBES integration. In addition, the LV distribution system in our case study can be operated as an isolated microgrid with an autonomous operation time of 26 % due to the support of the CeBES for each topology for the initial year.

Table IV-3 shows the simulation results at the end of the planning year. As the loads demand is increased year by year, all the PV production is locally consumed and no revers power flows appear at the MV/LV substaiton. As seen in Table IV-3, there is no energy stored in CeBES and then the autonomous time of the network is 0%. However, the energy used in network is still decreased by about 13% for strategy 1 and 12% for strategy 2 thanks to PV integration.

Table IV- 3 : Summary of simulation results for the end of the planning year in the urban area

Items	***Without-PV-CeBES* (strategy *1/* strategy *2)***	***With-PV* (strategy *1/* strategy *2)***	***With-PV-CeBES* (strategy *1/* strategy *2)***
Energy stored in CeBES [kWh]	0/0	0/0	0/ 0
Energy used [MWh/year]	1286.6/1343.6	1119.3/ 1175.2	1119.3/ 1175.2
Active power from grid [kW]	326.04/353.12	326.04/353.12	326.04/ 353.12
Autonomous operation time [%/year]	0/0	0/ 0	0/ 0

Furthermore, the histogram of simulation results at the end of the planning period are provided in Appendix IV-C.

IV.3.1.2.4 Comparison between SP-FFBP and MIQCP

In this part, the actualized cost is computed to compare the two different proposed algorithms. The total time study for the analysis is set to 15 years and the discount rate is estimated to 12 % [*VGBL17*]. The list of parameters for the economic analysis is the same as Table III-3 of chapter III.

The initial costs of the different algorithms for both cases without/with PV-BES integration are listed in Table IV-4 and Table IV-5. For this primary study, since there is no available information about construction cost of LV distribution, thus the actualized cost here is taken into account only for cable cost, distributed generation cost and cost of the energy used in order to validate both proposed algorithms.

Table IV- 4 : Initial cost without PV-BES integration of the proposed algorithms

Items	**Proposed method without PV-BES**			
	Strategy 1 : SP-FFBP		*Strategy 2: MIQCP*	
	Amount	Cost(kUSD)	Amount	Cost(kUSD)
70mm^2 cable	3440 m	3.440	2005 m	2.005
Energy used per year	818.98 MWh	147.416	841.38 MWh	151.448
Total cost	150.856 kUSD		153.453 kUSD	

Table IV- 5 : Initial cost with PV-BES integration of the proposed algorithms

Items	**Proposed method with PV-BES**			
	Strategy 1 : SP-FFBP		*Strategy 2: MIQCP*	
	Amount (unit)	Cost(kUSD)	Amount(unit)	Cost(kUSD)
$70mm^2$ cable	3440 m	3.440	2005 m	2.005
Energy used per year	653.13 MWh	117.563	674.97 MWh	121.495
PV	63.52 kWp	76.224	63.52 kWp	76.224
BES	88.37 kWh	11.488	86.80 kWh	11.284
Grid connected inverter	4*16[2] kWp	46.08	4*16 kWp	46.08
BES Bi-directional inverter	36[3] kW	41.58	36 kW	41.58
Total cost		296.375 kUSD		298.668 kUSD

It can be seen strategy 1 and 2 are quite equivalent in terms of costs. For the initial years, the cost of the solution PV-BES is the double of the cost without them.

Figure IV-13 shows the global actualized cost of the two strategies. As seen in this figure, in case without PV-BES integration, the actualized cost of the 1st strategy is about 8530 kUSD and 8856 kUD for 2nd proposed strategy. Also, these actualized costs have been reduced in the case with PV-BES integration for both algorithms. In all the cases, strategy 1 with PV-BES integration seems to be less expensive that strategy 2.

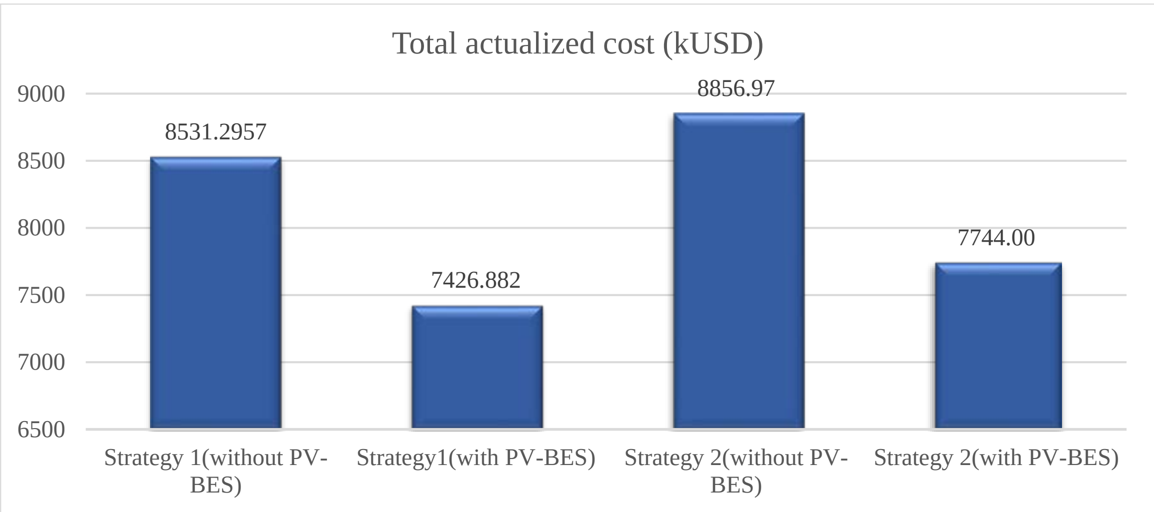

Figure IV- 13 : Total actualized cost of strategy 1 and strategy 2 over 15 years

[2] This value is selected from SMA company[*SMAS17*]
[3] This value is found by searching a maximum discharge of BES (algorithm) and select in SMA company

IV.3.2 In rural area

IV.3.2.1 Site study

A village in rural area has been selected to be a case study which is based on a non-electrified area. The village is named Sandek, located in Batheay district, Kampong Cham, Cambodia as depicted in Figure IV-14. The households are single-phase consumers, located along the road. The households are supplied by a 22-kV/0.4-kV Transformer from the 1st bus to the 129th buses. The total active power is 43 kW with a power factor of 0.95 for the initial year which are taken from normal distribution with a mean of 0.4 kW and a standard deviation of 0.05kW since there is presently no available information. In Cambodia, a classical conductor size usage is 50 mm^2 for main lines and 4 mm^2 for connecting each household to the pole in rural areas.

Figure IV- 14 : Site study in Sandek, Batheay, Kampong Cham, Cambodia [12°08'34.5'N 104°57'30.3'E]

Besides, detailed information on loads (peak demand and coordinates) are provided in Appendix IV-D. The same PV and load curves as the ones used in chapter III are taken.

IV.3.2.2 Simulation results and discussion

IV.3.2.2.1 Optimal topology

The radial topology is performed by using the SP-FFBP algorithm. Figure IV-15 presents an optimal topology with load balancing (Pload-A :13.97 kW, Pload-B : 14.29 kW and Pload-C : 14.73 kW).

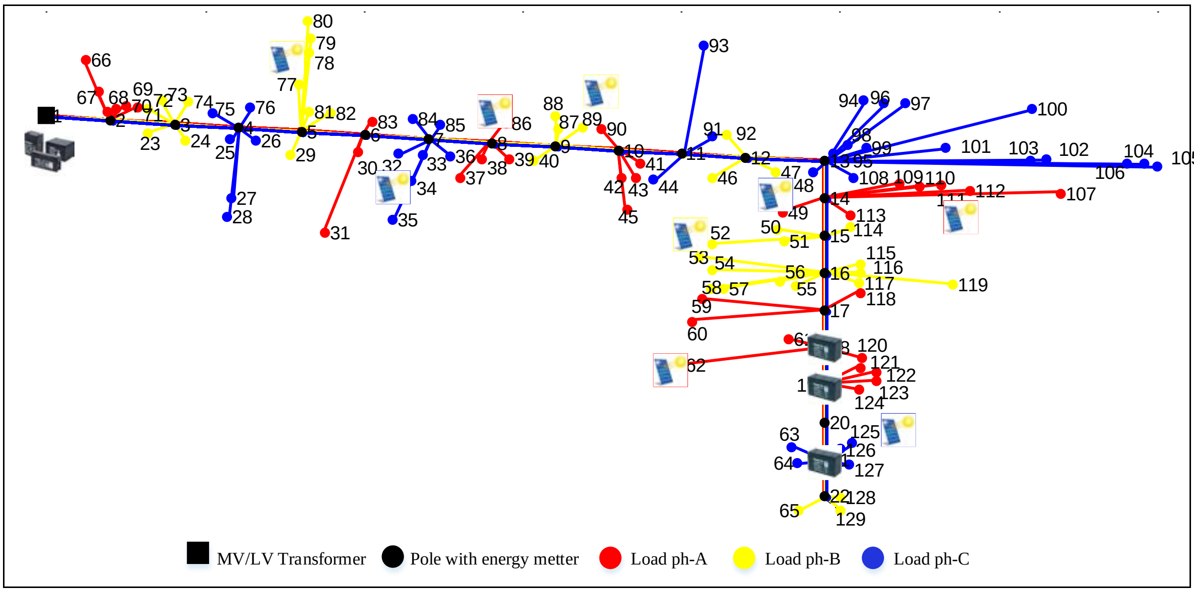

Figure IV- 15 : Radial topology with PV-DeBES-CeBES integration of Sandek village, Batheay, Kampong Cham, Cambodia

IV.3.2.2.2 PV penetration

A single-phase PV unit amount per phase will be assumed in order to validate the proposed method since there is no relevant information about PV integration. Therefore, three single-phase PVs per phase allocate to the highest demand are selected in this part to validate the proposed method. The size of PV is found by using the iterative technique of chapter III. Thus, the sizing of each PV unit which is integrated into the grid is listed in the following table.

Table IV- 6 : Simulation of PV penetration in rural area

Phase connection	Households with PV			Sizing
A	62	86	111	2.40 kWp
B	52	77	89	3.28 kWp
C	32	48	125	3.06 kWp

IV.3.2.2.3 Location and Sizing of DeBES

- **Location of DeBES**

In our work, we propose to use only one DeBES per phase which is integrated to the LV distribution system. By applying the algorithm of chapter III, the optimal location of DeBES is shown in Figure IV-15 and is located at buses 18 (Ph-A), 17 (Ph-B) and 21(Ph-C) which corresponds to the minimal power discharged at 19h to prevent from low voltage constraint. The fitness evolution of the applied GA to find the location and sizing of DeBES is shown in Appendix IV-E.

- **Reference voltage V_{set}**

This part aims at finding V_{set} by taking into account an uncertainty of +/- 5% on the load profile over the planning study. By applying the Monte-Carlo simulation on V_{set} searching by considering the loads at the end of the planning period over 1000 samplings, we obtained the histogram of V_{set} for each DeBES as presented in Figure IV-16 to Figure IV-18.

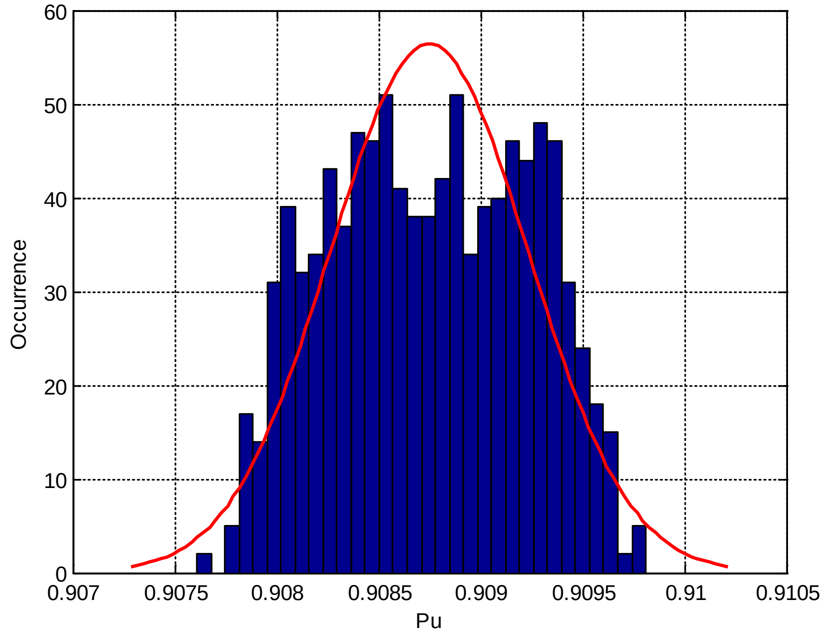

Figure IV- 16 : Histogram of the voltage of the DeBES of phase A at bus 18 for year 15

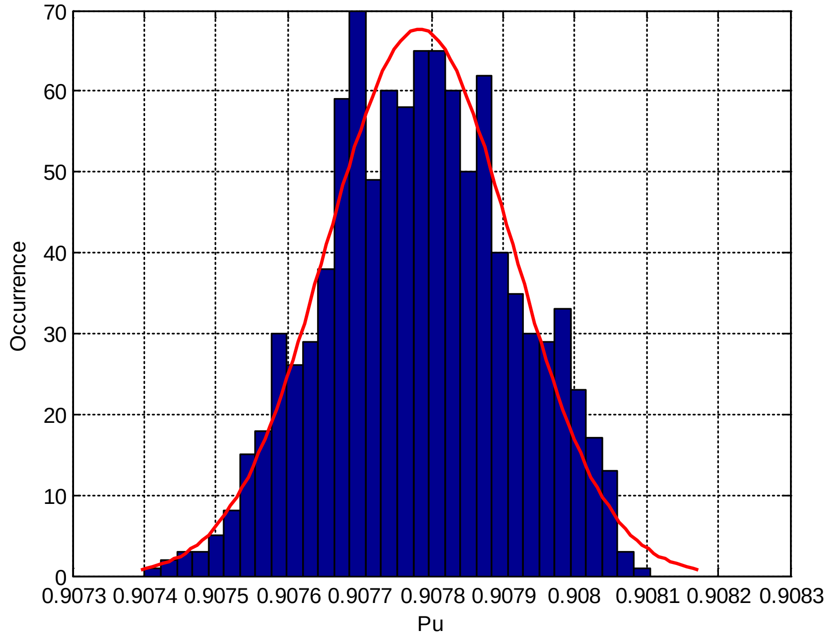

Figure IV- 17 : Histogram of the voltage of the DeBES of phase B at bus 17 for year 15

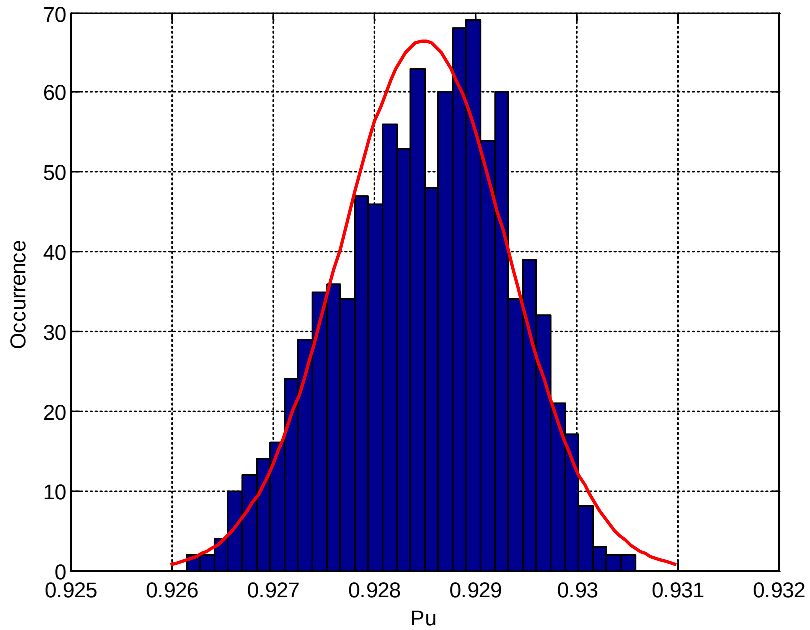

Figure IV- 18 : Histogram of voltage of the DeBES of phase C at bus 21 for year 15

According to these histograms, we can find the average of V_{set} for each DeBES. Therefore, the V_{set} of each DeBES are 0.9087 pu (DeBES phase A), 0.9078 pu (DeBES phase B) and 0.9285 pu (DeBES phase C). These values are used as the reference voltages of the decentralized control of the DeBES without using ICT.

- **Sizing of DeBES**

According to the optimal location of DeBES (see Figure IV-15), the sizing of that battery will be provided by using the iterative technique detailed in chapter III. Figure IV-19 to Figure IV-21 show the maximum charging and minimum discharging of DeBES at bus 18(A), 17(B) and bus 21 (C). The sizing of DeBES is determined by the sum of discharge power from 18h00 to 20h00 and increased by 20% in order protect the battery against extreme operating condition; therefore, the sizing of each DeBES is 13.73 kWh (A), 13.09 kWh (B) and 18.37 kWh (C). Furthermore, the maximum charging and minimum discharging of DeBES at lowest solar radiation are provided in Appendix IV-F.

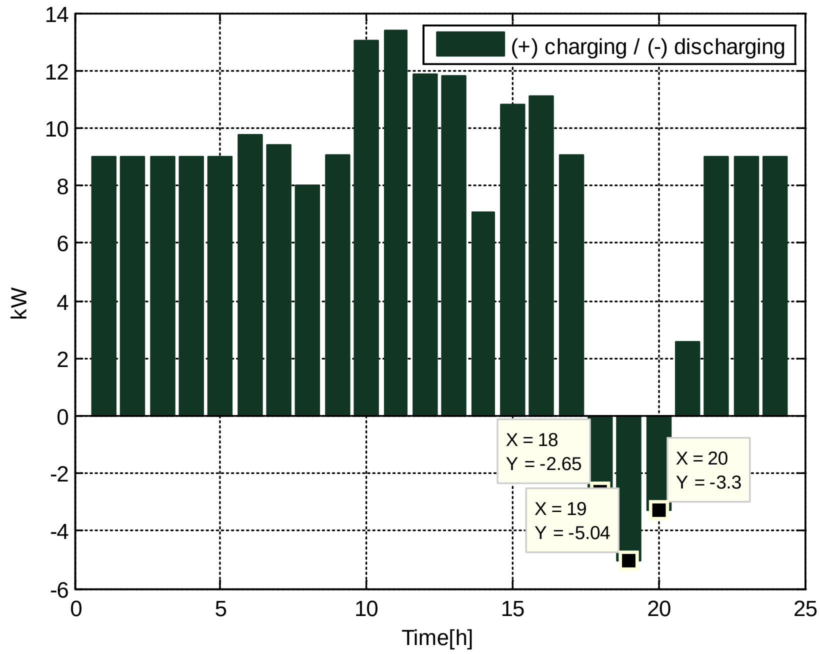

Figure IV- 19 : Max charging (+) and min discharging (-) of DeBES-A power at bus 18 at the end of planning

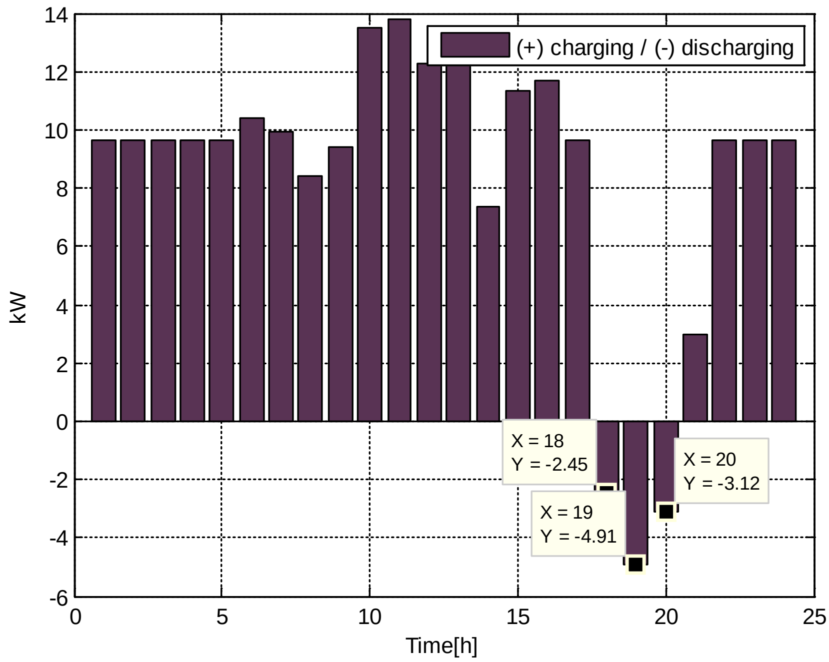

Figure IV- 20 : Max charging (+) and min discharging (-) of DeBES-B power at bus 17 at the end of planning

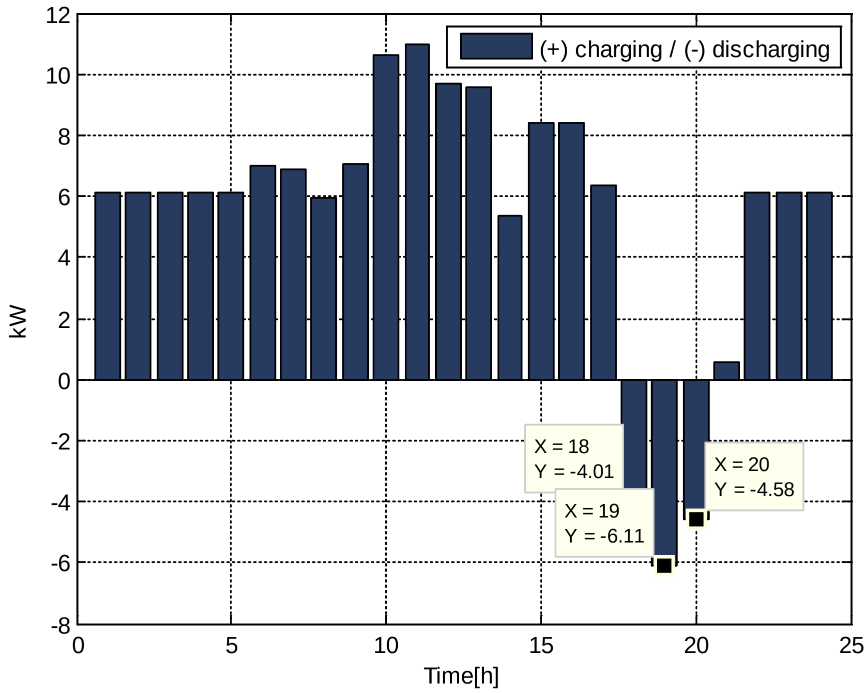

Figure IV- 21 : Max charging (+) and min discharging (-) of DeBES-C power at bus 21 for year 15

Figure IV-22 shows the voltage profile of the complete feeder at 19h00 (peak demand) with and without PV-DeBES integration. According to that figure, it can be seen that the system does not respect the voltage constraint without DeBES but it has been solved by injection power from DeBES.

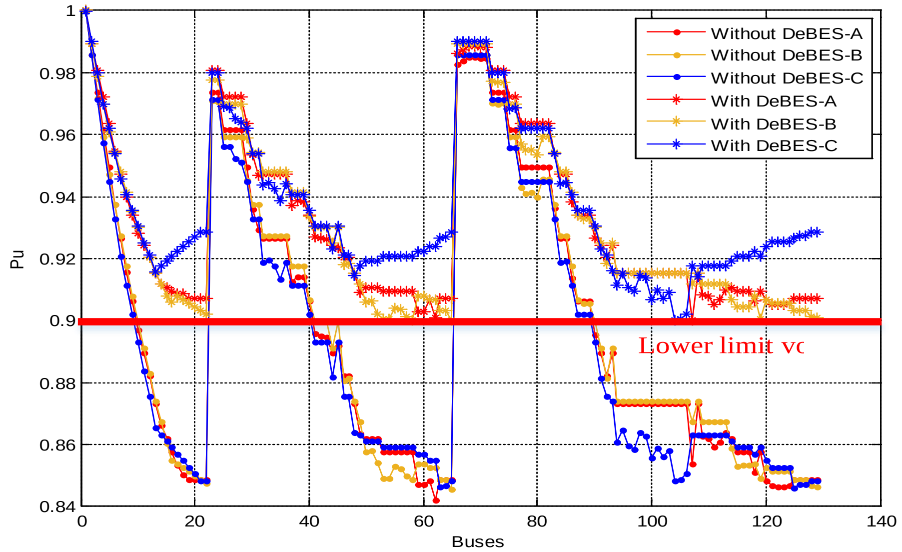

Figure IV- 22 : Voltage profile with/without DeBES at time=19h00 (peak load) at year 15

Figure IV-23 to Figure IV-24 show a result of scheduling and state of charge of DeBES by applying the decentralized control of DeBES over two days of different solar radiation. For this simulation, we assumed that 6/8 kW battery inverter (bi-directional inverter) of

SMA company [*SMAS17*] which is available in Cambodia is used in our case study as it is the maximal power of discharge required for the three batteries as seen in Figure IV-19 to Figure IV-21. As illustrated in Figure IV-23 to Figure IV-25, the operation of the DeBES by decentralized control at the highest and lowest solar radiation are the same. Also, this schedule will be repeated in over a year of simulation for each DeBES.

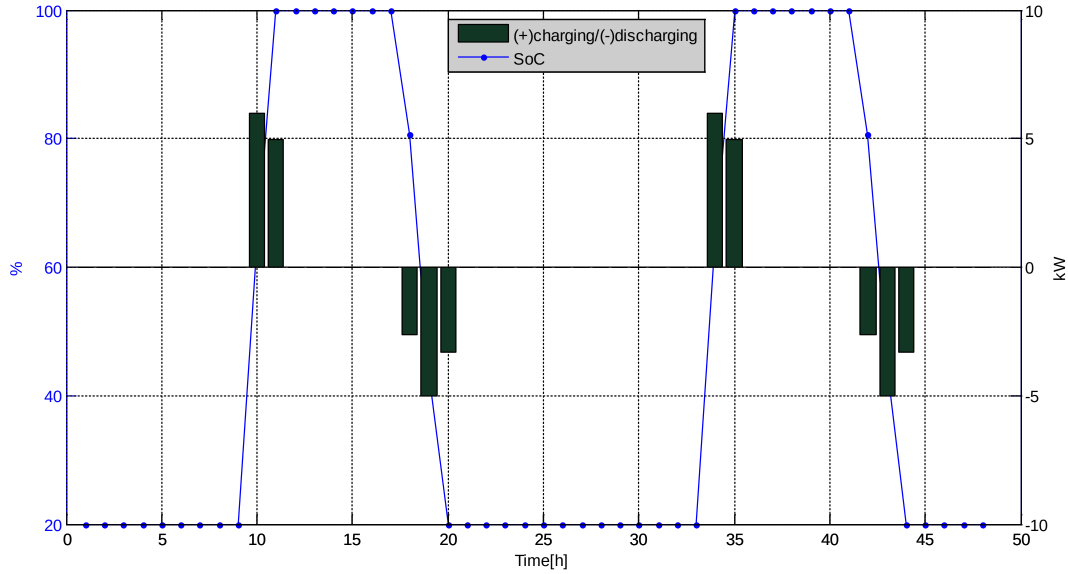

Figure IV- 23 : Operation of the DeBES-A and its State of Charge over two days of different solar radiation by decentralized control at the end of the planning period.

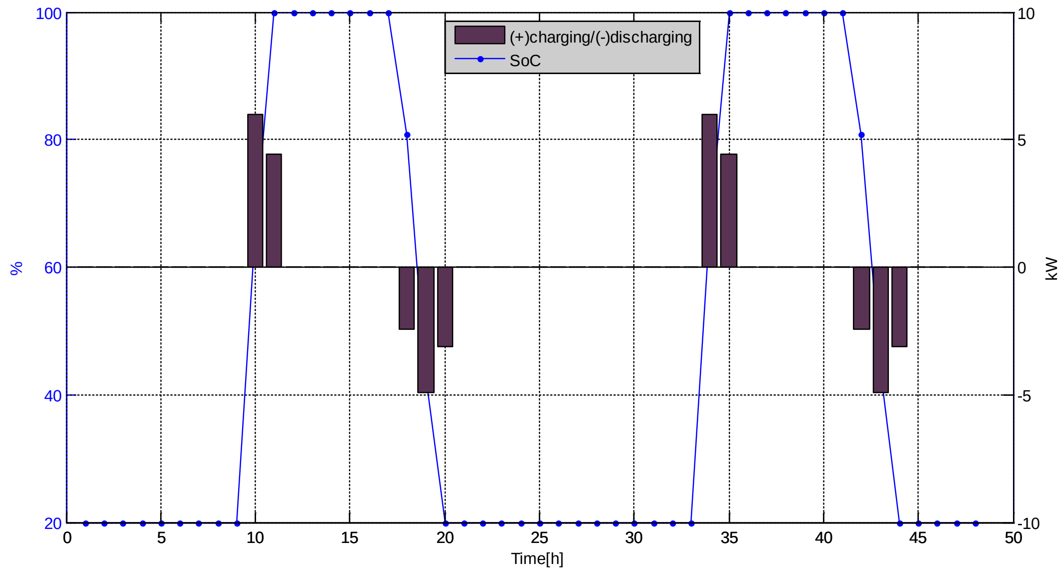

Figure IV- 24 : Operation of the DeBES-B and its State of Charge over two days of different solar radiation by decentralized control at the end of the planning period.

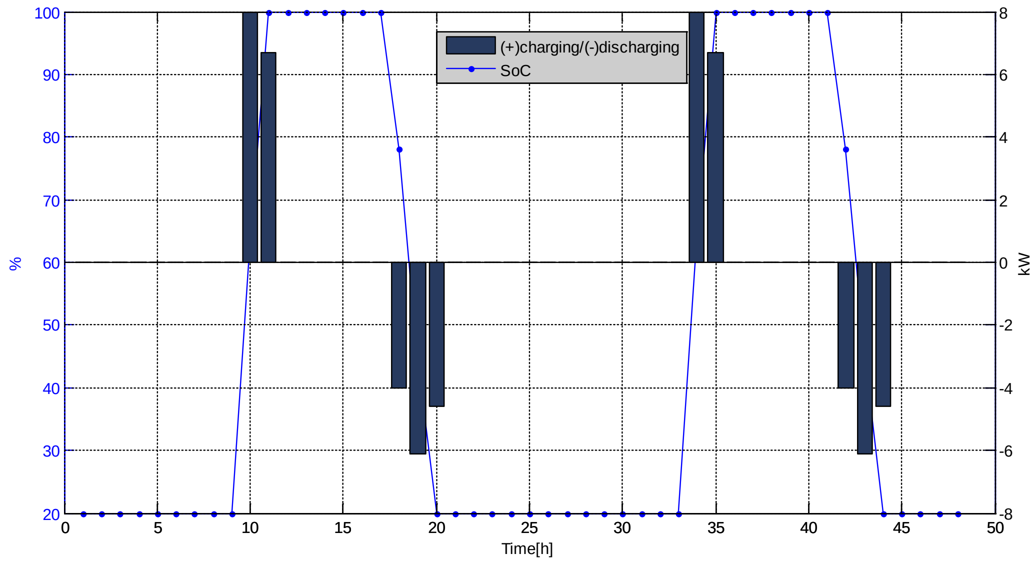

Figure IV- 25 : Operation of the DeBES-C and its State of Charge over two days of different solar radiation by decentralized control at the end of the planning period.

The minimum voltage profile of the system and the voltage profile at the DeBES nodes are shown in Figure IV-26. According to this figure, we can say that the decentralized controller is running well and no under voltage problems has occurred.

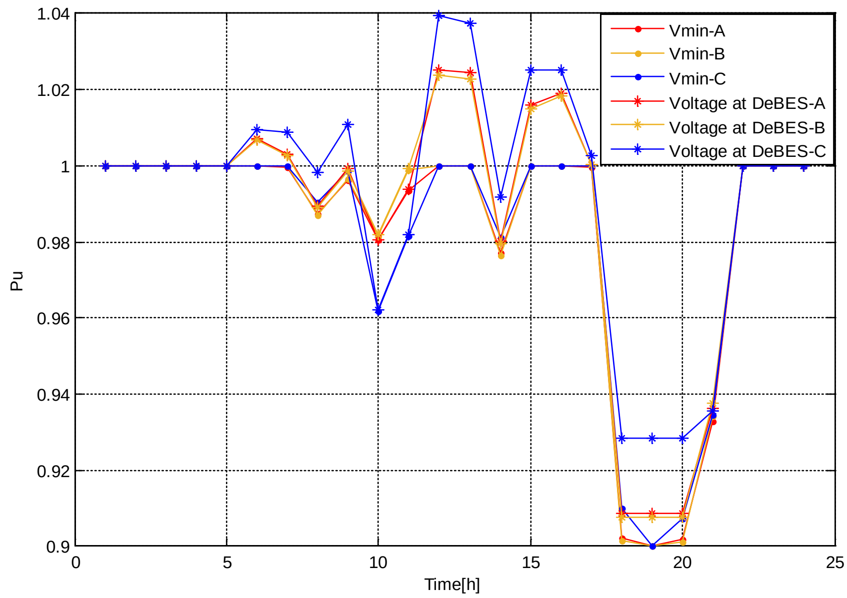

Figure IV- 26 : Minimum voltage profile of the system and voltage at the DeBES nodes at the highest solar radiation at the end of the planning period.

IV.3.2.2.4 Sizing of CeBES

Figure IV-27 shows the histogram of the annual power at the MV/LV substation without PV-BES integration for initial year; the maximum active power at the MV/LV substation is about 47 kW. If PV is added, there are some negative values (reverse power flows) at the MV/LV substation as depicted in Figure IV-28. However, this maximum active power has been reduced to 45 kW thanks to DeBES integration as given in Figure IV-29.

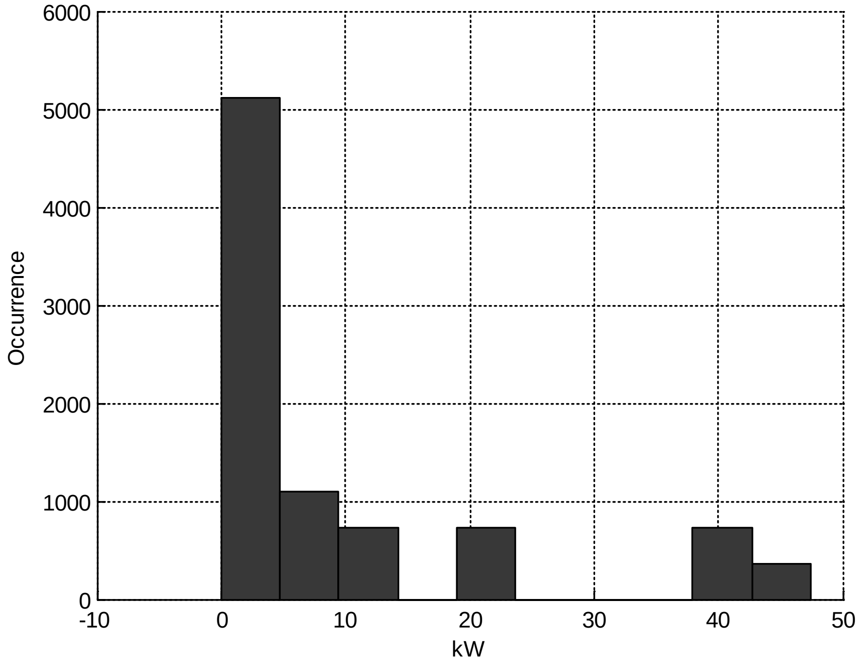

Figure IV- 27 : Histogram of the annual active power at the MV/LV substation without PV-DeBES-CeBES

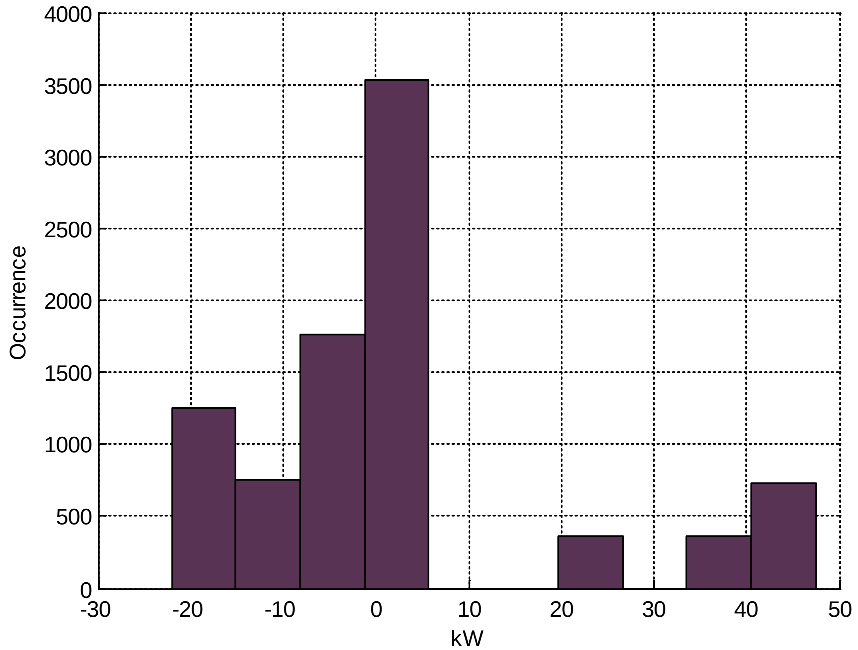

Figure IV- 28 : Histogram of the annual active power at the MV/LV substation with PVs integration

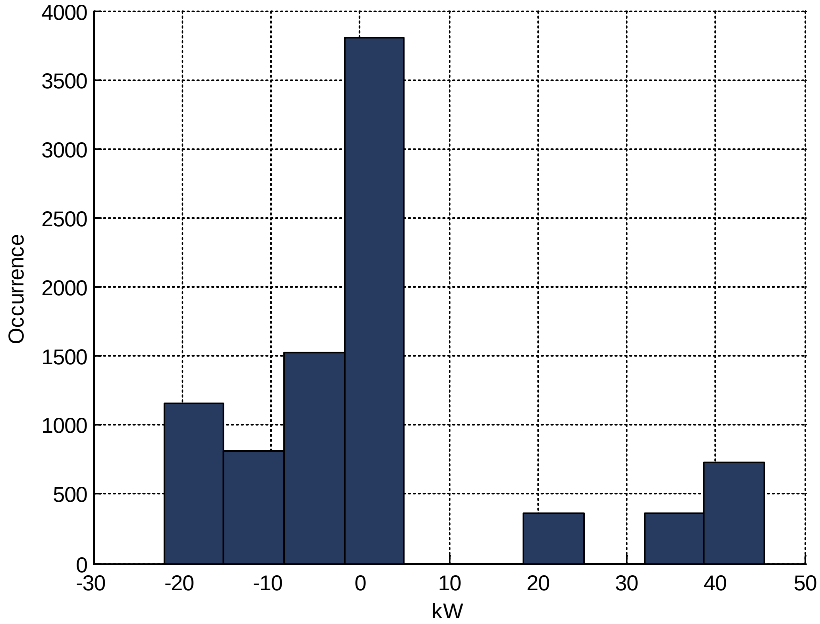

Figure IV- 29 : Histogram of the annual active power at the MV/LV substation with PVs-DeBES integration

Besides, the CeBES is used at the MV/LV substation for solving a problem of reverse power flows from the LV side to the MV side and also for enabling an autonomous operation time of the LV system. As shown in Figure IV-30, the negative powers have been stored in the CeBES and active power of the MV/LV substation is also reduced to 40 kW.

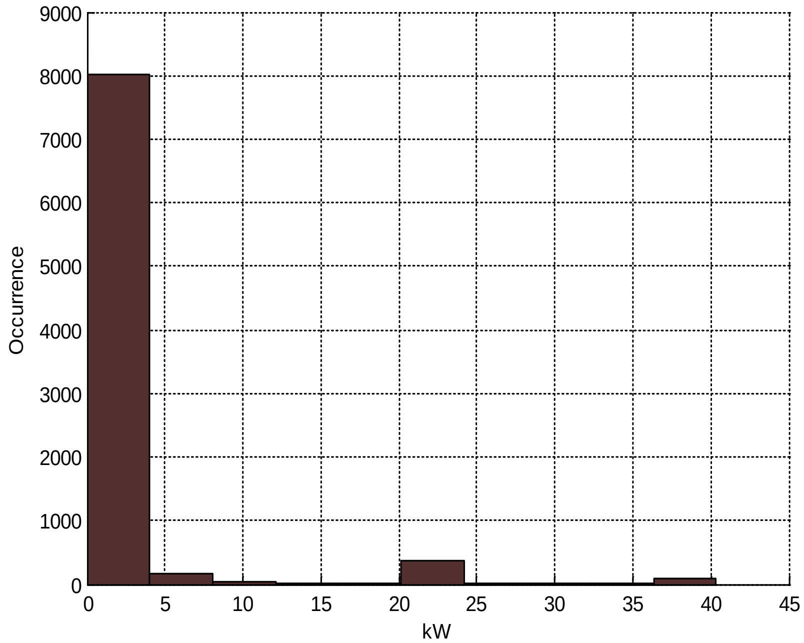

Figure IV- 30 : Histogram of the active power per year at the MV/LV substation with PV-DeBES-CeBES

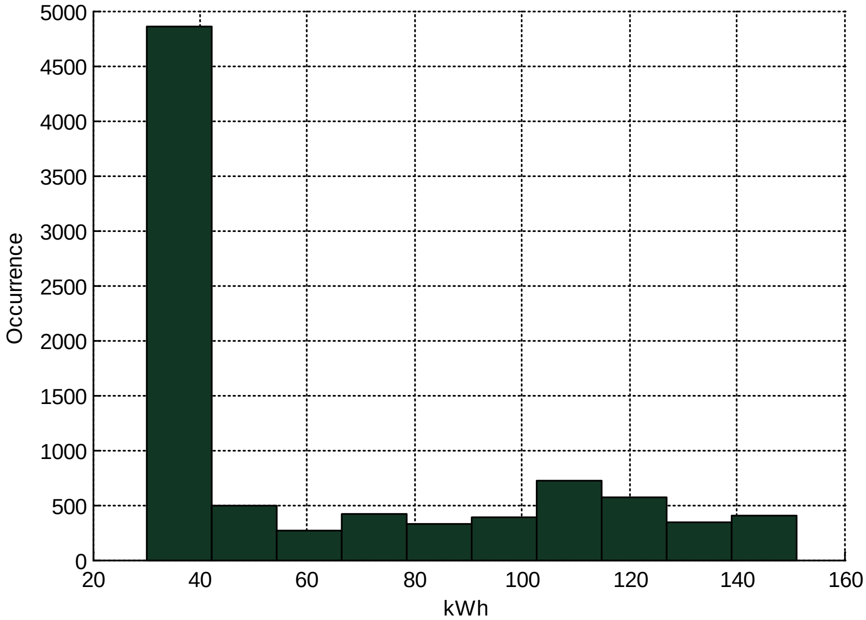

Figure IV- 31 : Histogram of the annual energy of centralized battery energy storage-CeBES

Table IV-7 lists the detailed simulation results in the rural area for the end of the planning year. According to this table, the active power coming from the MV grid has been decreased drastically by the PV-DeBES-CeBES integration from 47 kW to 40 kW. The energy supplied from the MV grid has been also decreased from 82 MWh to 14 MWh. Moreover, the LV distribution system is operated as an isolated microgrid with autonomous operation time of 90 % in the initial year. Besides, the capacity of CeBES is taken from Figure IV-31, so the capacity of the CeBES is 151 kWh. Furthermore, all the simulation results at the end of the planning year are provided in Appendix IV-G.

Table IV- 7 : Summary of simulation results for the initial year in rural area

Parameters	**Without-PV-DeBES-CeBES**	**With-PV**	**With-PV-DeBES**	**With-PV-DeBES-CeBES**
Three single-phases PV[A-B-C] -[kWp]	0	[2.4,3.28,3.06]	[2.4,3.28,3.06]	[2.4,3.28,3.06]
Decentralized BES [kWh]	0	0	[13.73,13.09,18.37]	[13.73,13.09,18.37]
Active power from grid [kW]	47.44	47.44	45.44	40.35

Energy used [MWh/year]	82.58	54.54	53.38	14.67
Autonomous time [%/year]	37.5 (no load)	79.44	79.44	90.9
Number of hours with voltage problem (V<0.9pu)/day	3	3	0	0

As seen in Table IV-7, the under voltage has been occurred in case without distributed generation, thus the grid-reinforcement is performed in order to remove this problem. Table IV-8 shows the minimal voltage and maximal current for cable reinforcement (i.e. 70mm^2 and 95mm^2) used in Cambodia at 19h where the peak load occurs at the end of planning period.

Table IV- 8 : Minimal voltage and maximal current for two types of cable reinforcement.

Cable size	**Min voltage (pu)**	**Max current (in % of the maximal admissible current)**	**Decision**
ABC-4x70mm2	0.89 pu	64.5 %	NO
ABC-4x95mm2	0.92 pu	51.9 %	**YES**

According to these results, the cable size of 95mm2 is selected for the grid reinforcement since there is no voltage and current constraints in our test system.

Furthermore, the actualized cost is computed to compare the grid reinforcement and PV-BES integration. The total time study for the analysis is set to 15 years. The list of parameters for the economic analysis is the same as Table III-3 of chapter III. The CAPEX at the initial year for the two strategies are detailed in Table IV-9.

Table IV- 9 : CAPEX of the grid-reinforcement and PV-BES integration

Items	**Solution**			
	Grid reinforcement		*PV-BES integration*	
	Values	Cost(kUSD)	Values	Cost(kUSD)
4x50 mm^2 cable	0 m	0	3409.42 m	2.728
4x95 mm^2 cable	3409.42 m	5.114	0 m	0
PV	0 kWp	0	[2.4,3.28,3.06]x3kWp	31.464
DeBES	0 kWh	0	[13.73,13.09,18.37]kWh	5.879
CeBES			151 kWh	19.630

Grid connected inverter	0 kW	0	2.5x3kW+3.3x6kW	19.656
BES Bi-directional inverter	0 kW	0	6-6-8 kW (DeBES) and 48 kW(CeBES)	78.54
Total cost		**5.114kUSD**		**157.892kUSD**

It can be seen that the initial CAPEX for the PV-BES integration is about 30 times higher than the grid-reinforcement. When the OPEX costs are integrated and the total actualized cost is computed, the tendency is reversed. The OPEX cost consists in the cost of the energy the DSO will have to pay. The PV-BES integration enables to increase the autonomy of the LV grid by decreasing the energy coming from the MV grid. The global actualized cost of the grid-reinforcement is about 229 kUSD and 225 kUSD for the PV-BES integration. The cost is almost the same for both strategies however the cost of the grid-reinforcement is expected to increase with the planning period. Also, two advantages which cannot be quantified are the cancelation of the reverse power flows and the ability of the LV network to be operated independently from the MV network. Therefore, we can conclude that the proposed solution with PV-BES integration is selected our test system in case without taking into account the line construction and maintenance costs.

IV.3.2.2.5 Impact of uncertainty on the load profile

This section deals with the impact on the LV system of the uncertainty on the load profile by using a MC simulation. As we got the V_{set} of each DeBES from the section IV.3.2.2.3, we applied these values to the decentralized control by taking into account the uncertainty on load profile. Figure IV-32 shows several samplings (1000) of load profiles considering an uncertainty of +/- 5%. With these load uncertainties, we obtain the variation of the daily minimum voltage of each phase with decentralized control of DeBES as illustrated in Figure IV-33 to Figure IV-35. As seen in these figures, the variation of the minimum voltage happens almost always between 18h00 and 21h00 due to high load consumption but these values are acceptable (Voltage > 0.9 pu).

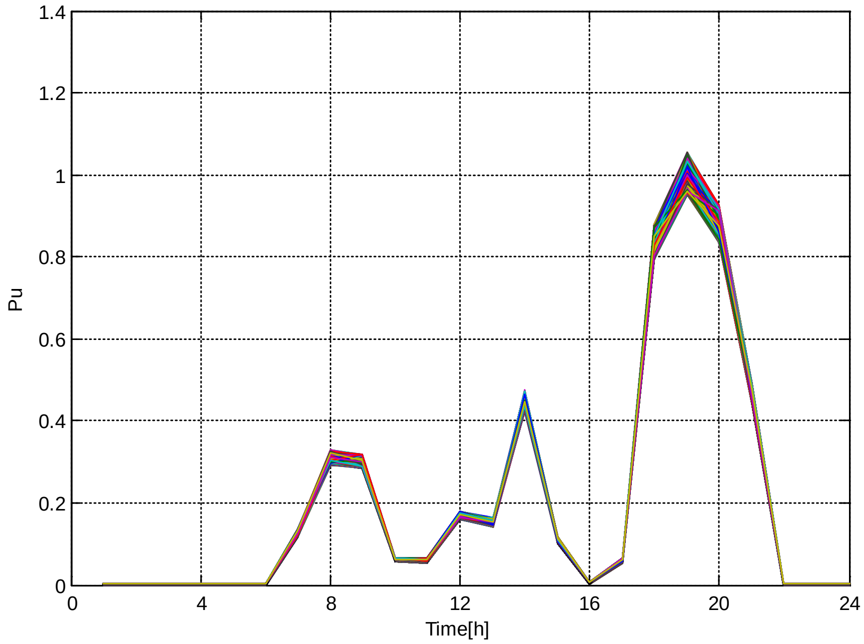

Figure IV- 32 : Daily load profile uncertainty of each household over 1000 samplings

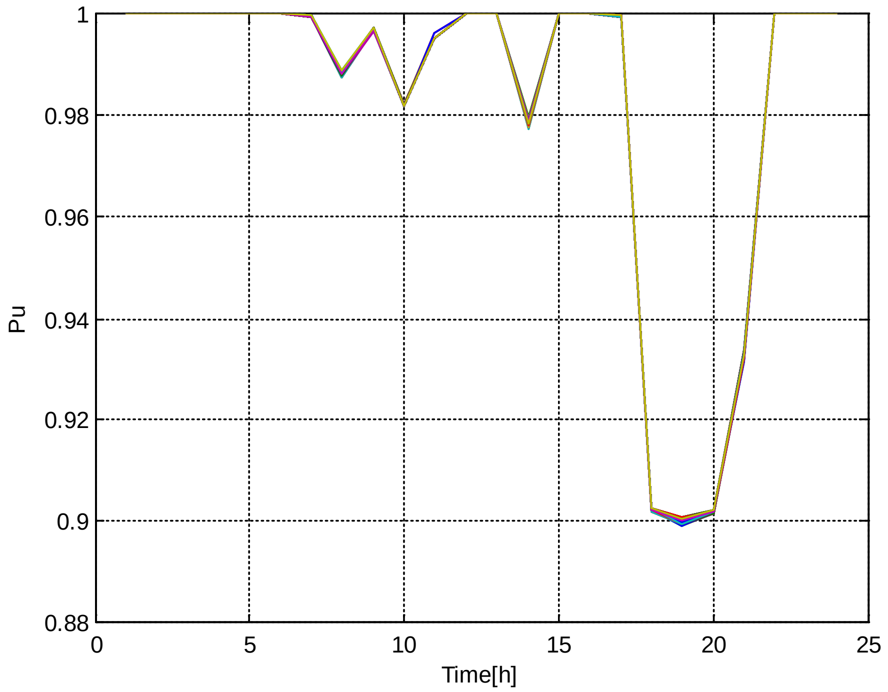

Figure IV- 33 : Daily variation of the minimum voltage for phase-A over 1000 samplings at the end of the planning study.

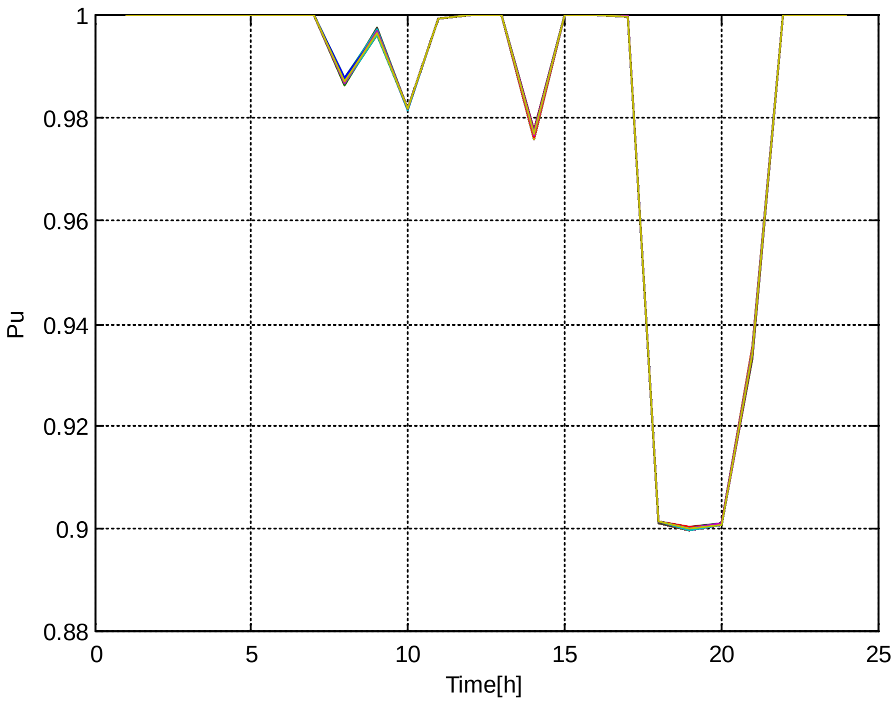

Figure IV- 34 : Daily variation of the minimum voltage for phase-B over 1000 samplings at the end of the planning study.

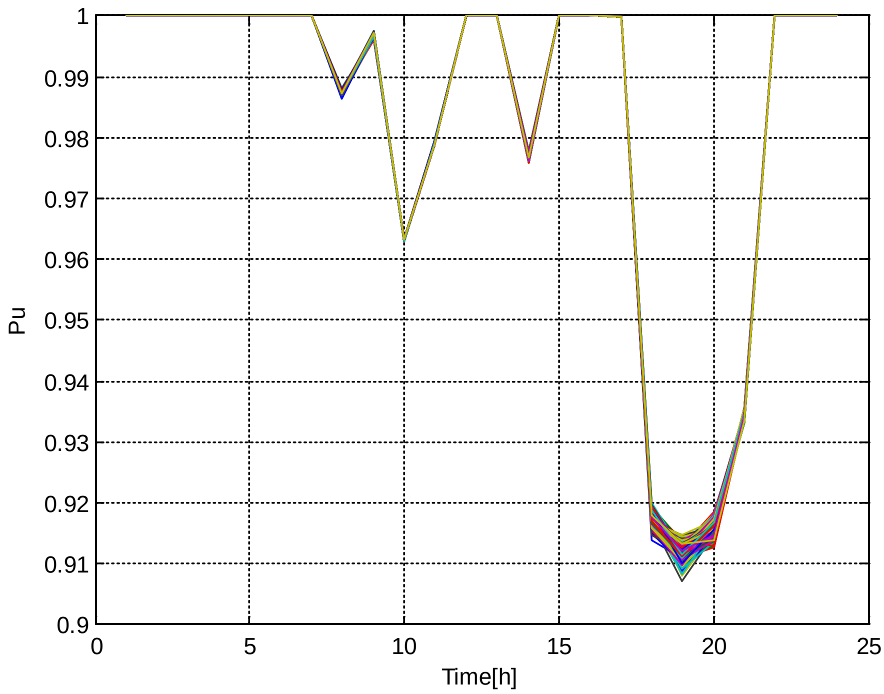

Figure IV- 35 : Daily variation of the minimum voltage for phase-C over 1000 samplings at the end of the planning study.

Furthermore, Figure IV-36 and Figure IV-38 also present histograms of the minimum voltages over the day which occur in the whole LV network with and without DeBES integration.

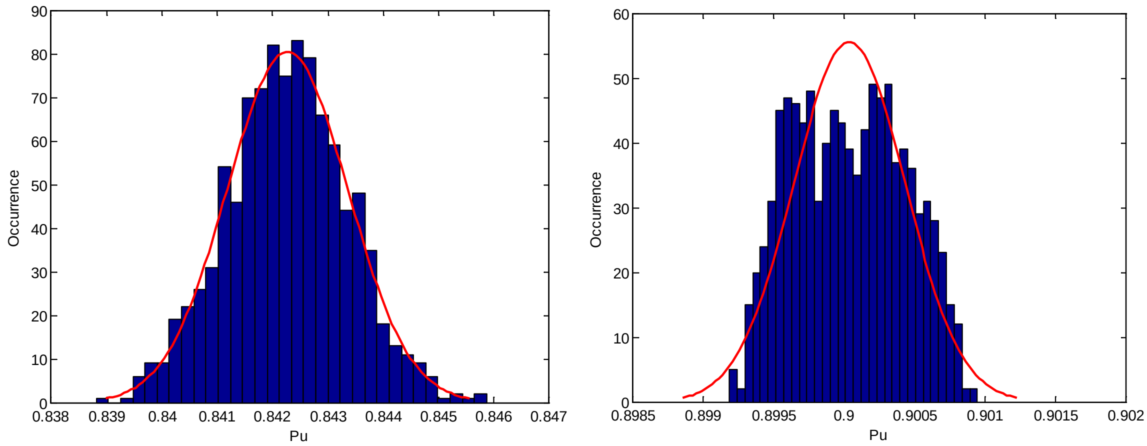

Figure IV- 36 : Histogram of the minimum voltage without (left) and with (right) DeBES-A integration over 1000 samplings

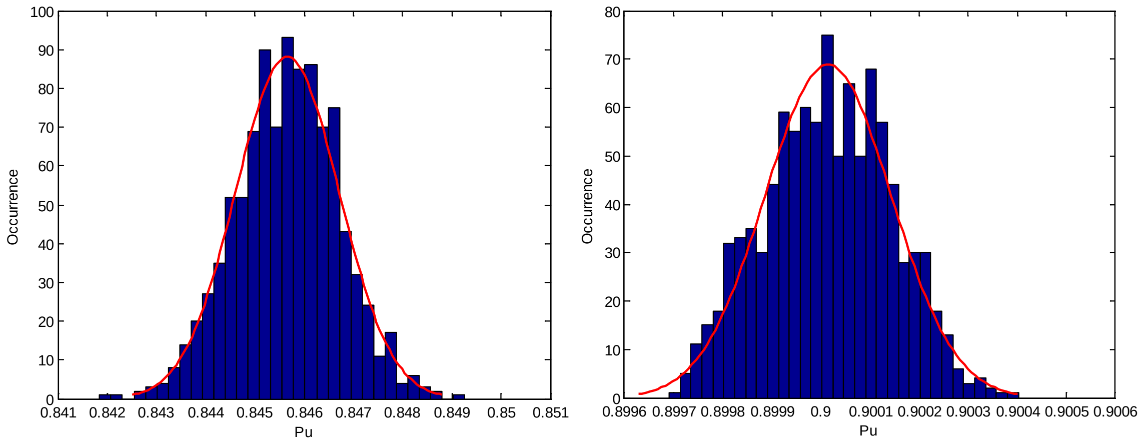

Figure IV- 37 : Histogram of the minimum voltage without (left) and with (right) DeBES-B integration over 1000 samplings

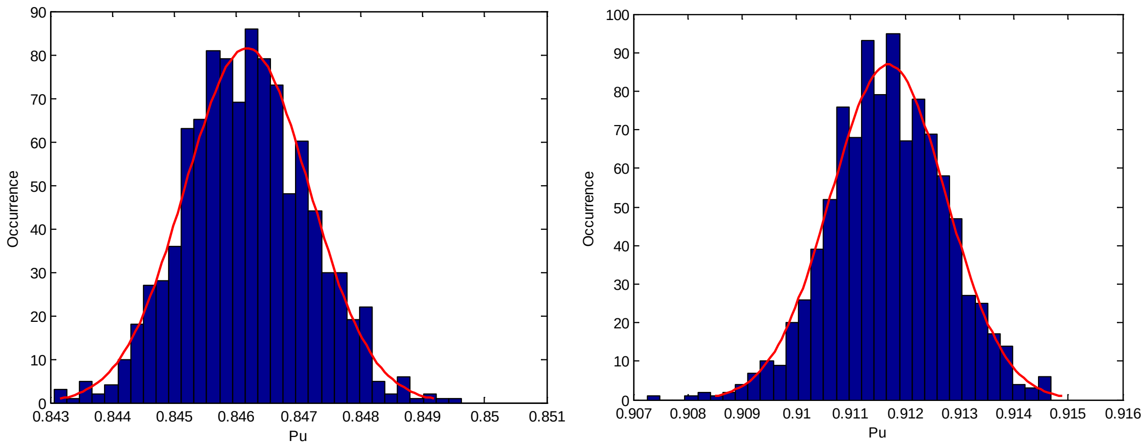

Figure IV- 38 : Histogram of the minimum voltage without (left) and with (right) DeBES-C integration over 1000 samplings

It can be seen that the under voltage problem has been completely removed thanks to the DeBES integration with the selected voltage reference (V_{set}). Therefore, we can notice that the V_{set} and the associated decentralized control are adapted for the management of the Decentralized Battery Storage without requiring developing an ICT network.

IV.4 Conclusion

In this chapter, the new planning principles presented in chapter III have been applied on both urban and rural areas. Even if additional simulations on other networks would be necessary to conclude, a first conclusion is that for developing country the integration of solar and battery into LV grids would not be more expensive that classical planning solutions (and even cheaper). This new way of planning could also bring other advantages such as cancelling reverse power flows and increasing the autonomy of the grids. LV microgrids could be created and isolated from the main grids reducing the investment in the MV network but further studies are required to quantify these advantages.

In addition, the impact of the value of the reference voltage for the DeBES control has been studied thanks to a Monte-Carlo Simulation method applied on the load profile uncertainty over the planning period in rural area. A small error of +/- 5% in the case studied does not seem to have a negative impact on network.

REFERENCES

[*Apcr11*] M.-C. Alvarez-Hérault, D. Picault, R. Caire, B. Raison, N. HadjSaid, and W. Bienia, "A Novel Hybrid Network Architecture to Increase DG Insertion in Electrical Distribution Systems," *IEEE Trans. Power Syst.*, vol. 26, no. 2, pp. 905–914, 2011.

[*Cora14*] A. F. Contreras and G. A. Ramos, "Fault location algorithm based on shortest path optimization problem for Distribution networks with DG," *2014 IEEE PES T&D Conf. Expo.*, pp. 1–5, 2014.

[*Eac15*] EAC, "Report on power sector of the Kingdom of Cambodia," 2015. [Online]. Available: https://eac.gov.kh/publication/report/.

[*Ecos17*] EcoSun, "EcoSun Solar Appliance Products," 2017. [Online]. Available: http://ecosun-products.webs.com/.

[*Iba93*] K. Iba, "Reactive power optimization by genetic algorithm," *Conf. Proc. Power Ind. Comput. Appl. Conf.*, pp. 1–6, 1993.

[*King04*] N. R. King, "General requirements of electric power technical standards of the kingdom of cambodia," 2004. [Online]. Available: http://eac.gov.kh/wp-content/uploads/2014/08/General-Requirements-of-Electric-Power-Technical-Standards.en_.pdf.

[*Mjcx14*] M. Mao, P. Jin, L. Chang, and H. Xu, "Economic analysis and optimal design on microgrids with SS-PVs for industries," *IEEE Trans. Sustain. Energy*, vol. 5, no. 4, pp. 1328–1336, 2014.

[*Nasa17*] Nasa, "ASDC _ Processing, archiving, and distributing Earth science data at the NASA Langley Research Center," 2017. [Online]. Available: http://eosweb.larc.nasa.gov.

[*Nipo05*] K. Nipon, "Photovoltaic Hybrid Systems for Rural Electrification in the Mekong Countries," University of Kassel, 2005.

[*Poch13*] K. Poch, "Renewable Energy Development in Cambodia: Status, Prospects and Policies," Jakarta, 2013.

[*Rara07*] S. V. K. Raja and P. H. Raj, “Balanced traffic distribution for MPLS using bin packing method,” *Proc. 2007 Int. Conf. Intell. Sensors, Sens. Networks Inf. Process. ISSNIP*, pp. 101–106, 2007.

[*Smas17*] S. SMA Solar Technology AG, “Battery Inverters,” 2017. [Online]. Available: http://www.sma.de/en/products/battery-inverters.html.

[*Vgba17*] V. Vai, E. Gladkikh, L. Bun, M.-C. Alvarez-Hérault, and B. Raison, “Planning of low-voltage distribution systems with uncertainty on load demand in urban areas,” in *IEEE International Conference on Environment and Electrical Engineering (EEEIC)*, 2017, pp. 1–6.

[*Vgba17*] V. Vai, E. Gladkikh, L. Bun, M.-C. Alvarez-Hérault, and B. Raison, “Study of low-voltage distribution system with integration of PV-battery energy storage for urban area in developing country,” in *IEEE International Conference on Environment and Electrical Engineering (EEEIC)*, 2017, pp. 1–6.

[*Vgbl17*] V. Vai, E. Gladkikh, L. Bun, M. C. L. Alvarez-Hérault, and B. Raison, “Low-Voltage Distribution System Planning under Load Demand Uncertainty: Growth Rate with Connection of New Loads,” in *IEEE International Electrical Engineering Congress (iEECON)*, 2017, pp. 1–4.

General conclusions and future works

The objectives of this thesis were focused on the long term planning of the low voltage distribution systems with the integration of small scale distributed generations (photovoltaic) to challenge the current issues of increasing the electrification and increase the renewable energy in Cambodia. The two main contributions of this thesis are:

- the development of optimization methods to design the LV distribution network with the objectives of minimizing the cost and balancing the network,

- to propose a new way of planning the distribution network by coupling the photovoltaic with storage in order to reduce the size of conductors used, to cancel the reverse power flows, to increase the autonomy of the LV grid and to reduce the peak power.

Chapter I has provided the current situation of the power system in Cambodia; it has given the necessary information for further researchers who are interested to current issues of electricity power sector in Cambodia or in developing countries with similar rules.

Chapter II developed two novel algorithms to obtain the optimal architecture for low voltage distribution grids by taking into account the uncertainty on load demand over the planning study (i.e. growth rate and new connected loads). The first one, SP-FFBP (Shortest path and First-Fit Bin-Packing) reduces power losses and improves the load balancing but increases the length of cable used. The second one, MIQCP (Mixt Integer Quadratic Constrained Programming) tries to minimize the total length of the grid and to improve the load balancing. The main conclusion of this chapter is to show that two different strategies can be applied regarding the scenario of uncertainty on the load demand. For urban networks, in case of growth rate evolution of only the existing load demand, the better strategy is to build the network at the initial year considering the predicted load demand at end of the planning study using MIQCP algorithm. If new loads appear during the planning study, the best approach is based on reinforcement principle (upgrading cable size) and building the grid year by year using the SP-FFBP. For rural networks, the main lines follow the road and the connection of customers will be done using the SP (in case of single phase MV/LV transformers) and SP-FFBP (in case of three phase MV/LV transformers).

Chapter III compared the traditional grid-reinforcement method with a new way of planning (PV-BES integration) so as to increase the electricity coverage area while integrating the presence of solar home systems. With this second solution, the electricity distributors do not need to reinforce the lines, but they have to purchase PV-BES and extend cables for new consumers. The maximum installed power of PV was calculated with respect to voltage and current constraints. Moreover, the peak load demand has been decreased thanks to battery energy storage integrated into the grid. Due to the integration of PV in grid, an autonomous operation of low voltage distribution is also possible; that means consumers will be supported by local generations (PV-BES). These two last effects could enable to decrease the required investment in MV planning. This chapter has thus demonstrated that the local generation from small scale solar energy and battery energy storage were useful for the electricity sector in Cambodia. Another contribution of this chapter is the proposed control of the BES without using a large information and communication technology (ICT) system.

Chapter IV applies and validates the new planning method developed in chapter III on two case studies. In urban area, the two algorithms developed in chapter II (SP-FFBP and MIQCP) for the optimal architecture have been used. Then the integration of PV and centralized BES is considered. A technical and economic comparison is made between the two optimal architectures including PV-BES integration by taking into account the global actualized cost. The two following results have been provided:

1- the SP-FFBP gives better results that the MIQCP,

2- the case of PV-BES integration is slightly more economic compared to the case without PV-BES integration for both architectures. The peak load power and the autonomous time of the LV grid are drastically increased.

The same study is conducted for the rural area. In this case, the SP-FFBP has been applied to find out the optimal architecture with load balancing. The maximum installed PV that can be integrated without violating voltage and current constraint was determined. The location and sizing of both centralized and decentralized BES have been performed in order to solve the under voltage problem due to the peak load and to cancel the reverse power flows at the MV/LV transformer. In this chapter, the effect of uncertainties of the hourly load profile on the settings of the control algorithm over the planning horizon has been integrated. The main conclusion of this chapter is that the integration of PV-BES in LV distribution planning tool is a promising solution which needs to be more investigated and experimented by the Cambodian government and electricity distributors. Additionally, with these developed algorithms, the low-distribution system can be operated as an isolated microgrid independently from main MV network with an autonomous operation time of 70 % and a peak load reduction of 23 % at the end of planning period.

However, to improve this current research, some future works can be recommended. In this research, the investment cost takes into account only equipment price for evaluating the actualized cost of the different case studies of low voltage distribution system. It should be considered to take into account the construction and maintenance costs for each equipment in order to give the general conclusion about the grid design. Moreover, only PV as renewable energy is considered in this thesis, thus other types of small scale renewable sources should be investigated such as biomass (gasification) and pico-hydropower plant which are abundant in some area in Cambodia. Likewise, the type of battery energy storage is not considered in this research since this thesis was focused on sizing optimization. Therefore, the comparison between different battery energy storage systems should be taken into account in order to select one among them for real application. Furthermore, this research has studied only the planning of low voltage distribution system. The novel method and algorithm should be modified and upgraded in order to be applied for current issues in medium voltage (MV) distribution system in further studies such as the optimal location and sizing of multiple distributed generations. The LV customers could then be split into microgrids linked together through the main grids which would require a global optimization. A sensitivity study has also to be made on some parameters such as the location of PV and the range of variation of the load growth and more case studies have to be run to generalize the conclusions. Finally, a Monte Carlo approach has been used to integrate uncertainties in the planning models. Other stochastic techniques have to be investigated such as the modelling of load and productions using probability density functions and a probabilistic load flow.

Increasing the electrification of the developing country is mandatory to bring social and economic progress. This Phd thesis is a first attempt to develop the LV distribution network with a modern and environmentally friendly way.

Appendices

Appendix II

Appendix II-A: Simplified Carson's Equations

The simplified Carson's equations for calculating self and mutual series impedance of system are shown below.

$$Z_{ii} = r_i + \pi^2 \cdot 10^{-4} \cdot f + j4\pi \cdot 10^{-4} \cdot f \cdot (\ln \frac{1}{GMR_i} + 6.4905 + \frac{1}{2}\ln\frac{\rho}{f})$$

$$Z_{ij} = \pi^2 \cdot 10^{-4} \cdot f + j4\pi \cdot 10^{-4} \cdot f \cdot (\ln \frac{1}{D_{ij}} + 6.4905 + \frac{1}{2}\ln\frac{\rho}{f})$$

Where:

Z_{ii} : self-impedance of conductor i in Ω / km

Z_{ij} : mutual-impedance of conductors i and j in Ω / km

GMR_i : geometric mean radius of conductor i in m

D_{ij} : distance between conductors i and j in m

ρ : resistivity of earth in $\Omega.m$

f : system frequency in Hz

Appendix II-B: Four-wires Unbalanced Load Flow

The unbalanced load flow simulation of radial system is carried out through forward/backward load flow program to solve load flow in four-wire unbalanced low-voltage.

- Bus Current Calculation

$$\begin{bmatrix} I_{ia} \\ I_{ib} \\ I_{ic} \\ I_{in} \end{bmatrix}^{(k)} = \begin{bmatrix} \left(\dfrac{S_{ia}}{V_{ia}}\right)^{(k-1)^*} \\ \left(\dfrac{S_{ib}}{V_{ib}}\right)^{(k-1)^*} \\ \left(\dfrac{S_{ic}}{V_{ic}}\right)^{(k-1)^*} \\ -(I_{ia}^{(k)} + I_{ib}^{(k)} + I_{ic}^{(k)}) \end{bmatrix}$$

Where S_{ia}, S_{ib}, S_{ic} are power injections at bus *i;* V_{ia}, V_{ib}, V_{ic} are voltages at bus *i* and $I_{ia}, I_{ib}, I_{ic}, I_{in}$ are the current injections at bus *i*.

- Backward Sweep: section current calculation

$$\begin{bmatrix} Iline_{la} \\ Iline_{lb} \\ Iline_{lc} \\ Iline_{\ln} \end{bmatrix}^{(k)} = \begin{bmatrix} I_{ia} \\ I_{ib} \\ I_{ic} \\ I_{in} \end{bmatrix}^{(k)} + \sum_{m \in M} \begin{bmatrix} Iline_{ma} \\ Iline_{mb} \\ Iline_{mc} \\ Iline_{mn} \end{bmatrix}^{(k)}$$

Where $Iline_{ia}, Iline_{ib}, Iline_{ic}$, and $Iline_{in}$ the current flow in line section and M is the set of line sections connected downstream to bus j.

- Forward Sweep: bus voltage calculation

$$\begin{bmatrix} V_{ja} \\ V_{jb} \\ V_{jc} \\ V_{jn} \end{bmatrix}^{(k)} = \begin{bmatrix} V_{ia} \\ V_{ib} \\ V_{ic} \\ V_{in} \end{bmatrix}^{(k)} - \begin{bmatrix} Z_{aa} & Z_{ab} & Z_{ac} & Z_{an} \\ Z_{ab} & Z_{bb} & Z_{bc} & Z_{bn} \\ Z_{ac} & Z_{bc} & Z_{cc} & Z_{cn} \\ Z_{an} & Z_{bn} & Z_{cn} & Z_{nn} \end{bmatrix} \times \begin{bmatrix} Iline_{la} \\ Iline_{lb} \\ Iline_{lc} \\ Iline_{\ln} \end{bmatrix}^{(k)}$$

- Convergence Criterion

The forward and backward sweep process is continued until the difference between the computed and specified voltage at the source is less than a specified tolerance.

Appendix II-C: Impedances matrix of cable

The impedance 4x4 matrix of cable type LV-ABC-4cores of 240mm^2 (Ω / km ,50Hz) is given as follows:

$$Z_{abcn-240} = \begin{bmatrix} 0.1743+j0.7338 & 0.0493+j0.6613 & 0.0493+j0.6396 & 0.0493+j0.6613 \\ 0.0493+j0.6613 & 0.1743+j0.7338 & 0.0493+j0.6613 & 0.0493+j0.6396 \\ 0.0493+j0.6396 & 0.0493+j0.6613 & 0.1743+j0.7338 & 0.0493+j0.6613 \\ 0.0493+j0.6613 & 0.0493+j0.6396 & 0.0493+j0.6613 & 0.1743+j0.7338 \end{bmatrix}$$

$$Z_{acn-240} = \begin{bmatrix} 0.1743+j0.7338 & 0 & 0.0493+j0.6396 & 0.0493+j0.6613 \\ 0 & 0 & 0 & 0 \\ 0.0493+j0.6396 & 0 & 0.1743+j0.7338 & 0.0493+j0.6613 \\ 0.0493+j0.6613 & 0 & 0.0493+j0.6613 & 0.1743+j0.7338 \end{bmatrix}$$

$$Z_{an-240} = \begin{bmatrix} 0.1743+j0.7338 & 0 & 0 & 0.0493+j0.6613 \\ 0 & 0 & 0 & 0 \\ 0 & 0 & 0 & 0 \\ 0.0493+j0.6613 & 0 & 0 & 0.1743+j0.7338 \end{bmatrix}$$

Appendix III

Appendix III-A: Load specification of LV distribution system

No. Bus	Coordinates		P(kW), pf=0.95	No. Bus	Coordinates		P(kW), pf=0.95	No. Bus	Coordinates		P(kW), pf=0.95
	X	Y			X	Y			X	Y	
1	0	0	0	31	178	163	0.343	61	370	733	0.465
2	17	40	0	32	252	98	0.322	62	359	738	0.310
3	34	80	0	33	252	147	0.394	63	379	729	0.299
4	51	120	0	34	246	161	0.393	64	376	742	0.282
5	68	160	0	35	258	186	0.339	65	374	751	0.340
6	85	200	0	36	284	200	0.319	66	403	729	0.339
7	102	240	0	37	139	270	0.351	67	404	739	0.393
8	119	280	0	38	151	287	0.420	68	393	759	0.265
9	136	320	0	39	161	310	0.341	69	419	769	0.411
10	153	360	0	40	168	329	0.379	70	443	819	0.298
11	170	400	0	41	194	361	0.331	71	-1	103	0.352
12	187	440	0	42	209	364	0.368	72	2	113	0.298
13	204	480	0	43	204	385	0.331	73	-2	131	0.304
14	221	520	0	44	300	350	0.297	74	24	159	0.399
15	238	560	0	45	283	373	0.354	75	31	175	0.267
16	255	600	0	46	287	394	0.337	76	30	192	0.291
17	272	640	0	47	206	422	0.379	76	47	212	0.467
18	299	680	0	48	210	439	0.440	78	86	303	0.353
19	316	720	0	49	228	455	0.353	79	113	389	0.246
20	354	760	0	50	226	474	0.279	80	107	405	0.409
21	394	800	0	51	300	437	0.254	81	114	481	0.330
22	434	840	0	52	305	451	0.368	82	151	460	0.317
23	25	5	0.401	53	241	504	0.372	83	237	633	0.322
24	35	33	0.317	54	256	506	0.385	84	231	642	0.315
25	42	50	0.353	55	256	539	0.380	85	250	657	0.427
26	58	82	0.366	56	315	664	0.413	86	342	796	0.302
27	60	117	0.373	57	332	682	0.339	87	361	829	0.342
28	67	115	0.357	58	351	674	0.321	88	371	829	0.402
29	76	123	0.366	59	351	710	0.343	89	381	863	0.353
30	74	134	0.326	60	359	723	0.255	90	391	889	0.302

Appendix III-B: Impedances matrix of cable

The impedance 2x2 matrix of cable types LV-ABC-2cores of 95-50-4mm^2 (Ω / km ,50Hz) are given as follows:

$$Z_{an-2\times 95} = \begin{bmatrix} 0.3693 + j0.7688 & 0.0493 + j0.6898 \\ 0.0493 + j0.6898 & 0.3693 + j0.7688 \end{bmatrix}$$

$$Z_{an-2\times 50} = \begin{bmatrix} 0.6903 + j0.7906 & 0.0493 + j0.7080 \\ 0.0493 + j0.7080 & 0.6903 + j0.7906 \end{bmatrix}$$

$$Z_{an-2\times 4} = \begin{bmatrix} 4.9993 + j0.8626 & 0.0493 + j0.7824 \\ 0.0493 + j0.7824 & 4.9993 + j0.8626 \end{bmatrix}$$

Appendix III-C: Load profile per 2 households on December 20th and 23rd 2016 for rural area-case study

Time	Power consumption (W)		
	1st Household (Name: CHUCH Vai)	**2nd Household** (Name: OUN Ean)	**Averaged curve (Pu)**
1:00	0	0	0
2:00	0	0	0
3:00	0	0	0
4:00	0	0	0
5:00	0	0	0
6:00	0	0	0
7:00	38.41667	0	0.122412
8:00	45.69444	36.23061	0.307828
9:00	0	79.33446	0.298094
10:00	0	15.42541	0.05796
11:00	0	15.0838	0.056676
12:00	36.38889	8.072657	0.167061
13:00	39.96822	0	0.150178
14:00	50.36111	68.55164	0.446807
15:00	0	28.19126	0.105927
16:00	0	0	0
17:00	0	15.28808	0.057444
18:00	76.36111	145.4657	0.8335
19:00	117.5	148.6389	1
20:00	81.63889	152.3357	0.879145
21:00	22.25	101.1856	0.463801
22:00	0	0	0
23:00	0	0	0
24:00	0	0	0

Appendix IV

Appendix IV-A: Load specification of LV distribution system for urban area-case study

No. Bus	Coordinates		P(kW), pf=0.95	No. Bus	Coordinates		P(kW), pf=0.95
	X	Y			X	Y	
1	0	0	0	24	170	15	4.61
2	0	5	0	25	190	15	4.68
3	0	15	0	26	5	35	4.32
4	0	35	0	27	30	35	4.48
5	0	45	0	28	50	35	5.52
6	5	5	4.97	29	70	35	5.47
7	30	5	4.03	30	90	35	5.40
8	50	5	4.89	31	110	35	5.50
9	70	5	6.12	32	130	35	4.99
10	90	5	4.72	33	150	35	5.08
11	110	5	5.19	34	170	35	5.37
12	130	5	5.26	35	190	35	5.47
13	150	5	5.20	36	5	45	6.30
14	170	5	5.04	37	30	45	4.51
15	190	5	4.68	38	50	45	5.06
16	5	15	5.18	39	70	45	5.22
17	30	15	5.13	40	90	45	4.41
18	50	15	5.09	41	110	45	4.24
19	70	15	5.31	42	130	45	5.08
20	90	15	4.91	43	150	45	4.64
21	110	15	4.40	44	170	45	5.00
22	130	15	5.53	45	190	45	4.51
23	150	15	5.36				

Appendix IV-B: Load profile per household from March 4th to May 19th 2017 for urban area-case study

Time	Consumption (kW)	Time	Consumption (kW)	Time	Consumption (kW)
1:00	0.957772727	9:00	0.475090909	17:00	0.354181818
2:00	0.739090909	10:00	0.287772727	18:00	0.5745
3:00	0.650772727	11:00	0.308772727	19:00	1.131954545
4:00	0.656863636	12:00	0.314954545	20:00	1.431909091
5:00	0.652136364	13:00	0.275818182	21:00	1.185136364
6:00	0.663272727	14:00	0.354681818	22:00	0.931909091
7:00	0.592545455	15:00	0.4535	23:00	0.871318182
8:00	0.563181818	16:00	0.3385	24:00	0.98952381

Figure IV-B-1: Set-Up of load profile measurements (Urban-left, Rural-right) by using Power Quality Analyzer-Fluke 435 series II

Appendix IV-C: Summary of simulation results at the end of planning year for urban area-case study

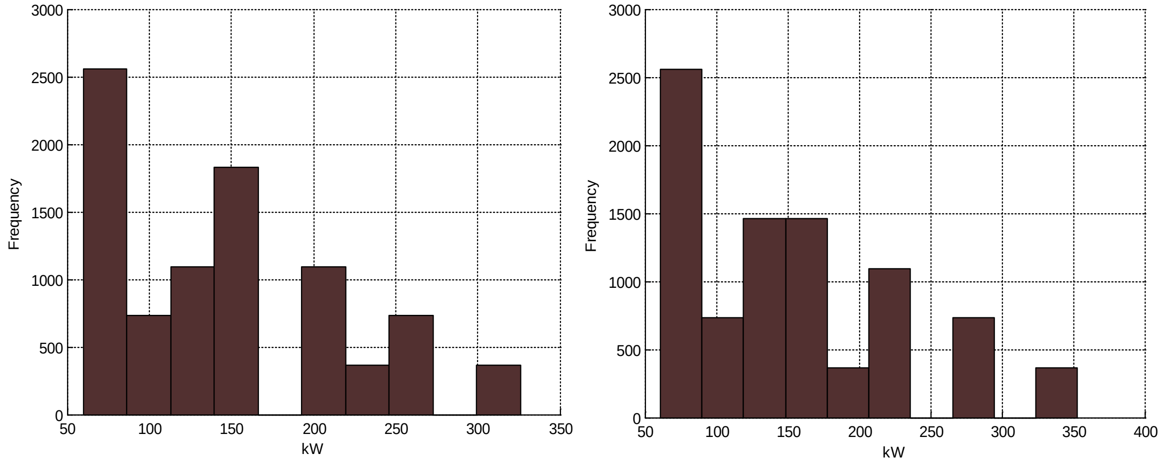

Figure IV-C-1: Histogram of the annual active power at the MV/LV substation without PV-CeBES (Algo1-left, Algo2-right)

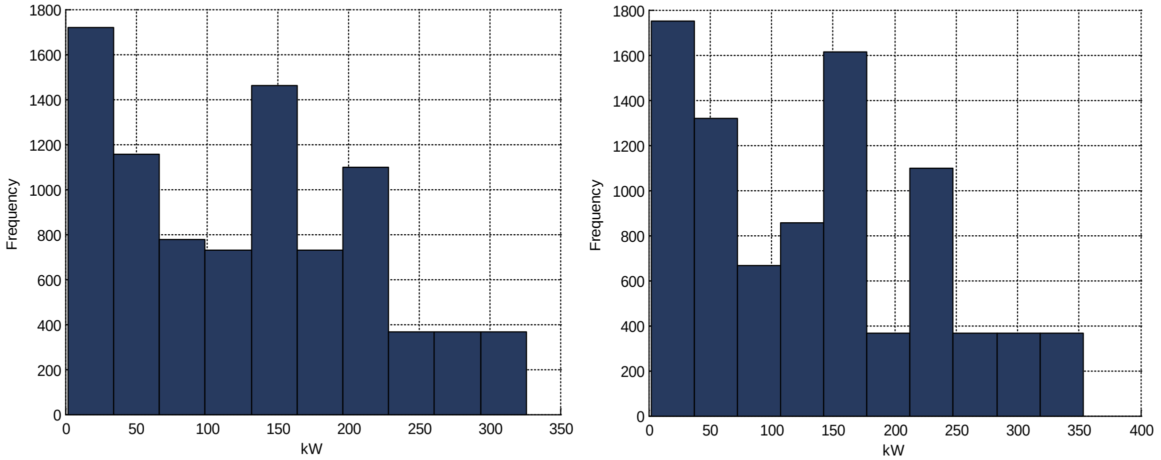

Figure IV-C-2: Histogram of the annual active power at the MV/LV substation with PVs integration (Algo1-left, Algo2-right)

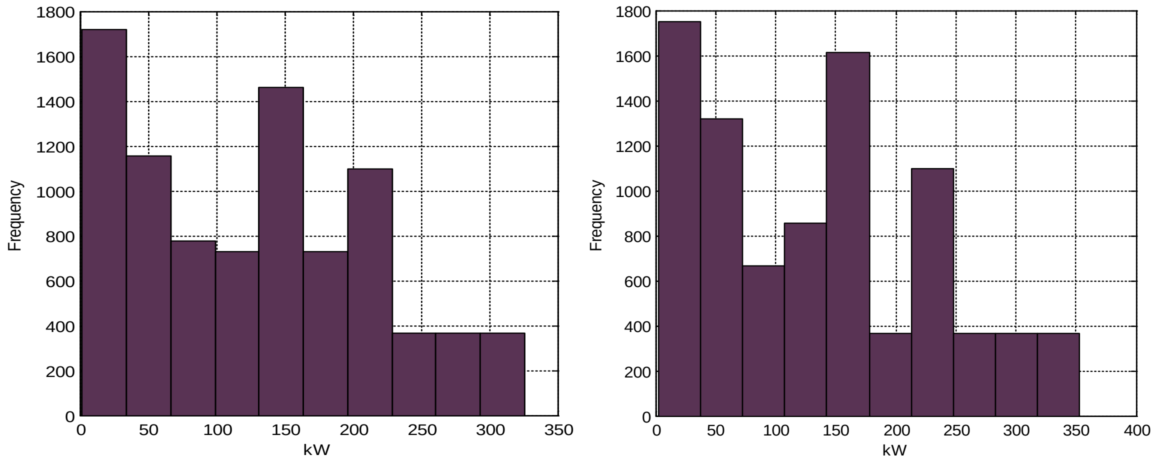

Figure IV-C-3: Histogram of the active power per year at the MV/LV substation with PV-CeBES (Algo1-left, Algo2-right)

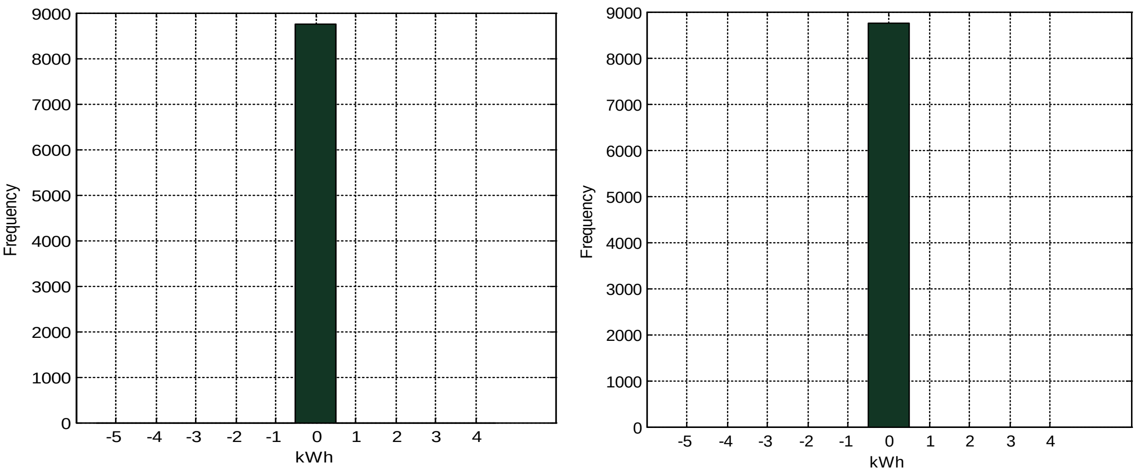

Figure IV-C-4: Histogram of the annual energy of centralized battery energy storage-CeBES (Algo1-left, Algo2-right)

Appendix IV-D: Load specification of LV distribution system for rural area-case study

No. Bus	Coordinates		P(kW), pf=0.95	No. Bus	Coordinates		P(kW), pf=0.95	No. Bus	Coordinates		P(kW), pf=0.95
	X	Y			X	Y			X	Y	
1	0	0	0	44	68	382	0.317	87	13	322	0.372
2	4	40	0	45	100	365	0.433	88	0	320	0.389
3	8	80	0	46	66	419	0.431	89	11	337	0.494
4	12	120	0	47	59	459	0.389	90	13	349	0.357
5	16	160	0	48	59	482	0.499	91	21	419	0.426
6	20	200	0	49	103	463	0.453	92	20	428	0.359
7	24	240	0	50	121	460	0.420	93	-77	413	0.439
8	28	280	0	51	134	464	0.405	94	-17	514	0.358
9	32	320	0	52	137	419	0.459	95	39	495	0.410
10	36	360	0	53	151	411	0.389	96	-14	527	0.416
11	40	400	0	54	164	419	0.434	97	-15	540	0.448
12	44	440	0	55	182	471	0.428	98	31	504	0.321
13	48	490	0	56	177	461	0.444	99	33	516	0.424
14	88	490	0	57	185	426	0.408	100	-8	620	0.365
15	128	490	0	58	185	418	0.444	101	33	566	0.437
16	168	490	0	59	196	412	0.423	102	45	629	0.357
17	208	490	0	60	220	406	0.393	103	48	619	0.304
18	248	490	0	61	239	467	0.422	104	51	680	0.465
19	288	490	0	62	267	399	0.464	105	51	691	0.430
20	328	490	0	63	354	469	0.411	106	53	699	0.369
21	368	490	0	64	372	472	0.434	107	82	638	0.437
22	408	490	0	65	423	473	0.437	108	65	508	0.428
23	18	63	0.296	66	-61	24	0.292	109	72	537	0.364
24	25	87	0.360	67	-27	32	0.369	110	75	549	0.358
25	24	115	0.420	68	-5	38	0.445	111	74	563	0.501
26	25	131	0.365	69	-8	43	0.446	112	80	581	0.313
27	87	116	0.376	70	-12	50	0.381	113	106	506	0.435
28	108	113	0.372	71	-10	57	0.333	114	119	506	0.389
29	41	153	0.399	72	-9	63	0.371	115	158	512	0.396
30	38	196	0.398	73	-17	72	0.435	116	168	512	0.382

31	124	175	0.443	74	-16	89	0.414	117	178	511	0.342
32	39	221	0.489	75	-4	104	0.423	118	189	512	0.402
33	41	236	0.421	76	-10	128	0.332	119	180	570	0.382
34	69	229	0.390	77	-34	158	0.477	120	259	513	0.415
35	111	217	0.455	78	-69	165	0.412	121	269	512	0.381
36	43	254	0.434	79	-84	166	0.336	122	275	522	0.345
37	66	260	0.385	80	-102	164	0.361	123	284	522	0.357
38	46	274	0.415	81	-6	165	0.382	124	293	511	0.456
39	46	291	0.417	82	-4	178	0.332	125	350	507	0.473
40	48	306	0.361	83	5	205	0.347	126	357	500	0.392
41	50	373	0.355	84	3	230	0.454	127	373	505	0.426
42	65	362	0.374	85	8	247	0.451	128	409	500	0.416
43	66	371	0.397	86	7	289	0.469	129	422	500	0.349

Appendix IV-E: Implementation of GA for location and sizing of DeBES

In the implementation of GA, we set 50 individuals, 300 generations, 10e-20 of tolerance constraint (TolCon) and 10e-20 of tolerance penalty fitness (TolFun) as inputs in optimization. As seen in Figure C-1 to Figure C-3, the algorithm is terminated at generation lower than 300 due to the average change in the penalty fitness value less than TolFun and constraint violation is less than TolCon.

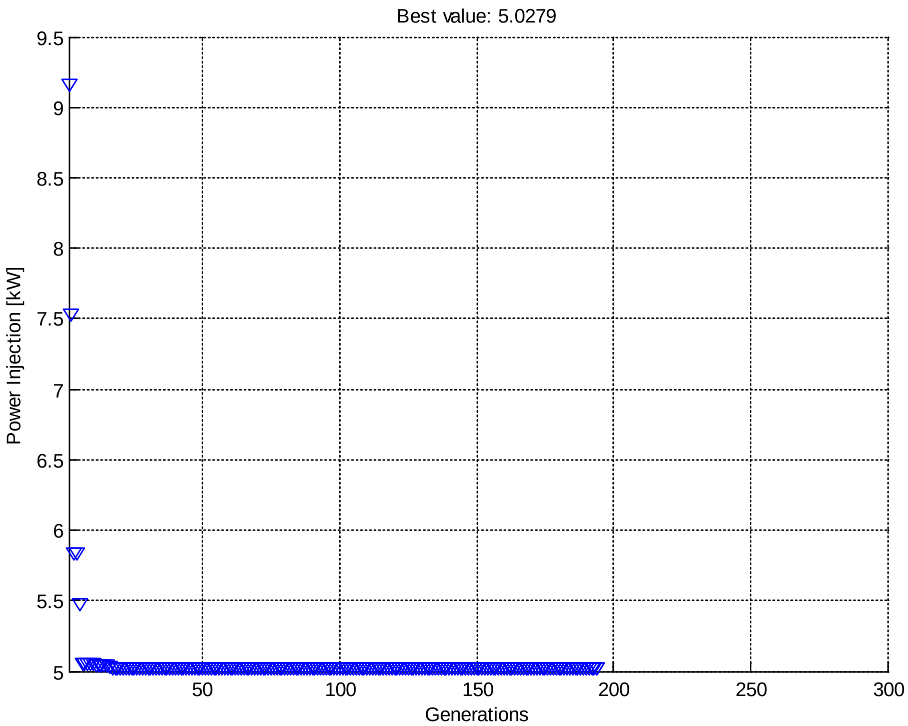

Figure IV-E-1: Evolution of the best DeBES-A location (18) and Sizing at 19h00 over 300 generations setting

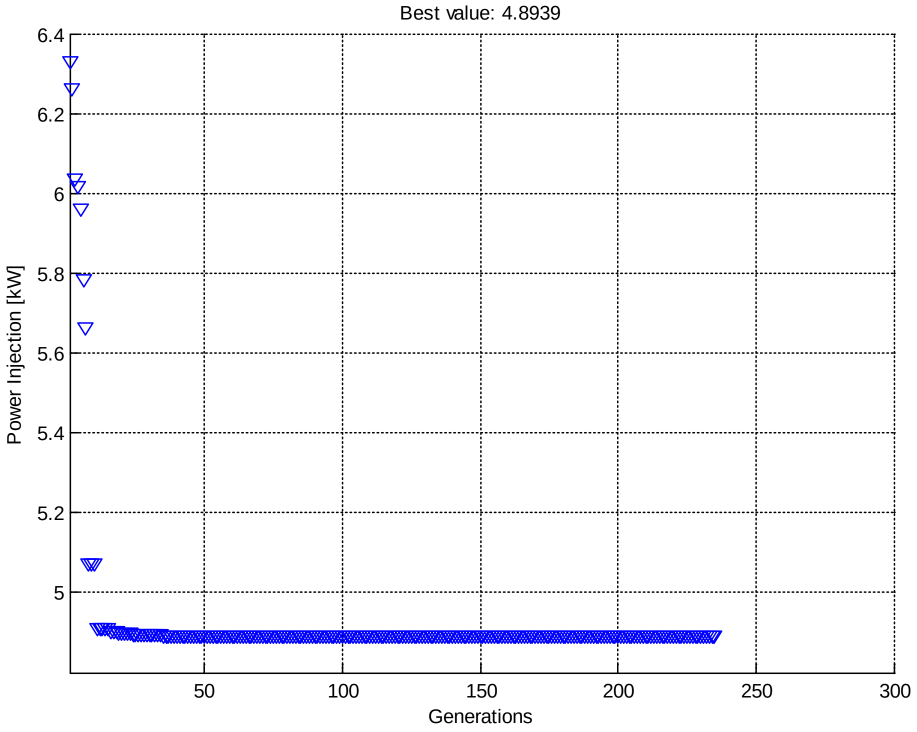

Figure IV-E-2: Evolution of the best DeBES-B location (17) and Sizing at 19h00 over 300 generations setting

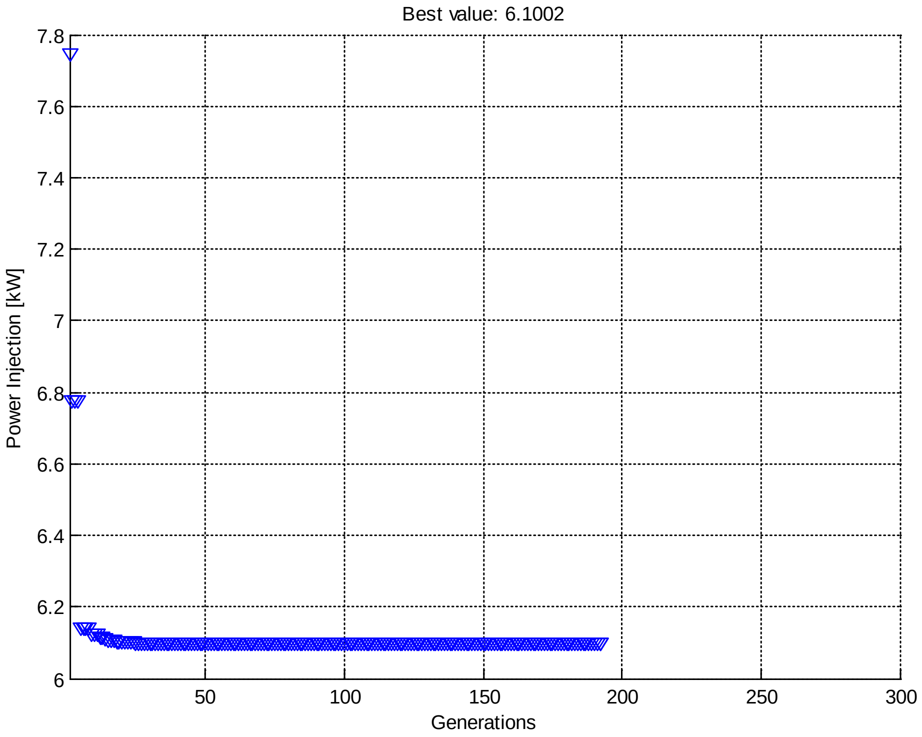

Figure IV-E-3: Evolution of the best DeBES-C location (21) and Sizing at 19h00 over 300 generations setting

Appendix IV-F: maximum charging and minimum discharging of DeBES at lowest solar radiation

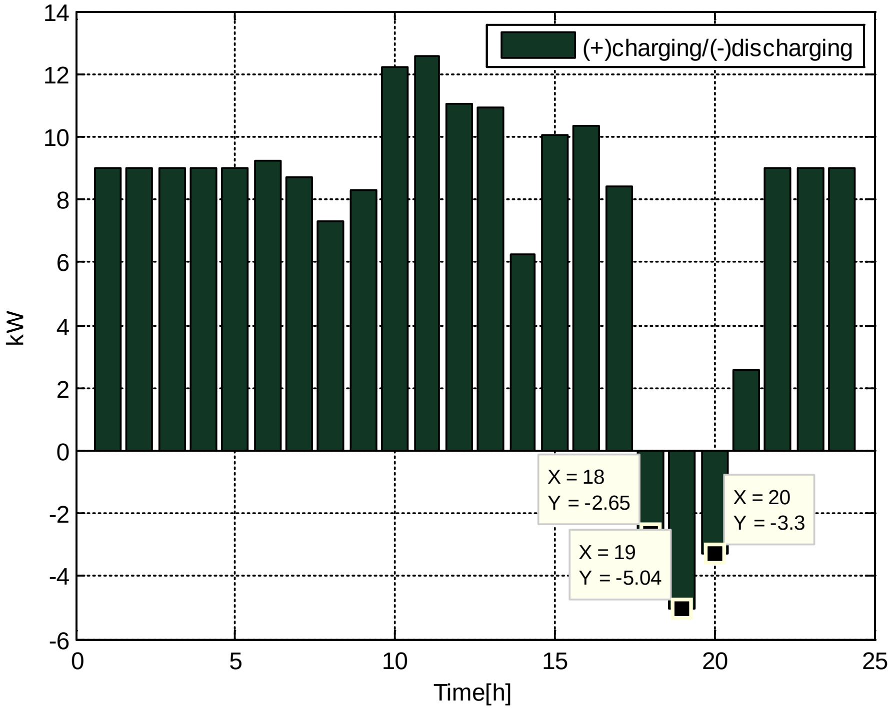

Figure IV- F-1: Max charging (+) and min discharging (-) of DeBES-A power at bus 18 in initial year

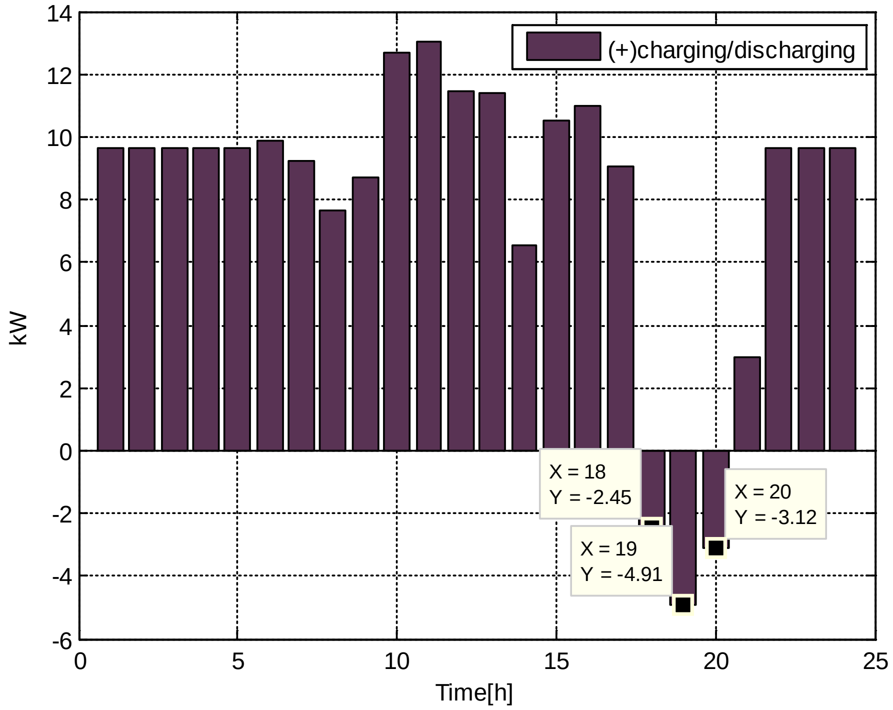

Figure IV- F-2: Max charging (+) and min discharging (-) of DeBES-B power at bus 17 in initial year

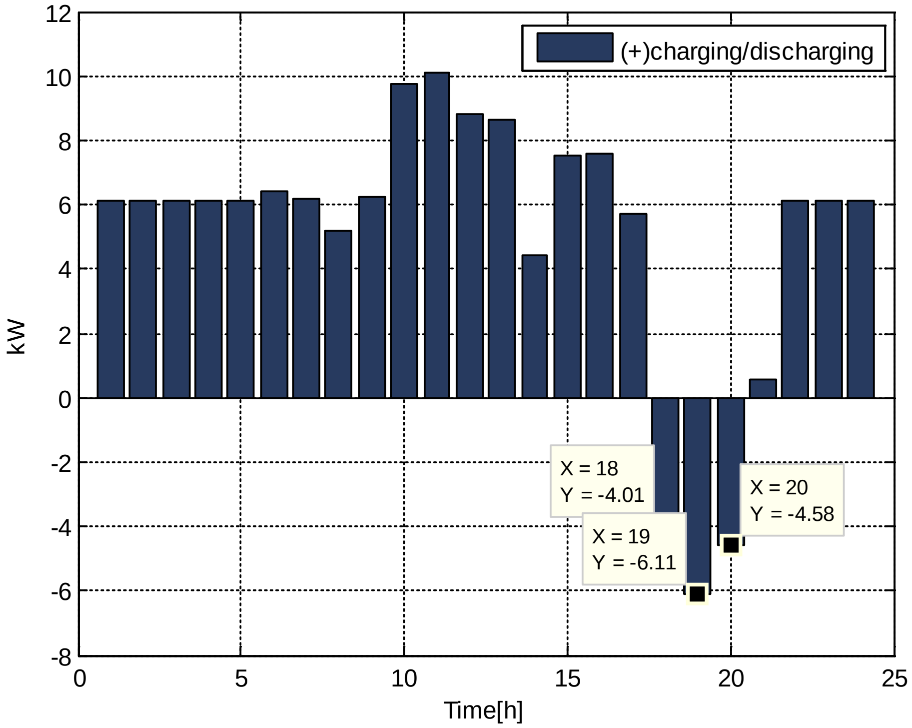

Figure IV- F-3: Max charging (+) and min discharging (-) of DeBES-C power at bus 21 in initial year

Appendix IV-G: Summary of simulation results at the end of planning year for rural area

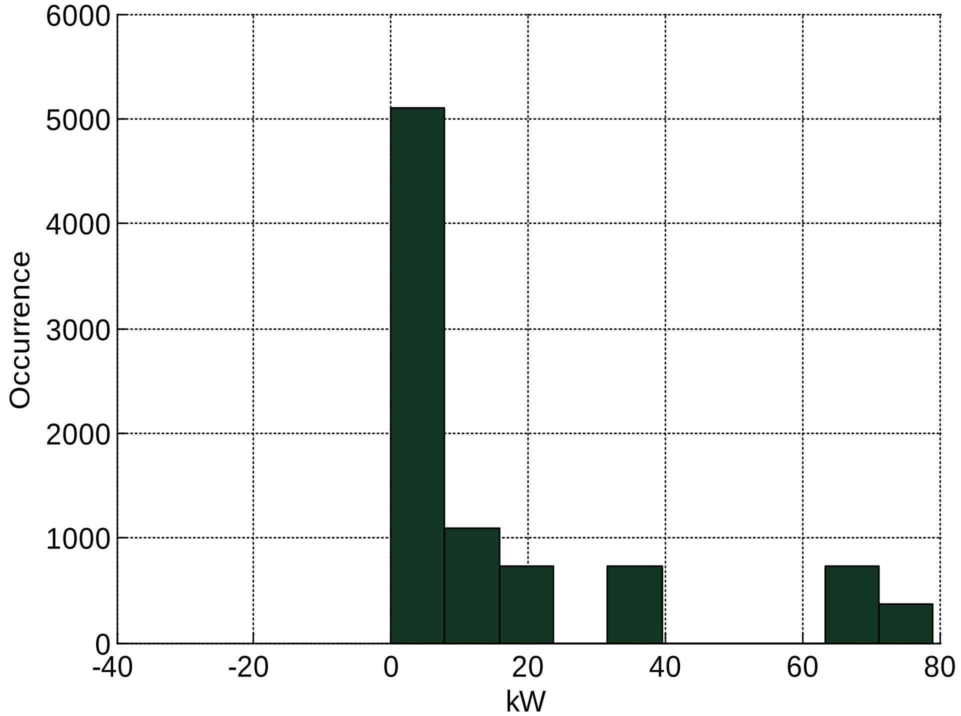

Figure IV-G-1: Histogram of the annual active power at the MV/LV substation without PV-DeBES-CeBES

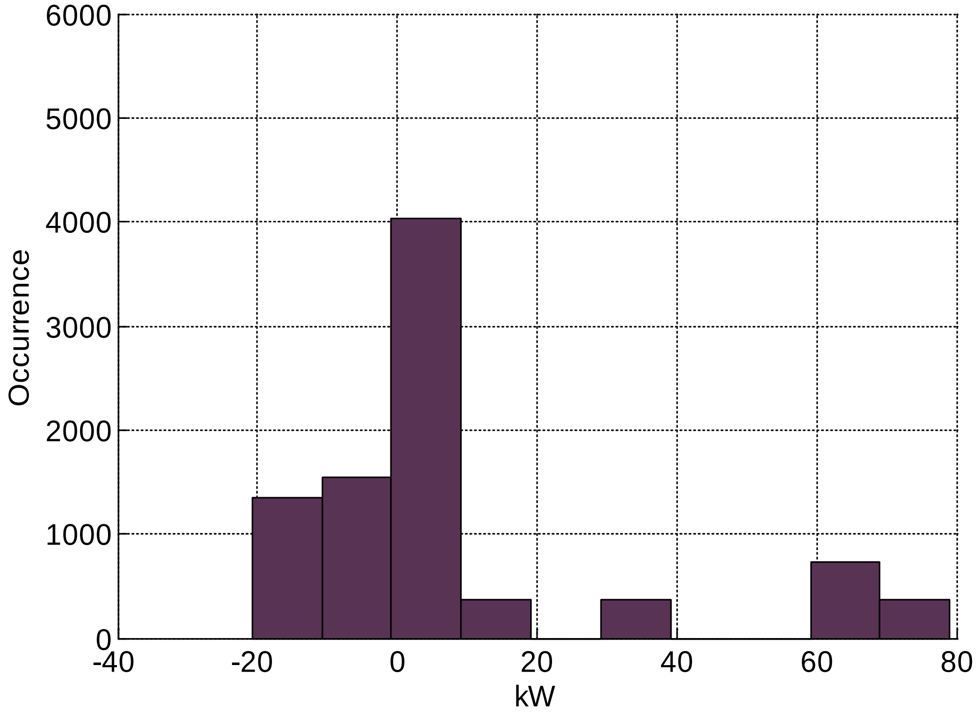

Figure IV-G-2: Histogram of the annual active power at the MV/LV substation with PV

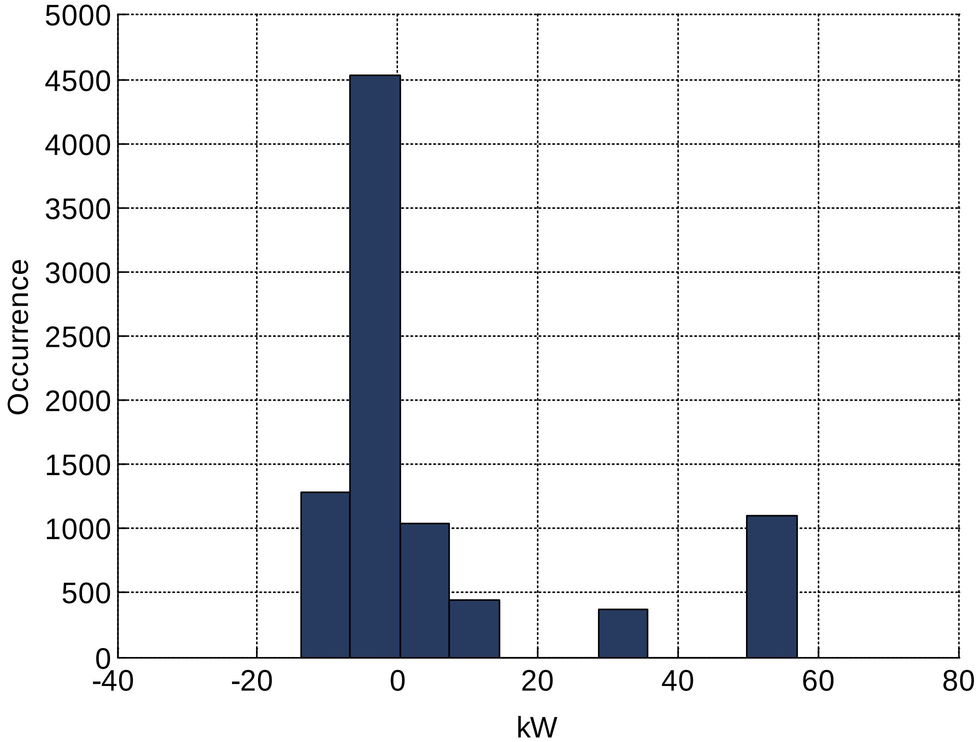

Figure IV-G-3: Histogram of the annual active power at the MV/LV substation with PV-DeBES

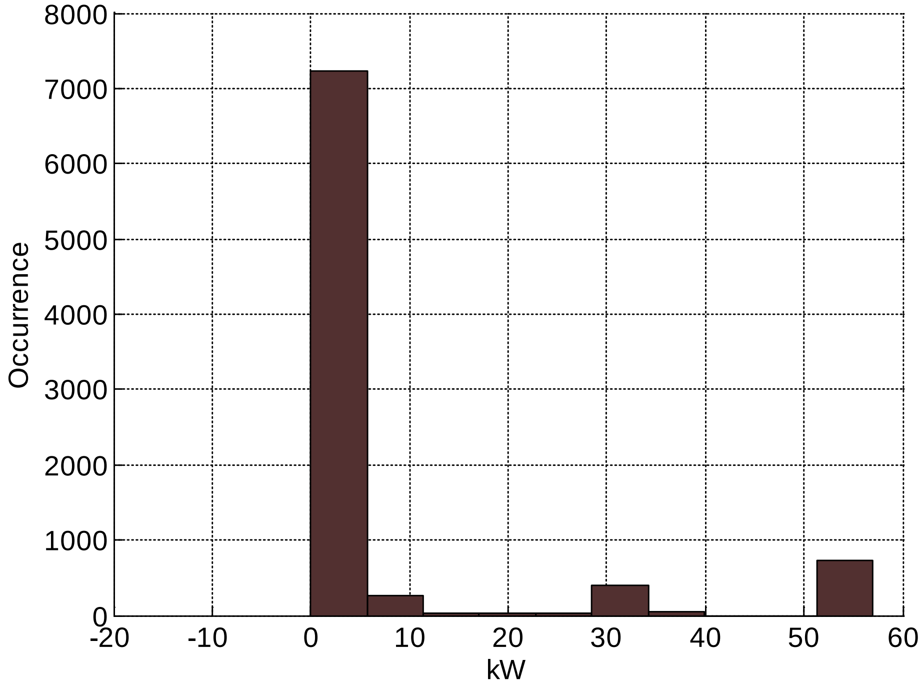

Figure IV-G-4: Histogram of the annual active power at the MV/LV substation with PV-DeBES-CeBES

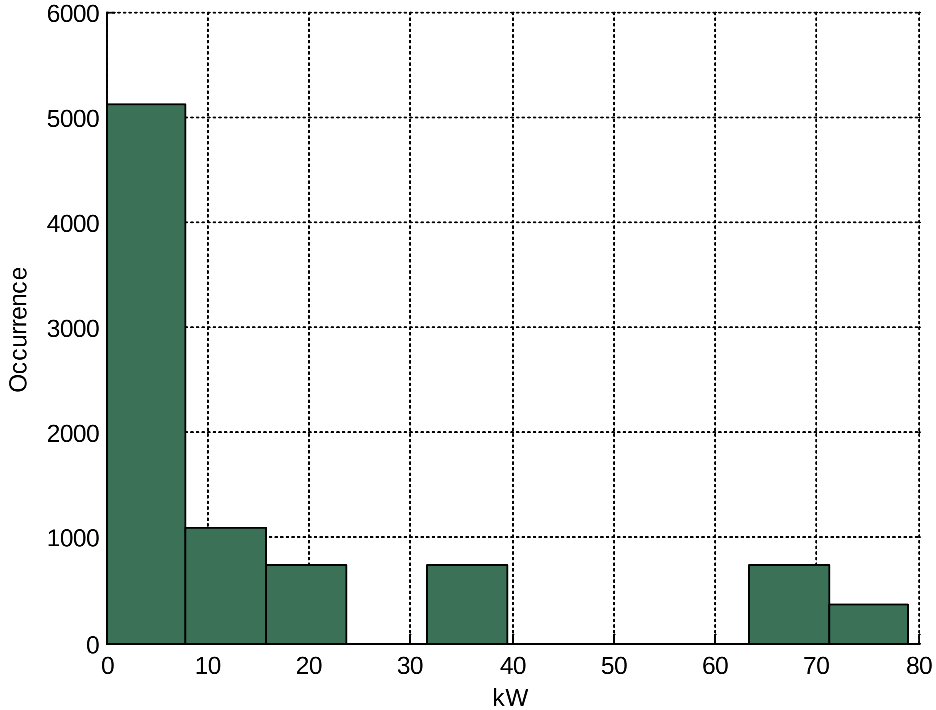

Figure IV-G-5: Histogram of the battery energy storage at the MV/LV substation with PV-DeBES-CeBES

Table IV-G-1 Summary of simulation results at the end of planning for rural area-case study

Parameters	**W/O-PV-DeBES-CeBES**	**With-PV**	**With-PV-DeBES**	**With-PV-DeBES-CeBES**
Three single-phases PV[A-B-C] -[kWp]	0	[2.4,3.28,3.06]	[2.4,3.28,3.06]	[2.4,3.28,3.06]
Decentralized BES [kWh]	0	0	[13.73,13.09,18.37]	[13.73,13.09,18.37]
Active power from grid [kW]	79.07	79.07	57.02	57.02
Energy used [MWh/year]	128.40	95.96	78.94	60.46
Autonomous time [%/year]	37.5 (no load)	69.62	65.46	77.14
Number of hours with voltage problem (V<0.9pu)/day	3	3	0	0

Résumé en français

Planification du réseau de distribution basse tension avec intégration de sources photovoltaïques et stockage-cas du réseau du Cambodge

1. Introduction générale

1.1. Contexte

De jour en jour, les consommations d'énergies ont continuellement augmenté dans le monde en raison de crossant d'habitants avec les styles de vie plus confortables. Actuellement, les besoins d'énergie ont alerté en concernant la réduction des fossiles, l'efficacité énergétique et les problèmes de réchauffement planétaire, ce qui conduit nos sociétés à chercher des sources d'énergies alternatives. Des sources d'énergie renouvelables ont été proposées pour réduire la dépendance de combustible fossile en transformant l'énergie des ressources naturelles à l'énergie thermique et électrique. Aujourd'hui, les sources d'énergie renouvelables sont largement utilisées pour fournir de l'énergie en tant que la génération distribuée connectée au réseau électrique. Les générations distribuées se situent à proximité des consommateurs, peuvent jouer un rôle important dans le réseau de distribution basse tension au futurs en raison de leurs impacts positifs potentiels sur l'amélioration de la fiabilité, la réduction des pertes, le support de tension et la réduction des émissions de CO2. Ainsi, l'intégration de la génération distribuée peut être considérée comme une option alternative attrayante pour la planification du réseau de distribution.

Au Cambodge, l'électricité est récemment fournie par quatre sources principales, i.e. le diesel, l'hydroélectricité, le charbon et l'importation des pays voisins. Dans le plan directeur du développement du secteur de l'électricité du pays, le gouvernement cambodgien a défini l'hydroélectricité et le charbon comme les deux sources principales de production d'électricité. Les sources d'énergie renouvelables (i.e. photovoltaïques) déjà existent, mais elles sont petites et encore isolées du réseau national ; elles s'appellent le Solar Home System (SHS) au Cambodge. Actuellement, environ 80 % de la population vit dans les zones rurales et 75 % des ménages vivent sans l'électricité même si ce pays a le potentiel élevé de ressources renouvelables. Afin de répondre aux besoins de la population et de la société pour l'électricité, le gouvernement cambodgien a établi la politique pour promouvoir et encourager le développement d'électricité ; tous les villages auront de l'électricité d'ici 2020 et au moins 70 % des ménages auront accès à la qualité d'électricité d'ici 2030. En outre, les réseaux de distribution basse tension sont renforcés et expansés en raison d'augmentation des charges électriques (i.e. croissance de la population et amélioration du standard de vie) ; ces points obligent le gouvernement cambodgien et les distributeurs d'électricité à effectuer la planification à la suite de ces problèmes actuels.

1.2. Objectifs

Pour réussir ces objectifs du contexte de travail, cette thèse étudie de novelles méthodologies pour dessiner les réseaux de distribution basse tension avec intégration de sources d'énergie renouvelables à petite échelle au Cambodge. Les objectifs principaux de thèse sont d'étudier la planification du réseau de distribution basse tension avec intégration de sources photovoltaïques et stockage et d'évaluer les solutions proposées prenant en compte les problèmes d'incertitude associés aux charges électriques. Cette thèse contribuera à l'électrification cambodgienne sur l'horizon de planification à long terme.

1.3. Plan de thèse

Dans le premier chapitre de cette thèse présentera la situation actuelle et l'évolution du réseau électrique, l'architecture du réseau de distribution basse tension pour les deux zones différentes (rural et urbain) et fournira également le principe de la planification du réseau de distribution au Cambodge.

Le deuxième chapitre détaillera le développement de la méthode de planification à long terme pour tacler le défi de l'incertitude des charges en zone urbaine. Dans cette partie, le nouvel algorithme sera développé pour chercher l'architecturer optimale de minimisation du coût d'investissement (CAPEX) et d'exploitation (OPEX) qui respecte l'ensemble de contraintes topologies et électriques (courant et tension). La programmation linéaire mixte en nombres entiers à contraintes quadratiques (PLMNECQ), le plus court chemin, first-fit bin-packing, et la méthode de Monte-Carlo seront utilisées pour résoudre ce problème.

Le troisième chapitre portera sur l'extension de la zone de couverture de l'électricité avec deux solutions possibles : le renforcement du réseau et l'intégration de photovoltaïques (PV)-stockage d'énergie de la batterie (BES). Le maximum d'intégration PV est trouvé dans le réseau BT afin d'optimiser l'autonomie énergétique du réseau électrique. Ensuite, des algorithmes seront mis en place pour trouver l'emplacement optimal et la capacité du BES qui sera intégré au réseau de distribution basse tension afin de résoudre le problème de sous tension ainsi que son contrôle. En fin, l'analyse de techno-économique sera effectuée pour comparer entre le renforcement du réseau et l'intégration de PV-BES.

Le dernier chapitre se concentrera sur la planification du réseau de distribution basse tension résidentielle BT pour les zones non électrifiées aux rural et urbain par l'architecture optimale et l'intégration de PV-BES des deux chapitres précédents. Nous développerons également l'algorithme pour contrôler le BES en tenant compte de l'incertitude de profil des charges sur l'horizon de planification.

Les conclusions générales et certaines perspectives d'avenir seront fournies à la fin de cette thèse.

2. Etat de l'art du réseau du Cambodge

Le Cambodge, officiellement connu sous le nom de Royaume du Cambodge, est un pays située dans le Sud-Est Asiatique. Il a une superficie de 181 035 km^2 avec la population de plus de 15 millions en 2014 [KING14]. Actuellement, l'électricité au Cambodge est fournie par quatre sources principales, i.e. le diesel, l'hydroélectrique, le charbon et les importations des pays voisins [EAC16]. En outre, les sources d'énergie renouvelables telles que le photovoltaïque et la biomasse déjà existent, mais elles sont petites et encore isolées du réseau national. Par ailleurs, le Cambodge est un pays agricole ou plus de 80% des personnes vivent dans les zones rurales, l'agriculture étant la source principale de subsistance [FAO11]. Parmi la région de l'Asie du Sud-Est, le Cambodge est l'un des tarifs d'électricité les plus chers (i.e. 0.18 USD/kWh aux urbains et 0.3 USD/kWh aux ruraux) selon un rapporte de [KOSA12] [EAC16]. Aujourd'hui, 74.80 % des villages et 65 % des ménages ont accès à l'électricité de qualité du réseau électrique [MME16]. De plus, environ 25 % des ménages cambodgiens ont accès à l'électricité en milieu rural même si ce pays a un potentiel élevé de renouvelable [PHOK16]. Ils survivent en utilisent du générateur diesel, de la batterie, du kérosène pour l'éclairage, de la télévision, du multimédia et d'autres appareils.

De même, pour réduire la pauvreté, améliorer le standard de vie et favoriser le développement économique, le gouvernement cambodgien a établi la politique de promotion et d'encouragement du développement de l'électrification [REF17] ; tous les villages du Cambodge auront accès à l'électricité d'ici 2020 et au moins 70 % de tous les ménages du Cambodge auront accès au réseau électrique de qualité d'ici 2030.

En outre, dans le plan directeur du développement du secteur de l'électricité dans le pays, le gouvernement a défini l'hydroélectrique et le charbon comme les deux sources principales de production d'électricité [KEIR09] [EAV11]. Cependant, comme les sources d'énergie renouvelables telles que l'énergie solaire sont abondantes dans certaines régions particulières, le gouvernement semble négliger sont plan de développement pour le secteur de l'électricité [MME16]. Il est donc très intéressé de mettre en évidence les avantages des générations distribuées à petite échelle (intégration de PV et stockage) au réseau de distribution basse tension afin d'encourager le gouvernement cambodgien et les distributeurs d'électricité avec ces sources. Par ailleurs, afin d'appliquer la conception de planification du réseau de distribution basse tension, il faut comprendre le fond du réseau électrique tel que sa situation actuelle et son évolution, ainsi que l'architecture du réseau de distribution basse tension au Cambodge. La première partie de ce chapitre présentera la situation actuelle du réseau électrique au Cambodge. Dans la deuxième partie, nous fournirons la structure du réseau de distribution basse tension au deux zones différentes (i.e. rural et urbain). Enfin, nous détaillons le principe de la planification du réseau de distribution dans la dernière partie de ce chapitre.

Dans ce chapitre, nous avons commencé par le contexte et le fond du réseau électrique au Cambodge. Il a été souligné qu'il y a environ 75 % de la production propre et que les 25 % restants sont importés des pays voisins, même si le Cambodge a le potentiel élevé de renouvelable. Actuellement, les lignes principales sont réparties en monophasée et triphasée le long des routes pour les zones rurales et sont presque triphasées pour les zones urbaines au Cambodge. Dans la planification traditionnelle, la génération locale n'est pas prise en compte ; il est donc intéressant d'étudier l'insertion de la génération locale, i.e. photovoltaïque (PV) et stockage d'énergie de la batterie (BES) dans la planification du réseau de distribution basse tension. Les contraintes prises en compte pour l'architecture optimale sont liées à la topologie et aux électrotechniques (i.e. tension et courant). Les problèmes principaux de cette thèse sont la recherche de l'architecture optimale et de l'impact de l'intégration de PV-BES au réseau de distribution basse tension sur l'horizon de planification. Ces problèmes seront pris en compte dans les trois chapitres suivants.

3. Planification du réseau de distribution basse tension sous incertitude des charges

Les réseaux de distribution basse tension (BT) sont renforcés et expansés dans dernières années en raison de l'augmentation de charge ; ces points obligent les distributeurs d'électricité à effectuer la planification suite à ces problèmes. Dans une procédure de planification du réseau de distribution, il est essentiel de chercher l'architecture appropriée afin de satisfaire l'aspectes techno-économique. Les réseaux de distribution basse tension sont le réseau radial presque déséquilibré en raison de diverses charges monophasées et triphasées au réseau. Pour faire face à ces problèmes, l'optimisation du réseau distribution radiale a été développée dans la littérature pour trouver le coût d'investissement le plus bas en utilisant l'algorithme de recherche de chemin [KUKS13] ou l'approche directe

[SSGS12]. En outre, les auteurs de [SWLM12] et [MRMM05] ont été étudiés sur le problème de l'acheminement des alimentations respectivement en utilisant le modèle MILP ou la programmation dynamique ; ces méthodes permettent de modéliser la réalité mais sont plus adaptées aux zones rurales et sont appliquées sur les réseaux de transmission. Pour construire l'architecture radiale en fonction de l'environnement, les chercheurs de [BOMP02] ont utilisé la méthode de programmation dynamique pour obtenir l'architecture. De même, le travail de [LITW96] est suggéré les heuristiques basées sur des mathématiques simples pour allouer les sous-stations et les alimentations du réseau de distribution. Mais [BOMP02] et [LITW96] ne sont pas adaptés à l'architecture d'alimentation. Les auteurs de [GOAR15] ont étudié la planification optimale du réseau de distribution urbaine sur sa topologie en utilisant l'algorithme de recuit simulé adapté ; cette méthode vise à minimiser le travail nécessaire du réseau existant pour l'expansion du réseau de distribution. Mais [GOAR15] a examiné sur la moyenne tension et souterrain du réseau triphasé équilibré. Cependant, on peut remarquer que les auteurs ont considéré les réseaux comme des alimentations à triphasés équilibrés. En outre, l'équilibrage de charge présente de nombreux avantages dans les réseaux de distribution ; les auteurs de [GRGL12] ont étudié la réduction des pertes par équilibrage de charge optimal ; cette méthode a réduit le courant de ligne et amélioré le facteur de tension déséquilibré. Par ailleurs, d'autres méthodes telles que la programmation en nombre entier mixte dans [ZHCZ98] et le recuit simulé dans [ZHU99] proposent de commuter la connexion de phase de charges individuelles pour réduire les pertes. Dans ces travaux de recherche, seule la topologie radiale existante est considérée. Le défi sur la planification du réseau de distribution basse tension manque encore tout en trouvant l'architecture optimale avec l'équilibrage de charge sous incertitude de charge aux réseaux déséquilibrés.

Par ailleurs, nous visons à développer la méthodologie de planification à long terme pour tacler le défi de l'incertitude de charge (i.e. taux de croissance et novelle charge connectée) au réseau de distribution basse tension. Nous développons le nouvel algorithme pour chercher l'architecture optimale en constatant quelle connexion de charge induit les coûts le plus bas (investissement et les pertes) et l'amélioration de l'équilibrage de charge. Dans la première partie, le modèle du réseau de distribution basse tension est décrite. Ensuite, la méthode proposée est décrite ainsi que l'étude de cas sur laquelle elles seront appliquées. Enfin, les résultats de simulation seront fournis et analysés pour valider la méthode proposée pour ce chapitre.

Dans ce chapitre, l'architecture radiale optimale et la stratégie de planification ont été réalisées en appliquant le PLMNECQ, le plus court chemin, le first-fit bin-packing, et la simulation de Monte-Carlo dans le logiciel ILOG-CPLEX et MATLAB. En outre, les trois cas sur l'incertitude de charge ont été proposés en tenant compte du taux de croissance et des nouvelles charges connectées au cours de l'étude de planification. La meilleure stratégie de conception est sélectionnée pour chaque cas de problème d'incertitude ; la 1ème stratégies est pour le cas 2 et le cas 3 et la 2ème stratégie est pour le cas 1. De plus, le diagramme triphasé est affiché automatiquement pour les planificateurs de voir la visualisation de l'architecture optimale. Cette méthode proposée est donc efficace et utile pour les distributeurs d'électricité pour dessiner les réseaux de distribution basse tension. Pour accomplir la planification du réseau de distribution basse tension, la planification composée de sources d'énergie renouvelables (RES), de stockage centralisé et décentralisé (CeBES-DeBES) sera étudiés dans les chapitres prochains.

4. Intégration de photovoltaïque en utilisant le stockage sur le réseau de distribution basse tension

La consommation d'énergie augmente d'année en année en raison de la croissance de la population et des conditions économiques dans les pays en voie de développement. Actuellement, environ 80 % de la population vivent dans les zones rurales et 75 % des ménages vivent sans l'électricité [PHOK16]. Afin de répondre aux besoins de la population et de la société en termes d'électrification, les distributeurs d'électricité trouvent une solution possible pour leurs consommateurs. Une solution possible a attiré l'intérêt des distributeurs d'électricité afin d'augmenter la couverture de l'électricité sont le renforcement/expansion de réseau et l'intégration de la production locale. En outre, les réseaux de distribution basse tension pour une faible densité de population dans les zones rurales sont caractérisés par une ligne principale monophasée, une faible densité de charge électrique et une utilisation fréquente des lignes aériennes.

Dans ce chapitre, nous étudierons un renforcement du réseau et l'intégration de PV-BES au réseau de distribution basse tension. L'objectif principale de ce chapitre est de proposer deux solutions différentes basées sur le renforcement et l'utilisation du PV-BES pour l'extension du réseau existant aux zones non-électrifiées. Ce travail vise à dimensionner la capacité de câble, le PV-BES décentralisé et le BES centralisé intégrés au réseau de distribution basse tension. Ce chapitre a été divisé en trois partie principales afin d'obtenir la solution. Tout d'abord, nous décrivons l'impact général de l'intégration de PV-

BES aux réseaux de distribution basse tension. Ensuite, la méthode proposée et les algorithmes développés sont présentés pour accomplir l'objectif de travail (sous tension et flux de puissance inversé). Les résultats de simulation du réseau de distribution basse tension testé sont fournis à la dernière partie.

L'impact des photovoltaïques et stockages intégré au réseau de distribution basse tension aérienne avec la ligne principale monophasé a été présenté dans ce chapitre. La comparaison entre le renforcement du réseau et l'intégration de PV-BES a également été fournie. Le dimensionnement du PV décentralisé (DePV) est déterminé en utilisant la technique itérative en considérant les contraintes de tension et de courant. En outre, l'emplacement optimal et le dimensionnement du BES décentralisé (DeBES) ont été soulignés par l'algorithme génétique (GA) et la technique itérative afin de résoudre le problème de sous tension du réseau. Par ailleurs, l'opération de DeBES a été réalisé avec l'algorithme de contrôle décentralisé. De même, la stratégie de dimensionnement du BES centralisé (CeBES) a été développée pour déterminer la capacité de CeBES afin d'éviter le flux de puissance inversé à poste source. De plus, la méthode proposée sera utile pour les distributeurs d'électricité qu'envisagent de faire l'extension de couverture d'électricité par le renforcement du réseau et l'intégration de PV-BES.

5. Planification du réseau de distribution basse tension avec photovoltaïque et stockage – études de cas

Dans les deux chapitres précédents, nous avons présenté le réseau de distribution basse tension sous l'incertitude de charge en recherchant l'architecture optimale avec la stratégie de conception et l'intégration de PV-BES en zone rurale avec la ligne principale monophasée. Cependant, ces deux chapitres ne tiennent pas compte de l'intégration de PV-BES (Chapitre II) et de l'incertitude sur le profil de charge avec la ligne principale triphasée (Chapitre III). La méthode proposée porte sur la planification du réseau de distribution basse tension résidentielle dans les zones rurales et urbaines par l'algorithme d'architecture optimale et l'intégration de PV-BES avec la ligne principale triphasée. La méthode proposée est décrite dans la première partie. Ensuite, les résultats de simulation du réseau de distribution résidentielle testée sont fournis. La conclusion est également fournie dans la dernière section du chapitre.

Ce chapitre a présenté la planification du réseau de distribution basse tension résidentielle avec l'intégration de DePV, DeBES et CeBES dans les zones rurales et urbaines du Cambodge, en particulier pour les zones non-électrifiées. L'algorithme d'architecture radiale optimale a été développé en utilisant le PLMNECQ, le plus court chemin et le first-fit bin-packing afin de dessiner l'architecture en minimisant l'utilisation des conducteurs et en améliorant l'équilibrage de charge. Par ailleurs, l'algorithme du dimensionnement de DePV a été développé comme la technique itérative sous les contraintes de tension et de courant du réseau électrique. L'emplacement et le dimensionnement de DeBES ont également été réalisés en utilisant l'algorithme génétique et la technique itérative afin de résoudre le problème de sous tension. En outre, la stratégie de dimensionnement de CeBES a été établie pour éviter le flux de puissance inversé du réseau de distribution BT vers le réseau de distribution MT et aussi pour augmenter le temps de fonctionnement autonome. De même, le contrôle décentralisé de DeBES a été développé sans utiliser les technologies de l'information et de la communication (TIC). L'impact de la référence de tension a été étudiée par la méthode de simulation de Monte-Carlo sous l'incertitude du profile de charge au cours de l'horizon de planification sans la zone rurale. De plus, la méthode proposée fournit des conseils et des concepts à ceux qui sont au début du dessin du réseau de distribution basse tension résidentielle.

6. Conclusion générale

6.1. Conclusion

Les objectifs de cette thèse ont été portes sur le développement à long terme de la planification des réseaux de distribution basse tension avec intégration de générations distribuées à petite échelle (photovoltaïques et stockage d'énergie de la batterie) pour défier les problèmes actuels au Cambodge. Les deux contributions principales de ce travail sont de rechercher d'abord l'architecture optimale du réseau de distribution basse tension et dimensionner les générations distribuées intégrées au réseau électrique. Les travaux présentés dans cette thèse peuvent être résumés comme suit :

Le chapitre I a fourni la situation actuelle du réseau du Cambodge. Il a fourni les informations nécessaires pour les chercheurs qui s'intéressent aux problèmes actuels du secteur de l'électricité au Cambodge ou les pays en voie de développement ayant des règles similaires.

Le chapitre II a développé le nouvel algorithme afin d'obtenir l'architecture optimale pour la conception du réseau de distribution basse tension en zone urbaine en tenant compte de l'incertitude de charges électriques sur l'horizon de planification (i.e. taux de croissance et nouvelles charges connectées). La conclusion principale de ce chapitre est de montrer que les deux stratégies différentes peuvent être appliquées en concernant le scenario d'incertitude de charges électriques. En cas d'évolution du taux de croissance de charges existantes seulement, la meilleure stratégie est de construire le réseau a l'année initiale en tenant compte de charges prévues à la fin d'année de planification en utilisant l'algorithme PLMNECQ. Si les nouvelles charges apparaissent lors de l'étude de planification, la meilleure approche est basée sur le principe de renforcement (câbles) et construction du réseau d'année en année en utilisant les algorithmes de plus court chemin et first-fit bin packing.

Le chapitre III a proposé les deux solutions possibles afin d'augmenter le couverture d'électricité pour le village rural pour résoudre le problème de sous tension en bout de ligne de réseau de distribution basse tension. Ces deux solutions possibles sont le renforcement de réseau et l'intégration de sources PV-stockage. Avec cette deuxième solution, les distributeurs d'électricité n'ont pas besoin de renforcer les lignes, mais ils doivent acheter des PV-stockages et des câbles d'extension pour les nouveaux consommateurs. La puissance installée maximale de PV a été calculée en fonction des contraintes de tension et de courant. De plus, la charge maximale (peak load) a été réduite grâce au stockage d'énergie de la batterie connecté au réseau. En raison de l'intégration de PV au réseau, l'opération autonome du réseau de distribution basse tension est également assurée ; cela signifie que les consommateurs seront soutenus par des générations locales (PV-BES). Ce chapitre a ainsi démontré que la générations locale d'énergie renouvelables à petite échelle et le stockage d'énergie de la batterie étaient utiles pour le secteur de l'électricité au Cambodge.

Le chapitre IV a concentré sur la planification du réseau de distribution résidentielle basse tension en particulier pour les zones non-électrifiées, en recherchant l'architecture optimale automatiquement et en dimensionnant de sources PV-BES au réseau sur l'horizon de planification. En zone urbaine, les deux algorithmes développés au chapitre II pour l'architecture optimale ont été utilisés. La première partie est basée sur la plus court chemin et le first-fit bin packing, et trouve l'architecture qui minimise la longueur totale et améliore l'équilibrage de charge. Cet algorithme réduit les pertes mais il augment l'utilisation du câble. La deuxième partie est l'algorithme PLMNECQ qui tente de minimiser l'utilisation du câble et d'améliorer l'équilibrage de charge. En conséquence, les pertes de l'architecture proposée pour cet algorithme sont supérieures à celles obtenues avec la première solution proposée. Une fois les architectures obtenues, l'intégration de PV-BES est considérée. La comparaison de techno-économique est faite entre les deux architectures optimales, y compris l'intégration de PV-BES en tenant compte du coût actualisé. Les deux résultats suivant ont été fournis :

1- le premier algorithme est meilleur que le deuxième.
2- le cas de l'intégration de PV-BES est plus économique que le cas sans l'intégration de PV-BES pour les deux architectures.

La même étude est menée pour le réseau de distribution résidentielle basse tension en zone rurale. Dans ce cas, le plus court chemin et le first-fit bin-packing ont été appliqués afin d'obtenir l'architecture optimale avec l'équilibrage de charge. La puissance installée maximale de PV qui peut être intégrée au réseau a été déterminé en fonction des contraintes de tension et de courant. L'emplacement et le dimensionnement du BES centralisé et décentralisé ont été effectués afin de résoudre le problème de sous tension et de diminuer le dimensionnement du transformateur MT/BT. L'autre contribution de ce chapitre est le contrôle proposé du BES sans utiliser les technologies de l'information et de la communication (TIC). L'algorithme a été développé en tenant compte de l'hypothèse d'incertitude du profil de charge sur l'horizon de planification. Ce chapitre a conclu que le réseau de distribution basse tension triphasée en tant que la ligne principale avec l'équilibrage de charge et l'intégration de PV-BES est la solution possible que le gouvernement cambodgien et les distributeurs d'électricité devraient considérer. En outre, avec cet algorithme développé, le réseau de distribution basse tension peut être joué le rôle de réseau-micro isolée indépendant du réseau de distribution moyenne tension (MT) principale avec les temps de fonctionnement autonome de 70 % et 37 % de la réduction maximale de capacité du transformateur MT/BT à la fin de l'horizon de planification.

6.2. Perspectives

Malgré notre objectif de fournir la méthode de planification de réseau de distribution avec intégration de sources photovoltaïques et stockage-cas du réseau du Cambodge, il est évident que de nombreuses perspectives peuvent êtres recommandés dans ces travaux. Dans cette recherche, le coût d'investissement ne tient compte que le prix de l'équipement pour évaluer le coût actualise de l'architecture différente du réseau de distribution basse tension. Il faut tenir compte des coûts de construction et de maintenance pour chaque équipement afin de fournir la conclusion générale sur la conception du réseau de distribution basse tension. De plus, le type de source PV seulement comme l'énergie renouvelable est considéré pour l'étude primaire dans cette thèse, donc d'autres types de sources renouvelables à petite échelle devraient être étudiés comme la biomasse et le picohydroélectrique, qui sont abondantes dans certaines régions du Cambodge. De même, le type de stockage d'énergie de la batterie n'est pas considéré dans ce travail puisque cette thèse était portée sur l'optimisation du dimensionnement. Par conséquent, la comparaison entre différents stockages devrait être prise en compte afin de sélectionner l'un d'entre eux pour une application réelle. Par ailleurs, ce travail n'a étudié que la planification du réseau de distribution basse tension. La nouvelle méthode et l'algorithme devraient être modifiés afin d'appliquer pour les problèmes actuels au réseau de distribution moyenne tension dans l'autres études telles que l'emplacement et le dimensionnement optimal de générations distribuées multiples. Le denier point consiste à tester plus d'études de cas avec l'algorithme présenté et à développer un modèle d'incertitude précisé pour tacler à un comportement intermittent de charge et de génération distribuée afin de fournir une conclusion générale, en particulier pour les pays en voie de développement.

Publications

Conference Papers

[1] **V. Vai**, E. Gladkikh, L. Bun, M.-C. Alvarez-Herault, B. Raison, "Study of Low-Voltage Distribution System with Integration of PV-Battery Energy Storage for Urban Area in Developing Country", *IEEE-EEEIC / I&CPS Europe 2017,* June 2017, Italy.

[2] **V. Vai**, E. Gladkikh, L. Bun, M.-C. Alvarez-Herault, B. Raison, "Planning of Low-Voltage Distribution Systems with Uncertainty on Load Demand in Urban Areas", *IEEE-EEEIC / I&CPS Europe 2017,* June 2017, Italy.

[3] **V. Vai**, E. Gladkikh, L. Bun, M.-C. Alvarez-Herault, B. Raison, "Low-Voltage Distribution System Planning under Load Demand Uncertainty: Growth Rate with Connection of New Loads", *IEEE-iEECON 2017*, March 2017, Thailand.

[4] **V. Vai**, L. Bun, M.-C. Alvarez-Herault, B. Raison, "Study of Low-Voltage Distribution System with Decentralized PV-BES and Centralized BES for Rural Village in Developing Country", *IEEE-iEECON 2017*, March 2017, Thailand.

[5] **V. Vai**, E. Gladkikh, L. Bun, M.-C. Alvarez-Herault, B. Raison, "Planning of Low Voltage Distribution Systems with Uncertainty on Load Demand", *RCEnE 2016*, November 2016, Cambodia.

Submitted to Journal Paper

[1] **V. Vai**, L. Bun, M.-C. Alvarez-Herault, B. Raison, "Optimal design of microgrids for the electrification of developing countries-case studied of Cambodia", Submitted to IET Generation, Transmission & Distribution, 2017.

PLANIFICATION DU RÉSEAU DE DISTRIBUTION BASSE TENSION AVEC INTÉGRATION DE SOURCES PHOTOVOLTAÏQUES ET STOCKAGE - CAS DU RÉSEAU DU CAMBODGE

Résumé: La consommation d'énergie augmente d'année en année en raison de la croissance de la population et des conditions économiques. Dans ce contexte, le gouvernement Cambodgien a mis en place une politique de promotion et d'encouragement du développement de l'électrification ; tous les villages devront être électrifiés d'ici 2020 et au moins 70% des domiciles auront accès au réseau électrique d'ici 2030. Par ailleurs, de nombreux foyers non électrifiés sont équipés de panneaux solaires afin d'avoir accès à l'électricité. L'objectif de cette thèse est donc de développer des outils de planification du réseau de distribution basse tension afin de contribuer à l'électrification du pays. La première partie de cette thèse se concentre sur le développement d'outils d'optimisation de l'architecture afin de minimiser le coût d'investissement (CAPEX) et d'exploitation (OPEX) qui respecte l'ensemble des contraintes topologies et électriques (courant et tension) tout en intégrant les incertitudes liées au développement des consommateurs basse tension. La deuxième partie de la thèse propose une nouvelle solution de planification afin d'intégrer les productions solaires présentes et à venir sur le réseau basse tension. Cette solution consiste à ajouter du stockage centralisé (en milieu urbain et rural) et du stockage décentralisé (en milieu rural). Les principaux avantages seraient d'une part de réduire le pic de consommation du transformateur moyenne tension/basse tension et donc de réduire les investissements moyenne tension mais également le dimensionnement de « microgrids » basse tension pouvant être autonomes une grande partie de l'année. Une comparaison technico-économique avec la solution classique de renforcement permet d'évaluer l'intérêt de cette nouvelle solution.

Mots clés: *Méthode de Monte Carlo, optimisation, planification, photovoltaïque, réseau de distribution basse tension, stockage, théorie de graphe*

PLANNING OF LOW VOLTAGE DISTRIBUTION SYSTEM WITH INTEGRATION OF PV SOURCES AND STORAGE MEANS- CASE OF THE POWER SYSTEM OF CAMBODIA

Abstract: The energy consumption increases year by year due to the growth of the population and the economic conditions. In this context, the Cambodian government promotes and encourages the development of the electrification through several policies; all the villages must be electrified by 2020 and at least 70 % of the households will be connected to the network by 2030. Besides, lots of non-electrified homes are equipped with solar panels so as to have access to the electricity. Then, the objective of this thesis is to develop planning tools of the low voltage distribution network to contribute to the electrification of the country. The first part of this thesis focusses on the development of architecture's optimization methods to minimize the capital expenditure (CAPEX) and operational expenditure (OPEX) while respecting both topological and electrical constraints (current and voltage) and integrating the uncertainties on the future development of the low voltage customers. The second part of the thesis proposes a new planning solution so as to integrate the current and future solar productions on the low voltage network. This solution consists in adding centralized storage (in urban and rural areas) and decentralized storage (in rural areas). The main advantages would be first to reduce the consumption peak of the medium voltage /low voltage transformer and consequently to reduce the medium voltage investments but also to size low voltage "microgrids" which can be autonomous a big part of the year. A technical and economic comparison with the classic solution of reinforcement allows estimating the interest of this new solution.

Keywords: *Monte Carlo method, optimization, planning, photovoltaic, low voltage distribution system, storage, graph theory*

G2Elab - Laboratoire de Génie Electrique de Grenoble (UMR 5269 CNRS / Grenoble INP / UGA)
Bâtiment GreEn-ER, 21 avenue des martyrs
CS 90624, 38031 Grenoble